

Acute Cardiac Responses to Respiratory Muscle Unloading at Different Exercise Intensities

by

Sarah A. Angus

A thesis

presented to the University of Waterloo

in fulfillment of the

thesis requirement for the degree of

Master of Science

in

Kinesiology

Waterloo, Ontario, Canada, 2022

© Sarah A. Angus 2022

AUTHOR'S DECLARATION

I hereby declare that I am the sole author of this thesis. This is a true copy of the thesis, including any required final revisions, as accepted by my examiners. I understand that my thesis may be made electronically available to the public.

ABSTRACT

Respiration is accomplished by alterations in intrathoracic pressure (ITP) and has physiological implications on the heart. For example, the negative ITP during inspiration is transmitted to the right atrium, which augments venous return, preload, stroke volume (SV), and cardiac output (\dot{Q}). We sought to determine the impact of respiration on \dot{Q} during semi-supine cycle exercise by using a proportional assist ventilator to attenuate ITP changes and the work of breathing (W_b). Thirteen healthy participants (6 females) completed three discrete exercise trials at 30%, 60% and 80% peak power (W_{max}) with unloaded and spontaneous breathing. Intrathoracic and intraabdominal pressure were measured with balloon catheters placed in the esophagus and stomach. Stroke volume was determined via echocardiography and the Simpson's biplane method. An electrocardiogram measured heart rate (HR) and a customized metabolic cart measured ventilatory and mixed expired variables such as ventilation and oxygen consumption ($\dot{V}O_2$). Mean esophageal pressure was greater during unloaded relative to spontaneous breathing at all exercise intensities ($p < 0.0001$). Esophageal pressure swings per breath (between spontaneous and unloaded breathing) were different at 30%, 60% and 80%; (-3.5 ± 3.4 vs. -6.8 ± 6.4 vs. -11.9 ± 7.9 cmH₂O, respectively ($p = 0.01$)). However, the decrease in W_b was not different between exercise intensities (39 ± 22 vs. 46 ± 14 vs. $51 \pm 14\%$ from spontaneous breathing for 30%, 60%, and 80% W_{max} , respectively, all $p > 0.05$). Cardiac output decreased during unloaded breathing by -1.2 ± 1.3 vs. -1.7 ± 1.4 vs. -1.8 ± 2.0 L min⁻¹ from spontaneous breathing at 30%, 60% and 80% W_{max} , respectively (all $p < 0.05$). Heart rate decreased during unloaded breathing by -2 ± 3 vs. -6 ± 4 bpm at 60% and 80% W_{max} , respectively (both $p < 0.05$), with no change at 30% W_{max} ($p = 0.2$). Stroke volume decreased during unloaded breathing by -10.7 ± 11.2 vs. -10.1 ± 10.2 vs. -8.0 ± 12.3 mL from spontaneous breathing at 30%, 60% and 80% W_{max} , respectively (all $p < 0.05$). Oxygen

consumption decreased during unloaded compared to spontaneous breathing at 80%W_{max} (2.5 ± 0.6 vs. 2.6 ± 0.7 L min⁻¹, $p=0.002$) with no change at 30% and 60%W_{max} (both $p>0.05$). In summary, attenuating ITP swings resulted in a reduction in \dot{Q} at all exercise intensities. At 30% W_{max}, the decrease in \dot{Q} may be due to a reduction in SV. At 60%W_{max}, \dot{Q} decreases likely because of a reduction in SV and HR. At 80%W_{max}, \dot{Q} may decrease due reductions in SV, HR and $\dot{V}O_2$. In conclusion, the normally occurring swings in ITP developed during spontaneous breathing is helpful for maintaining cardiac function during exercise.

ACKNOWLEDGEMENTS

I am truly grateful for all of my participants. My study protocol was not easy and without you this thesis would not be possible.

I would like to extend my thanks to my supervisor, Dr. Paolo Dominelli. Thank you for providing me with so many opportunities to learn and to succeed. My Masters experience has far exceeded my expectations, thank you for your support and guidance. To my committee, Dr. Richard Hughson and Dr. Jason Au, thank you for providing your expertise to my thesis. Both of you have helped me learn and for that I am grateful.

Next, I would like to sincerely thank Dr. Alex Williams and Dr. Eric Stöhr. Alex, thank you for taking time out of your busy schedule to collect all of the cardiac images for this study. Eric, thank you for taking time every week for several months to teach me how to perform the cardiac analysis, without your help I wouldn't have been able to learn and truly appreciate how amazing the heart is. I am truly grateful for both of you, without both of you this study would not be possible.

To my lab mates, Leah Mann, Jason Chan, Connor Doherty, Ben Thompson, Victoria Chang, and Maddie Wright. Thank you for always making the lab (and office) a fun place to be. There was never a time when I was with you guys and I didn't have a great time. Thank you all for being amazing lab mates and friends.

Next, I would like to thank my friends and family. Fasih, thank you for constantly being there for me and for supporting me throughout this journey. I am truly grateful for your support and encouragement throughout my time knowing you, thank you for everything you do for me. Mom, thank you for your constant support. Even though I know you don't know what I do in school half the time you still fully support me nonetheless, I'm eternally grateful for you, thank you and I love you. Lorrie & Eric, thank you for your unending support, I love you guys.

Lastly, I am truly grateful for the strength Allah tala has provided me to complete this thesis. Without His help and guidance, this thesis would not be possible.

DEDICATION

To Mom, Lorrie and Eric, thank you for always caring for me, supporting me and loving me.

This thesis is for you.

TABLE OF CONTENTS

AUTHOR'S DECLARATION	ii
ABSTRACT.....	iii
ACKNOWLEDGEMENTS	v
DEDICATION.....	vi
LIST OF FIGURES	ix
LIST OF TABLES	x
LIST OF EQUATIONS.....	xi
LIST OF ABBREVIATIONS	xii
1.0 LITERATURE REVIEW	1
1.1 Cardiorespiratory Interactions in Health During Rest and Exercise	1
1.1.1 Influence of Intrathoracic Pressure on Cardiac Function	1
1.1.2 Influence of Ventilation and Lung Volumes on Cardiac Function	6
1.1.3 Influence of Abdominal Pressure, Volume Status and Venous Return on Cardiac Function	9
1.2 Cardiorespiratory Interactions Differ with Exercise Intensity.....	12
1.3 Cardiorespiratory Interactions During Mechanical Ventilation	14
1.4 Techniques Used to Study Cardiorespiratory Interactions.....	17
1.5 Proportional Assist Ventilation to Unload the Respiratory Muscles.....	19
1.6 Implications of Respiratory Muscle Unloading on Cardiac Output and Oxygen Consumption	20
2.0 STUDY RATIONAL	22
3.0 RESEARCH QUESTIONS AND HYPOTHESES	23
4.0 METHODS	24
4.1 Ethics	24
4.2 Participants.....	24
4.3 Experimental Overview	25
4.3.1 Day One: Screening, pulmonary function testing and $\dot{V}O_{2max}$ test	25
4.3.2 Day Two: Familiarization.....	26
4.3.3 Day Three: Experimental Protocol	26
4.4 Data Collection	27
4.4.1 Respiratory Flow and Volume.....	27
4.4.2 Intrathoracic/intrabdominal Pressure Surrogate (Esophageal/Gastric Pressure).....	28
4.4.3 Echocardiography	29
4.4.4 Manipulation of Intrathoracic Pressure	30
4.5 Data Analysis	31
4.5.1 Respiratory Flow and Volume.....	31
4.5.2 Heart Rate and Blood Pressure	31
4.5.3 Pressure.....	32
4.5.4 Echocardiography	32
4.5.5 Work of Breathing	34

4.6 Statistical Analysis.....	35
5.0 RESULTS	37
5.1 Participant Demographics and Baseline Data	37
5.2 Respiratory Muscle Unloading and Work of Breathing.....	37
5.2.1 Evidence of Respiratory Muscle Unloading via Proportional Assist Ventilation	37
5.2.2 Inspiratory and Total Work of Breathing Reduced by Proportional Assist Ventilation	41
5.3 Metabolic Implications of Respiratory Muscle Unloading.....	45
5.4 Cardiovascular Changes with Respiratory Muscle Unloading.....	46
5.5 Integrative Influence of Respiratory Muscle Unloading on Cardiovascular and Metabolic Variables.....	49
6.0 DISCUSSION	61
6.1 Main Findings.....	61
6.2 Cardiac Output Decreases During Respiratory Muscle Unloading	61
6.2.1 Reductions in Stroke Volume with Respiratory Muscle Unloading	62
6.2.2 Reductions in Heart Rate with Respiratory Muscle Unloading	70
6.3 Relationship Between Cardiac Output and Oxygen Consumption	71
6.4 Case Studies	73
6.4.1 Participant with the Greatest Reduction in Cardiac Output also had the Greatest rise in Intrathoracic Pressure.....	74
6.4.2 Participant with the Smallest Change in Cardiac Output had the Smallest Reduction in the Magnitude of Intrathoracic Pressure Swings	76
6.5 Technical Considerations and Limitations	78
6.6 Future Directions.....	81
7.0 CONCLUSION	83
REFERENCES.....	84

LIST OF FIGURES

Figure 1. Cardiorespiratory interactions depicted at rest and exercise.	4
Figure 2. Series and direct ventricular interactions during inspiration and expiration.	5
Figure 3. Cardiorespiratory interactions during mechanical ventilation and exercise.	16
Figure 4. Schematic of day 3 experimental protocol.	27
Figure 5. Representative figure of one participant exercising at 80%W _{max} during unloaded and spontaneous breathing.	38
Figure 6. Respiratory pressures during unloaded and spontaneous breathing at each exercise intensity.	39
Figure 7. Work of breathing and ventilatory data during unloaded and spontaneous breathing at each exercise intensity.	42
Figure 8. Metabolic variables during unloaded and spontaneous breathing at each exercise intensity.	45
Figure 9. Relationship between oxygen consumption and the work of breathing.	46
Figure 10. Cardiac variables during unloaded and spontaneous breathing at each exercise intensity.	47
Figure 11. Cardiovascular variables during unloaded and spontaneous breathing at each exercise intensity.	48
Figure 12. Relationship between the absolute change in cardiac output and oxygen consumption between unloaded and spontaneous breathing at each exercise intensity.	50
Figure 13. Relationship between cardiac output and oxygen consumption when considering breathing condition.	50
Figure 14. Change in the relationship between cardiac output and oxygen consumption depending on breathing condition.	51
Figure 15. Relationship between cardiac output and oxygen consumption at each exercise intensity during unloaded and spontaneous breathing.	52
Figure 16. Movement of the cardiac output and oxygen consumption relationship from the control trendline during unloaded breathing for each participant at each exercise intensity.	53
Figure 17. Relationship between cardiac output and the magnitude of esophageal pressure swings.	54
Figure 18. Relationship between stroke volume and the magnitude of esophageal pressure swings.	55
Figure 19. Relationship between left ventricular end-diastolic volume and the magnitude of esophageal pressure swings.	56
Figure 20. Relationship between left ventricular end-systolic volume and the magnitude of esophageal pressure swings.	56
Figure 21. Relationship between mean arterial pressure and the magnitude of esophageal pressure swings.	57
Figure 22. Relationship between heart rate and oxygen consumption.	58

LIST OF TABLES

Table 1. Participant inclusion and exclusion criteria. 25
Table 2. Participant demographics and baseline data. 37
Table 3. Relative (percent) differences for each exercise intensity from spontaneous (POST) to unloaded (PAV) breathing. 59
Table 4. Absolute differences for each exercise intensity from spontaneous (POST) to unloaded (PAV) breathing..... 60

LIST OF EQUATIONS

Eq 1. $P_{mus} = VE + \dot{V}R + \dot{V}I$	20
Eq 2. $P_{mus} + P_{aw} = VE + \dot{V}R + \dot{V}I$	20
Eq 3. $MAP = [DBP + 1/3(SBP-DBP)]$	32

LIST OF ABBREVIATIONS

Pab	Abdominal pressure
Paw	Airway pressure
ANOVA	Analysis of variance
Fb	Breathing frequency
CO ₂	Carbon dioxide
$\dot{V}CO_2$	Carbon dioxide output
\dot{Q}	Cardiac output
COPD	Chronic obstructive pulmonary disease
Pdi	Diaphragmatic pressure
DBP	Diastolic blood pressure
E	Elastance
ECG	Electrocardiogram
Pes	Esophageal pressure
\dot{V}	Flow
\ddot{V}	Gas acceleration
Pgas	Gastric pressure
HR	Heart rate
I	Inertance
IVC	Inferior vena cava
ICU	Intensive care unit
ITP	Intrathoracic pressure
LA	Left atrium
LV	Left ventricle
LVEDV	Left ventricular end-diastolic volume
LVSV	Left ventricular stroke volume
V	Lung volume
HRmax	Maximal heart rate
$\dot{V}O_{2max}$	Maximal oxygen consumption
MAP	Mean arterial pressure
Pm	Mouth pressure
MSNA	Muscle sympathetic nerve activity
O ₂	Oxygen
$\dot{V}O_2$	Oxygen consumption
Wmax	Peak power
Pmus	Pressure required of the respiratory muscles
PSV	Pressure support ventilation
PTP	Pressure time-product
PAV	Proportional assist ventilator
PVR	Pulmonary vascular resistance
R	Resistance
RER	Respiratory exchange ratio
RAP	Right atrial pressure
RA	Right atrium
RV	Right ventricle

RVEDV	Right ventricular end-diastolic volume
RVESV	Right ventricular end-systolic volume
RVSV	Right ventricular stroke volume
SV	Stroke volume
SNA	Sympathetic nerve activity
SBP	Systolic blood pressure
TPR	Total peripheral resistance
VR	Venous return
\dot{V}_E	Ventilation
W_b	Work of breathing

1.0 LITERATURE REVIEW

The cardiovascular and respiratory systems work together to intake oxygen and transport this oxygen around the body, while also removing carbon dioxide. Since the heart and lungs are enclosed in the thoracic cavity, they are also exposed to the same intrathoracic pressures (1,2), causing both systems to interact with each other (3).

1.1 Cardiorespiratory Interactions in Health During Rest and Exercise

The heart is comprised of two ventricles and two atria that are enclosed by a fibrous pericardium. The pericardium functions to anchor the heart and limit bi-ventricular volume, such that an increase in volume of one ventricle will decrease the compliance of the other (4). The pericardium limits bi-ventricular volume to protect the heart from overdistention. Removing the pericardium in canines increases stroke volume (SV), cardiac output (\dot{Q}) and maximal oxygen consumption ($\dot{V}O_{2max}$), thereby suggesting that the pericardium limits exercise performance in normal circumstances (5). The two ventricles of the heart share an interventricular septum which plays a substantial role in direct ventricular interactions and ventricular compliance (4,6,7). For example, if the volume of the right ventricle increases, the interventricular septum will shift leftwards into the left ventricle effectively impeding the filling (compliance) and function of the left ventricle. Cardiorespiratory interactions in health at both rest and exercise can be divided into three components based on causative mechanism (2): 1) intrathoracic pressure (ITP) changes, 2) lung volume changes, and 3) volume status and abdominal pressure (P_{ab}) changes.

1.1.1 Influence of Intrathoracic Pressure on Cardiac Function

Within the thoracic cavity, the surrounding pressure of the heart is considered pericardial pressure and pleural pressure is the surrounding pressure of the lung, yet it is universally assumed that both pericardial and pleural pressure equal ITP under healthy conditions (3). Therefore, ITP

is the surrounding pressure of both the heart and the lungs. As such, any change in ITP will be transmitted to the cardiac structures, such as the heart chambers (i.e., right atrium) and intrathoracic blood vessels (i.e., pulmonary vein, proximal portion of the inferior vena cava, etc.) (2,8). Intrathoracic pressure changes cyclically during a respiratory cycle whereby ITP becomes more negative during inspiration (from ~ -5 to $-8\text{cmH}_2\text{O}$) and passively returns to baseline pressures during expiration at rest (~ -2 to $-5\text{cmH}_2\text{O}$) (9). During exercise, ITP swings can range from $-15\text{cmH}_2\text{O}$ to $-30\text{cmH}_2\text{O}$ (nadir) during inspiration and from $10\text{cmH}_2\text{O}$ to $20\text{cmH}_2\text{O}$ (peak) during expiration (10), but can be greater depending on breathing pattern and total ventilation. Exercise requires an increase in both the magnitude and frequency of ITP swings because as exercise progresses, more of the inspiratory and expiratory reserve volumes will be used and the rate of inspiratory and expiratory flow increases, subsequently causing large ITP swings (2,11). Ventilation at rest involves active inspiration and passive expiration. However, during exercise, expiration becomes active (12–14) in order to reduce lung volume below functional residual capacity, consequently leading to more positive expiratory ITPs as a result. Moreover, the greater magnitude swings in ITP with exercise are in part due to a reduction in lung compliance at high lung volumes. As end-inspiratory lung volume approaches total lung capacity during exercise, the lung can become less compliant and require greater pressures to inflate (15).

At both rest and exercise, the more negative ITP during inspiration is transmitted to the right atrium (RA), thereby reducing right atrial pressure (RAP). Right atrial pressure at rest is approximately $2\text{--}6\text{ cmH}_2\text{O}$ (16). During inspiration when ITP becomes more negative, RAP will decrease and become less positive (becoming closer to $0\text{ cmH}_2\text{O}$), without becoming negative. As RAP decreases (becoming less positive), the rate of venous return (VR) will increase (17). The pressure gradient for VR is between mean systemic pressure and RAP (1). As such, the rate of VR

can be altered by either changing RAP or mean systemic pressure (**Figure 1A&B**). For example, increasing abdominal pressure (as with inspiration) will increase the pressure gradient for VR (by increasing mean systemic pressure) (18). As such, inspiration will cause an immediate increase in VR which will increase right ventricular end-diastolic volume (RVEDV) and right ventricular stroke volume (RVSV) on the subsequent heart systole (1,19). A greater volume of blood returning to the right heart can cause a reduction in left ventricle (LV) compliance (especially during exercise) as the large negative ITP swings increase RVEDV, decreasing the transseptal pressure gradient and subsequently causing a leftward septal shift (via direct ventricular interaction) (4,20) (**Figure 2C**). Inspiration facilitates an increase in intrathoracic blood volume (21) as a more negative ITP enhances VR and decreases left ventricular stroke volume (LVSV) at rest (2,12,22,23) (**Figure 1A**). During exercise, the large negative ITP swings will increase VR during inspiration (24) and will enhance LVSV during expiration (25).

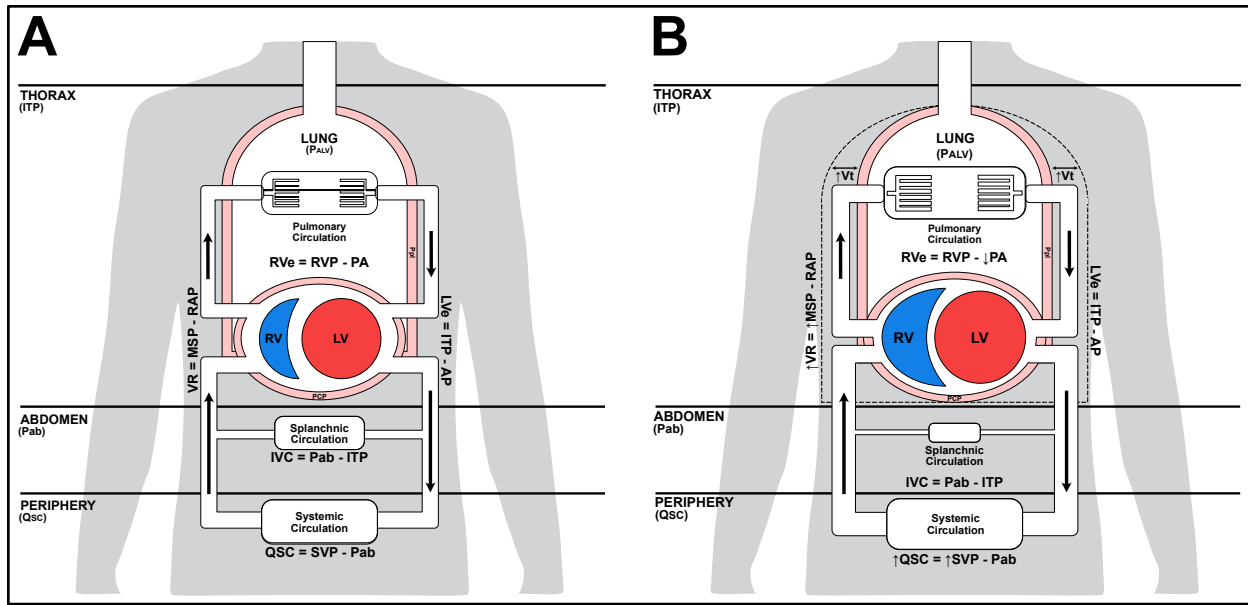


Figure 1. Cardiorespiratory interactions depicted at rest (A) and exercise (B). The lungs are surrounded by pleural pressure (Ppl) and the heart is surrounded by pericardial pressure (PCP). In the healthy individual, Ppl and PCP equal intrathoracic pressure (ITP). As such, the surrounding pressure for the heart and the lungs is assumed to be ITP. At rest (A), blood flow to the pulmonary circulation can be met with some resistance as some pulmonary capillaries are collapsed. Blood flow to the splanchnic circulation remains normal. During exercise (B), tidal volume (Vt) is elevated and the magnitude of ITP swings is enhanced. Circulating blood volume increases, therefore absolute blood flow through the heart and to the pulmonary circulation is increased. There is greater recruitment and distention of the pulmonary vasculature to accommodate the increased blood volume which will mitigate pulmonary vascular resistance (PVR). Blood flow to the splanchnic circulation is reduced while more is directed to the exercising skeletal muscle and to the skin (thermoregulation) in the periphery. Elevated pressures in the periphery (from exercising skeletal muscles) will increase mean systemic pressure (MSP) which will facilitate venous return (VR) (skeletal muscle pump). P_{ALV}, alveolar pressure; P_{ab}, abdominal pressure; QSC, systemic circulation blood flow; R_{Ve}, right ventricular ejection; R_{VP}, right ventricular pressure; P_A, pulmonary artery pressure; R_V, right ventricle; L_V, left ventricle; R_{AP}, right atrial pressure; L_{Ve}, left ventricular ejection; A_P, arterial pressure; I_{VC}, inferior vena cava; S_{VP}, systemic venous pressure. Modified from: Cheyne WS, Harper MI, Gelin JC, Sasso JP, Eves ND. Mechanical cardiopulmonary interactions during exercise in health and disease. *J Appl Physiol Bethesda Md* 1985. 2020 May 1;128(5):1271–9.

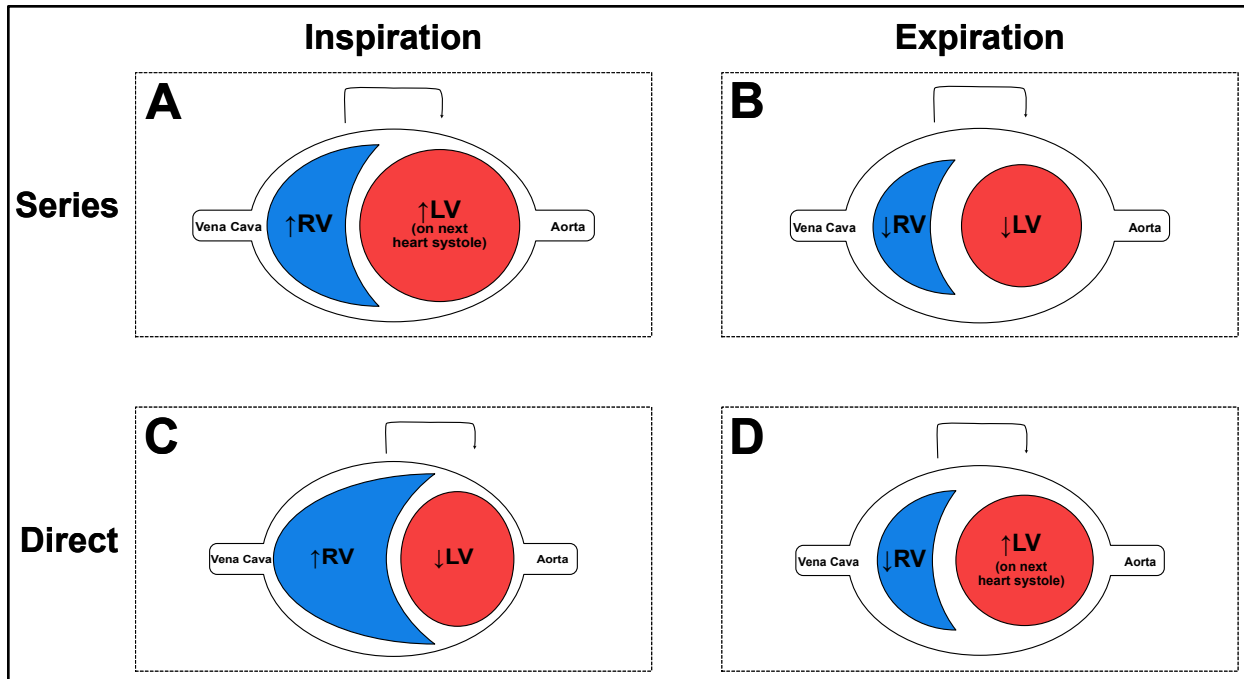


Figure 2. Series (A, B) and direct (C, D) ventricular interactions during inspiration (A, C) and expiration (B, D). RV, right ventricle; LV, left ventricle. Adapted from Neil Eves' Graduate Seminar presentation at the University of Waterloo on October 27, 2021.

During inspiration, there is an increase in VR and RVEDV which will cause the interventricular septum to shift leftwards and decrease the compliance and therefore stroke volume of the LV (via ventricular interdependence) (26) (**Figure 2C**). As ITP becomes more negative (especially during exercise) left ventricular afterload increases due to a rise in LV transmural pressure (2,21,26–30). Intrathoracic pressure changes can influence LV function by altering both LVEDV and LV ejection pressure (21). Left ventricular ejection pressure is arterial pressure relative to ITP (21,31) (**Figure 1A&B**). Therefore, when ITP becomes more negative during inspiration, this pressure gradient is increased (i.e., LV transmural pressure increases) meaning that myocardial wall stress and LV afterload are elevated (2,3,21), which can reduce or constrain LVSV (27). However, the healthy cardiovascular system is much more sensitive to changes in preload rather than afterload (32). Moreover, during exercise, LVSV increases during expiration due to the increases in RVEDV accumulated during the previous inspiration (**Figure 2D**). For

example, a greater RVEDV (during inspiration) will cause a greater LVSV via series interaction (during expiration) (**Figure 2A**). During exercise, there is a large reduction in systemic vascular resistance primarily due to vasodilation of the working skeletal muscle vasculature, as well as to the skin (thermoregulation). As such, the adverse effects of an elevation in LV afterload (due to large negative ITP swings) on LVSV are minimized (2,32) (**Figure 1B**).

Conversely, the less negative (more positive) ITP during expiration at rest (from $\sim -8\text{cmH}_2\text{O}$ to $-3\text{cmH}_2\text{O}$) will be transmitted to the RAP and will increase RAP making it more positive (i.e., starting from $\sim 3\text{cmH}_2\text{O}$ to $6\text{cmH}_2\text{O}$), thereby decreasing the rate of VR (1,19). As VR decreases, through series interaction, RVEDV, left ventricular end-diastolic volume (LVEDV) and \dot{Q} will decrease as a reduction in the initial blood volume returning to the heart (i.e., VR) will cause a reduction of blood passed through and pumped out of the heart (4,8,12,33) (**Figure 2B**). Expiration facilitates a decrease in intrathoracic blood volume as LV afterload is reduced (21,28,29), thereby promoting blood flow out and into the systemic circulation (1,21). Left ventricular afterload is determined not just by arterial pressure, but by wall stress. Wall stress includes arterial pressure, LV radius and LV thickness; however, LV radius and thickness do not change acutely. As such, afterload can be considered just arterial pressure when performing acute cardiac measurements. Taken together, there are considerable breath-by-breath alterations in VR and \dot{Q} . However, when considering the entire respiratory cycle, VR and \dot{Q} are relatively constant at rest (12). Only in situations of exercise and disease do the breath-by-breath alternations become considerably more prominent.

1.1.2 Influence of Ventilation and Lung Volumes on Cardiac Function

During exercise, there is a progressive increase in ventilation that begins with a rise in tidal volume with modest decreases in end-expiratory lung volume below functional residual capacity

(due to increasing abdominal effort (12,13,34,35)) and larger increases in end-inspiratory lung volume reaching approximately 85-90% of total lung capacity once near maximal exercise (36). As exercise progresses, tidal volume will eventually plateau, therefore any further increases in ventilation will occur with a rise in breathing frequency (12,15,37). As such, lung volume changes at both rest and exercise can influence cardiopulmonary interactions in three main ways: 1) changes in autonomic tone (26), 2) pulmonary vascular resistance (PVR) (38), and 3) cardiac compression (39).

First, autonomic tone changes cyclically during a resting respiratory cycle as lung volume fluctuates (26). During eupnea, tidal volumes can range from 400-600mL and will alter sympathetic vasomotor outflow to skeletal muscle (i.e., muscle sympathetic nerve activity). Muscle sympathetic nerve activity decreases during inspiration and increases during expiration due primarily to the lung stretch receptors and arterial baroreceptors (40). The lung stretch receptors function to inhibit lung overdistention and will therefore fire more with inspiration and subsequently lower muscle sympathetic nerve activity (41). However, the lung stretch receptors may be inactive in adult humans unless tidal volumes exceed 1000mL such as during exercise, and this breath-by-breath modulation of muscle sympathetic nerve activity will continuously increase to approximately 60% peak power (W_{max}), but no further increases were observed at 80% W_{max} (40).

Second, the influence of lung volumes on PVR primarily depends on the degree of lung inflation (42). At rest, lung volumes fluctuate during inspiration and expiration, but tidal volume remains at ~ 500mL with ventilation ranging from ~5-8 L/min. During exercise, there is a greater oxygen demand and ventilatory requirement as more gas exchange is needed to meet the body's metabolic demands. As such, there are more frequent alternations in lung volume and greater

increases in ventilation (upwards of 90-120L/min) which can influence cardiopulmonary interactions independent of changes in ITP. Pulmonary vascular resistance is lowest at functional residual capacity and will increase as the lung volume deviates (26). Functional residual capacity describes a lung volume at the end of expiration during quiet breathing where the outward pull of the chest wall and inward recoil of the lungs is equal. Pulmonary vascular resistance increases at lung volumes below functional residual capacity due to extra-alveolar vessel collapse (26,38). Likewise, PVR increases at lung volumes above functional residual capacity because the elevated alveolar pressures can cause alveolar vessel compression and/or collapse (26,38,43,44). Pulmonary vascular resistance is substantially higher at lung volumes above functional residual capacity as alveolar vessel compression outweighs the effect of extra-alveolar vessel distention (38,45). When lung volumes are both above and below functional residual capacity, PVR and therefore right ventricular (RV) afterload will increase (2,39,46). As PVR increases, the pressure gradient between the RV and pulmonary circulation increases thereby impeding RV ejection (38). Since the right ventricular pressure remains the same, if PVR increases, there is a greater afterload placed on the RV and a larger pressure gradient required by the RV to open the pulmonary valve. As such, right ventricular end-systolic volume (RVESV) will rise and if VR remains constant, RVEDV will continue to increase, leading to a reduction in LV diastolic compliance. A reduction in LV diastolic compliance will occur via direct ventricular interaction or ventricular interdependence whereby the heart is limited in how much blood volume it can hold at a given time (due to the pericardium) (**Figure 2C**). Therefore, if RVESV increases, then the volume remaining in the RV may induce a leftward shift of the interventricular septum and limit how much the LV can fill during the subsequent beat (2,4,8,20,47).

A decrease in RV ejection and/or RVSV will cause a reduction in LV ejection and/or LVSV via series interaction (26) (**Figure 2B**). With respect to the healthy cardiovascular system, the right heart is relatively unaffected by changes in PVR as it has the capacity to overcome small increases in PVR (27). Specifically, during exercise, PVR usually decreases despite large increases in lung volume because of greater extra-alveolar vessel recruitment and distention as a result of an elevation in \dot{Q} (48). As \dot{Q} increases, there is more circulating blood available to return to the heart and be pumped to the lungs to become oxygenated. Therefore, with increases in pulmonary blood flow, pulmonary artery and pulmonary venous pressures will increase and potentially exceed alveolar pressure (41). When pulmonary artery and pulmonary venous pressure exceed alveolar pressure, this increases West's zone 3 lung condition which will promote increases in blood flow to the left atrium (LA) despite high end-inspiratory lung volumes (2,49). However, gravity is not the predominant factor in determining regional pulmonary blood flow distribution in upright individuals (50). Research in upright primates suggests that there is heterogeneity in blood flow distribution in an isogravitational environment and that these driving pressures of the typical hydrostatic column (John West lung zones concept) may not be entirely correct. Nonetheless, greater recruitment and distension of alveolar arterioles and capillaries will decrease PVR during exercise to accommodate the increase in \dot{Q} .

1.1.3 Influence of Abdominal Pressure, Volume Status and Venous Return on Cardiac Function

Volume status and abdominal pressure changes impact cardiopulmonary interactions primarily by contraction of the diaphragm, however, aspects such as body position (i.e., supine versus upright) can influence this as well. The diaphragm is the main respiratory muscle responsible for changes in lung volumes during quiet breathing (12,15). During a respiratory cycle, the diaphragm will contract downwards into the abdominal cavity during inspiration and will relax

upwards during expiration. As the diaphragm contracts, Pab will increase and this can compress the inferior vena cava (IVC) and decrease VR from the lower limbs (12,51) (**Figure 1B**). The IVC transverses through the tendinous portion of the diaphragm from the abdominal cavity into the thoracic cavity and is therefore exposed to Pab, diaphragmatic pressure (Pdi) and ITP (51). During inspiration, there is a more negative ITP and increased Pab which will enhance blood flow from the abdominal cavity towards the thoracic cavity, namely the abdomino-thoracic pressure gradient. However, whether there will be an increase in IVC flow and VR depends on volume status (49). Specifically, diaphragm descent promotes blood flow from the abdominal to thoracic cavity yet impedes blood flow from the lower limbs to the abdominal cavity (51,52). When Pab increases, IVC flow will increase until Pab becomes greater than IVC intraluminal pressure. Following this, the IVC will collapse (51) and flow will become zero (24). A 1-2cmH₂O increase in Pab above IVC intraluminal pressure is sufficient to collapse both the canine (53) and human IVC (18) and a 5cmH₂O increase in Pab above IVC intraluminal pressure can cause a complete cessation of VR from the lower limb circulation (17).

Volume status of the IVC is critical because when IVC blood volume is elevated, compression will increase relative VR (promoting more blood flow from the abdominal cavity towards the thoracic cavity). However, if IVC blood volume is low, compression will likely leave VR unchanged or decreased relative to the previous amount of blood flow back to the heart (52). Additionally, if IVC blood volume increases considerably, the pressure inside the IVC will prevent its collapse. Under normal circumstances, IVC blood volume is typically elevated prior to inspiration and low prior to expiration (12,51). When considering the impact of diaphragm descent on cardiopulmonary interactions, there are substantial breath-by-breath changes in VR. However, when considering VR over many respiratory cycles, VR is relatively unchanged at rest (17).

Moreover, during exercise, the abdominal wall will move outward as the abdominal muscles relax thereby causing P_{ab} to decrease during inspiration (12,54,55). Moreover, during strenuous exercise, P_{ab} can become negative during inspiration which will prevent IVC collapse and allow for increased systemic VR from the exercising lower limbs (12).

The primary mechanisms of enhancing VR during exercise are the respiratory pump and skeletal muscle pump. Venous return is largely dependent on pressures produced by both pumps as well as the capacitance and compliance of the venous vasculature (17,56). The veins are suited with one-way valves which facilitate a unidirectional flow of blood through the venous system. Therefore, when the peripheral muscles contract during exercise, this will cause compression of the intramuscular and surrounding veins to facilitate blood flow through the one way-valves and back to the heart (12,17,25,57,58). Conversely, the respiratory pump refers to the changes in ITP and RAP that promotes VR (17,25). The respiratory and skeletal muscle pumps work together to maximally enhance VR both at rest and during exercise. During exercise, there is an increase in diaphragmatic displacement during inspiration which will increase P_{ab} and the gradient for VR from the abdominal to thoracic cavity, while decreasing the gradient for systemic VR to the abdominal cavity (17,59). Despite this modest decrease in VR to the abdominal cavity when P_{ab} is elevated during inspiration, it is likely that the high intramuscular pressures associated with exercise, are able to overcome P_{ab} and enhance blood flow towards the thoracic cavity during inspiration or the subsequent expiration (17). Moreover, VR may be enhanced during exercise due to splanchnic vasoconstriction decreasing splanchnic blood flow (60) (**Figure 1B**). Contraction of the spleen may occur in times of stress so that erythrocytes can be deposited into the circulation in an attempt to improve oxygen transport and aerobic performance. Splanchnic contraction has been observed in animals (61) but remains controversial in humans, yet it appears that the spleen

regulates its volume based on the intensity of activity or stressor (62). As such, splanchnic vasoconstriction in conjunction with diaphragm descent and increases in P_{ab} may further increase VR during exercise (63,64). Taken together, cardiovascular function is enhanced rather than impeded during exercise (2).

1.2 Cardiorespiratory Interactions Differ with Exercise Intensity

Information regarding cardiorespiratory interactions and exercise intensity have been investigated in clinical populations such as chronic obstructive pulmonary disease (COPD) (65–68) and congestive heart failure (69), yet there is limited information examining healthy individuals. The cardiorespiratory interactions of clinical populations fail to translate to healthy individuals due to the physiological differences manifesting in pathology. For example, an individual with COPD and a healthy individual cycling at the same wattage on an ergometer (*e.g.* 50 Watts) will generate a similar \dot{Q} . However, for the COPD individual, this may be maximal \dot{Q} while only submaximal for the healthy individual. Individuals with COPD have different respiratory pressures than healthy individuals, thereby causing them to generally have a higher W_b . As such, a diseased individual with a high W_b and relatively low \dot{Q} will have different physiology compared to that of a healthy individual. Therefore, the cardiorespiratory interactions are not easily translatable between these two populations, making information regarding cardiopulmonary interactions in health during different exercise intensities limited.

Despite the lack of information regarding cardiopulmonary interactions and exercise intensity in health, there is substantial information regarding hemodynamic alterations in healthy individuals with differing exercise intensities. Generally, as exercise intensity increases, so too do most hemodynamic and metabolic variables (70). When transitioning from rest to submaximal intensity exercise, most variables (*i.e.*, heart rate (HR), oxygen consumption ($\dot{V}O_2$) and \dot{Q}) increase

and display a linear relationship with exercise intensity (71), while others eventually plateau as the body adjusts to the exercise demand (i.e., SV) (70). The relationship between \dot{Q} and $\dot{V}O_2$ is of particular interest as it differs between exercise intensities. At low-moderate exercise intensities (<50-70% $\dot{V}O_{2max}$), there is typically a 4-6L/min increase in \dot{Q} for every 1L/min increase in $\dot{V}O_2$ (72–80); however, this relationship may differ at high exercise intensities as a disproportionate relationship has been observed at maximal exercise (81), likely the result of a plateau in work. Additionally, at maximal exercise, the cardiovascular system becomes constrained and \dot{Q} is maximized as there is a plateau or reduction in SV at maximal exercise (82–92). The reasons for a reduction in SV are not fully elucidated, but could be the result of reductions in ventricular filling time, greater LV afterload, ventricular function, and venous return (93). As maximal exercise is achieved, HR will progressively increase to its maximum and this will decrease ventricular filling time, therefore RVEDV and LVEDV will decrease. Moreover, LVEDV does not appear to increase from moderate to maximum exercise (94) and has been observed to decrease when HR was increased with atrial pacing (95). When HR is increased above maximal during atrial pacing, $\dot{V}O_{2max}$ and exercise performance was not improved, thereby suggesting that HRmax and myocardial work capacity do not impair $\dot{V}O_{2max}$ at maximal exercise (96). Rather, it appears that LV filling is the primary factor of a reduced cardiac preload, SV and \dot{Q} at maximum exercise (96). Likewise, an increase in HRmax via atrial pacing caused a reduction in LV transmural filling pressure at all exercise intensities and increase RAP at high cycling intensities. Therefore, suggesting that a reduction in LV filling pressure decreases SV during atrial pacing and constricts \dot{Q} during maximal exercise (96).

Cardiorespiratory interactions differ greatly between rest and exercise primarily due to changes in intrathoracic pressures, lung volumes, and greater circulating blood volumes. When considering

cardiorespiratory interactions at different exercise intensities, current information is limited to studies investigating clinical populations which have physiology very different from that of healthy individuals. Moreover, with respect to cardiorespiratory interactions during mechanical ventilation, the current knowledge is limited to studies of patients in the intensive care unit (ICU) or animal studies. Individuals in the ICU are likely sedated, lying supine, and usually have some type of comorbidity, making the physiology between these individuals and those that are healthy, exercising, upright and spontaneously breathing very different. As such, translating knowledge of cardiorespiratory interactions from ICU studies to healthy, exercising individuals is challenging and unorthodox.

1.3 Cardiorespiratory Interactions During Mechanical Ventilation

Mechanical ventilation can be employed in different situations, such as when individuals require artificial ventilation to improve pre-existing respiratory and/or cardiovascular ailments, and functions to keep the body in a relatively stable state so as to allow the body to heal following surgery. Mechanical ventilation can alter cardiorespiratory interactions and can influence cardiac function and hemodynamic stability (1,3,4,26,97). The function of mechanical ventilation is to reduce the work of the respiratory muscles and maintain adequate alveolar ventilation which also decreases whole body oxygen consumption (1,21). There are many different forms of mechanical ventilation with the most common form being pressure support ventilation (PSV). Pressure support ventilation involves providing a positive airway pressure through an endotracheal tube or through an inspiratory line which causes air to flow into the lungs until the ventilator terminates the positive pressure. The influence of PSV on cardiopulmonary interactions can be divided into three main components: 1) ITP changes, 2) lung volume changes and 3) abdominal pressure changes.

The primary differences between PSV and spontaneous breathing are the differences in ITP swings and the energy required to produce them (1,19,21). Pressure support ventilation controls the patients respiratory efforts and provides a positive pressure during inspiration, thereby making ITP positive which is opposite compared to inspiration during spontaneous breathing (increasing negative pressure) (1,21). Since there is a positive ITP during inspiration with PSV, RAP will also be more positive which will decrease the pressure gradient and reduce VR (3,12,21,27) (**Figure 3**). As the pressure gradient for VR decreases with PSV, this may lead to an inspiratory reduction in transmural RAP and RVEDV which will cause a decrease in RVSV and LVEDV via series interaction (12,27). The reduction in VR associated with PSV can be mitigated by increases in Pab (26). Pressure support ventilation can impact LVEDV and subsequently LVSV by decreasing VR and/or decreasing LV diastolic compliance (27). Left ventricular diastolic compliance may be reduced with PSV if the lungs are being hyperinflated by the ventilator (does not usually happen), in which case, this can increase PVR and subsequently RV afterload and RVESV which will decrease LVEDV by a leftward septal shift (27,98). Moreover, PSV primarily acts to improve LV function. Since PSV mitigates the large negative ITP swings, LV afterload can decrease without reducing VR. Venous return will remain constant until ITP becomes positive (18,21,99,100). Left ventricular afterload will decrease with PSV, because if ITP becomes positive and arterial pressure remains constant (due to baroreceptors and/or medication), then transmural LV pressure and thus LV afterload will decrease (1,3,21,26,28,29,101) (**Figure 3**). However, if RVSV decreases, then LVSV will also decrease via series interaction which will in turn cause a reduction in \dot{Q} and MAP will decrease. The opposite is true, as ITP becomes more negative (as with spontaneous breathing), LV afterload will increase (1,21,26,28,29).

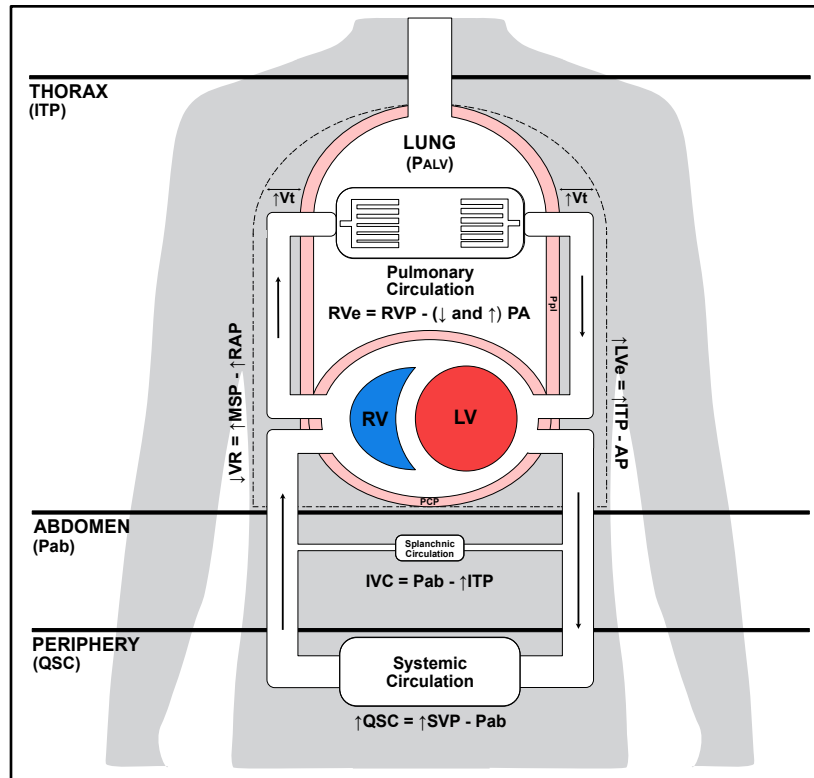


Figure 3. Cardiorespiratory interactions during mechanical ventilation and exercise. Pressure support ventilation (and proportional assist ventilation) will attenuate intrathoracic pressure (ITP) changes by providing a positive airway pressure during inspiration. With smaller ITP changes, right atrial pressure (RAP) will not change as much, therefore the pressure gradient for venous return (VR) is reduced. However, mean systemic pressure (MSP) is elevated due to skeletal muscle activity in the periphery. Since tidal volume (V_t) increases with exercise, pulmonary vascular resistance (PVR) and pulmonary artery pressure (PA) will increase. However, with exercise there is greater recruitment and distention of the pulmonary capillaries which will decrease PVR and PA. The elevated ITPs will enhance left ventricular ejection (LVE) as the left ventricle (LV) will not have to generate as high of pressures to pump blood into the aorta (transmural pressure is reduced). P_{ALV} , alveolar pressure; P_{ab} , abdominal pressure; QSC, systemic circulation blood flow; RVe, right ventricular ejection; RVP, right ventricular pressure; RV, right ventricle; AP, arterial pressure; IVC, inferior vena cava; SVP, systemic venous pressure. Modified from: Cheyne WS, Harper MI, Gelinas JC, Sasso JP, Eves ND. Mechanical cardiopulmonary interactions during exercise in health and disease. *J Appl Physiol Bethesda Md* 1985. 2020 May 1;128(5):1271–9.

Alterations in lung volumes with PSV depends on the tidal volume provided by the mechanical ventilator. Pressure support ventilation can either increase or decrease PVR. When PSV is applied to enhance alveolar recruitment in order to increase the partial pressure of alveolar oxygen, PVR and RV afterload will decrease and enhance RV ejection (1,26,27). Conversely, in

certain disease states where alveolar ventilation is considerably low, positive end-expiratory pressure ventilation can be used to keep the airways open rather than collapse during expiration. However, ventilatory methods such as high positive end-expiratory pressure and large tidal volume ventilation can increase PVR by compressing the pulmonary vasculature due to a high airway pressure (P_{aw}) (1,27,101–103). Furthermore, severe lung hyperinflation may mechanically limit LV filling and subsequently decrease LVSV via direct ventricular interactions due to pericardial constraint (2,47,104).

Like spontaneous breathing, PSV will inflate the lungs, compress the abdominal compartment via diaphragmatic descent and increase P_{ab} (21,52,105). As the diaphragm descends, P_{ab} will increase thereby translocating the large intra-abdominal blood volume towards the thorax. This central translocation of blood will maintain VR. As such, VR may not be reduced as much during PSV (18,21,99,100). The translocation of blood centrally is the primary mechanism of mitigating alterations in VR with PSV (26). However, this is only applicable at rest since blood is distributed peripherally during exercise and there is a reduction in abdominal blood volume. Overall, both positive and negative inspiration (PSV and spontaneous breathing, respectively) can impact preload by increasing VR from the abdominal vasculature by an increase in P_{ab} due to diaphragmatic descent (1,52,105).

1.4 Techniques Used to Study Cardiorespiratory Interactions

To study cardiopulmonary interactions, researchers have increased and decreased the magnitude of ITP swings to investigate the hemodynamic response. By altering the magnitude of ITP swings, the amount of work the respiratory muscles must perform to inflate the lungs, namely the work of breathing (W_b) will also change (1). Conversely, studies aiming to reduce the W_b can observe an attenuation of ITP swings as a result.

To increase the W_b , researchers have added resistive loads to the breathing circuit or have had participants breathe through smaller tubes (2,106–109). Adding resistive loads to the breathing circuit functions to decrease the cross-sectional area of the inspiratory or expiratory line, thereby increasing resistance to airflow (106,107). Moreover, the high W_b associated with COPD can be experimentally mimicked by generating large negative ITP swings, inducing dynamic hyperinflation (with added expiratory resistance) and hypoxic-mediated increases in PVR (106). Both techniques increase the W_b and induce large negative ITP swings (27), which will cause RAP to become less positive (closer to 0cmH₂O). Venous return can become flow-limited as the IVC collapses in the intrathoracic domain and remains open in the extrathoracic domain (18,110). Once VR becomes flow-limited, continuing to increase the more negative ITP will not improve venous flow compared to that of less negative ITP, it will only enhance LV afterload and impede LV ejection (4).

To study the hemodynamic responses to a reduction in W_b , researchers have had individuals inhale heliox (111–115) or breathe on a proportional assist ventilator (PAV) (116–118). Compared to atmospheric air (~21% oxygen and 79% nitrogen), heliox is a gaseous mixture in which nitrogen has been replaced with helium as an inert backing gas. Helium is less dense than nitrogen, thereby promoting more laminar air flow and thus decreasing the resistive component of the W_b (111,119). However, the total W_b consists of both elastic and resistive components. The elastic component involves the work required to changes the shape of the chest wall during inspiration and expiration, while the resistive component involves the work required to overcome the resistance to airflow in the airways (120). As such, heliox only reduces one component of the total W_b (resistive component). Therefore, the elastic component of the W_b will not be impacted by heliox and will continue to be elevated during both inspiration and expiration (121). Moreover, the effectiveness

of heliox is flow dependent and will alter the W_b differently for different flows. Therefore, heliox is less effective at rest and at low exercise intensities with its effect being amplified at high exercise intensities because of the higher flows (120). To provide a more uniform reduction in the W_b , researchers have used proportional assist ventilation.

1.5 Proportional Assist Ventilation to Unload the Respiratory Muscles

Proportional assist ventilation is unique compared to conventional mechanical ventilation (i.e., pressure support ventilation) in that it can be used in spontaneously breathing humans during dynamic exercise (117) and works by generating a positive mouth pressure (P_m) during inspiration. The positive P_m reduces the magnitude of change in ITP required by the inspiratory muscles and subsequently decreases the energetic W_b (122). Proportional assist ventilation is a non-invasive form of positive pressure mechanical ventilation that relieves the work of the respiratory muscles and reduces the W_b during exercise (120,123). The PAV can be used at both rest and exercise and provides a positive inspiratory pressure in proportion to the magnitude of the initial inspiration from the spontaneous breathing individual and functions on a continuous basis. The PAV was originally designed to help wean patients off of conventional mechanical ventilators. Proportional assist ventilation is unique in that it allows an individual to maintain control over all aspects of breathing (i.e., pressure, volume, timing) (121) while amplifying the individual's breathing efforts.

The proportional assist ventilator uses the equation of motion to determine the level of ventilatory assistance. During spontaneous breathing, the total pressure applied to the respiratory system is solely from the respiratory muscles (P_{mus}) and is the sum of the elastic, resistive and inertial components. The elastic component is the product of lung volume (V) and elastance (E),

the resistive component of flow (\dot{V}) and resistance (R), and the inertial component is the product of gas acceleration (\ddot{V}) and inertance (I), this is described in equation 1:

$$\text{Eq 1. } P_{\text{mus}} = V_E + \dot{V}R + \ddot{V}I$$

The PAV provides a positive airway pressure in proportion to the inspiration initiated by the individual and the level of assist can be manipulated. As such, when breathing on the PAV, the total pressure applied to the respiratory system involves the respiratory muscles (P_{mus}) and the positive airway pressure produced by the PAV (P_{aw}), this is denoted in equation 2:

$$\text{Eq 2. } P_{\text{mus}} + P_{\text{aw}} = V_E + \dot{V}R + \ddot{V}I$$

Of note, the inertial component is negligible at ventilations below ~ 70 breaths min^{-1} as the inertia of the respiratory system is not enough to contribute to the pressure applied to the respiratory system. Moreover, as mentioned previously, the PAV functions to amplify individual effort. Therefore, if the PAV was set to 50% assist, the individual would have to contribute 50% of the total work. Essentially, the PAV functions to unload the respiratory muscles and reduce the W_b such that for a given ventilation, an individual breathing on the PAV would have to do less work than an individual during unloaded breathing.

1.6 Implications of Respiratory Muscle Unloading on Cardiac Output and Oxygen Consumption

Cardiac output has a finite rate that is typically achieved at maximal exercise (124), at which point vital organs (*e.g.* brain, lungs) and exercising muscles will compete for blood flow. As exercise progresses and respiratory muscle work increases, more blood flow will be redistributed to the respiratory muscles and away from the working skeletal muscles (via the respiratory metaboreflex). The concept of ‘competing’ for cardiac output during exercise has been studied both at submaximal and maximal exercise intensities. During maximal exercise, respiratory muscle

$\dot{V}O_2$ is ~ 10-15% of $\dot{V}O_{2max}$ (125) and ~ 14-16% of \dot{Q} is redistributed to the respiratory muscles to support the high metabolic demands and tissue beds will compete for blood flow via sympathetically mediated vasoconstriction (126). This competition for \dot{Q} does not exist at submaximal exercise intensities because \dot{Q} has not yet become limited or maximized (in health).

When respiratory muscle work and the W_b is minimized, $\dot{V}O_2$ is significantly reduced compared to that of control and loaded breathing (127). As such, less blood flow will be distributed to the respiratory muscles and more will be available to the working skeletal muscle and exercise performance and capacity can be enhanced (127). Moreover, at maximal exercise during respiratory muscle unloading, \dot{Q} decreased disproportionately to a decrease in $\dot{V}O_2$ (126). The disproportional relationship observed between \dot{Q} and $\dot{V}O_2$ is of particular interest as $\dot{V}O_2$ and \dot{Q} typically have a proportional relationship. Oxygen consumption is expected to decrease since the respiratory muscle work is lower and therefore the metabolic demand is lower during unloaded breathing, yet \dot{Q} decreased more than it should have (126). It was suggested that the reduction in \dot{Q} was the result of a decline in SV, which was likely due to: 1) a reduction in metabolic demand, 2) an increase in PVR and 3) the less negative ITPs associated with the PAV. Since the PAV provides a positive Paw during inspiration, the attenuated ITP changes can reduce VR and subsequently LV preload and SV (126). Moreover, the positive airway pressure generated by the PAV functions to increase PVR which can increase RV afterload and impede RV ejection and subsequently LVSV via series and direct ventricular interactions (126). However, the study did not measure ITP or investigate changes in cardiac volumes during respiratory muscle unloading.

2.0 STUDY RATIONAL

At maximal exercise during respiratory muscle unloading, $\dot{V}O_2$ and \dot{Q} decreases, yet \dot{Q} decreases disproportionately to a reduction in $\dot{V}O_2$ (126). The proposed mechanisms as to why this occurs during respiratory muscle unloading is suggested to be the result of a reduction in metabolic demand, changes to intrathoracic pressure (from the PAV) and increases in pulmonary vascular resistance, yet the direct mechanism(s) responsible for this remains unknown. As such, the aim of this study was to investigate how respiration influences cardiac function and to directly determine how \dot{Q} may be influenced with respiratory muscle unloading. Since previous work has investigated maximal exercise, the aim of this study was to determine if \dot{Q} is impacted differently at different exercise intensities. Therefore, unloading the respiratory muscles allows for the investigation of ‘normal’ cardiac function with minimal respiratory influence because if ‘normal’ cardiac function is not understood, then effectively treating ‘abnormal’ or disease states becomes considerably difficult.

3.0 RESEARCH QUESTIONS AND HYPOTHESES

Research Questions:

1. Does respiratory muscle unloading alter cardiac output at different exercise intensities?
2. If cardiac output changes, are these changes due to HR, SV or $\dot{V}O_2$?

Hypotheses:

1. Cardiac output will be reduced at all exercise intensities with respiratory muscle unloading relative to spontaneous breathing.
2. Cardiac output will decrease at low and moderate exercise intensities (30% and 60% W_{max}), primarily by reductions in SV and HR. At high intensity exercise (80% W_{max}), cardiac output will decrease due to both reductions in HR and SV as well as decreases in $\dot{V}O_2$.

4.0 METHODS

4.1 Ethics

The experimental procedures for this study have been approved by the Clinical Research Ethics Board at the University of British Columbia (CREB #H20-01210) and the Office of Research Ethics at the University of Waterloo (ORE #43421). The research methods and protocols adhere to the recommendations outlined by the *Declaration of Helsinki* concerned with the use of human participants, except for registrations in a database.

4.2 Participants

The sample size of this study was 13 participants; 7 males and 6 females. Sample size was calculated prior to testing using a repeated measures analysis of variance (ANOVA) using G*Power 3.1.9.6. A sample size of n=20 was determined based on an effect size of 0.86 that was determined from a study that investigated cardiorespiratory interactions with augmented intrathoracic pressures in healthy participants (109).

Participants were young healthy adults between the ages of 18-40 years with no known respiratory or cardiovascular conditions to effectively investigate healthy cardiorespiratory responses to respiratory muscle unloading. Table 1 outlines the specific inclusion and exclusion criteria for the participants.

Table 1. Participant inclusion and exclusion criteria.

Inclusion Criteria	Exclusion Criteria
<ul style="list-style-type: none">• Age: 18-40 years• Language: Fluent in English• Active: 3+ days per week for 30+ minutes• Normal pulmonary function	<ul style="list-style-type: none">• Smoker• Obesity: BMI >30kg/m²• Females: Pregnant or nursing• Allergies: latex and lidocaine• Cardiovascular disease• Respiratory disease• Gastrointestinal disease• Diabetes• Chest wall disorders• Asthma (includes exercise-induced)• Hypertension• Recent nose/throat surgery• Arthritis• Esophageal ulcers or tumors

4.3 Experimental Overview

All participants completed three testing days. Day one consisted of screening, pulmonary function testing and a $\dot{V}O_2$ max test to determine subsequent workloads. Day two consisted of familiarizing participants with equipment that will be used and day three consisted of the experimental protocol. A description of the procedures conducted on each day is detailed below.

4.3.1 Day One: Screening, pulmonary function testing and $\dot{V}O_2$ max test

Day one of testing began with participant screening followed by pulmonary function testing. Measurements taken included forced vital capacity, forced expiratory volume in 1 second (FEV₁), %FVC expired in FEV₁, forced expiratory flow at 25-75% of expiration, 12 second maximal voluntary ventilation and full body plethysmography to measure absolute lung volumes. These measures conformed to ATS standardization (128,129) and were compared to reference values. Pulmonary function measures were completed to ensure that the participants do not have any obstructive lung diseases (i.e., asthma).

Participants performed a 15-minute self-selected warm up on a modified semi supine cycle ergometer. Next, participants performed a $\dot{V}O_{2\max}$ test. All participants began the $\dot{V}O_{2\max}$ test at 100 Watts and increased by 20 Watts every 2 minutes.

4.3.2 Day Two: Familiarization

Day two of testing was used to ensure the participants were sufficiently familiarized with both the PAV and the cardiac ultrasound imaging positions. The participants cycled on the same modified ergometer as day one at a low intensity while breathing on the PAV. Participants also practiced finding the most comfortable position for their left arm, as this arm was required to be placed behind the participants head to obtain the most accurate cardiac images.

4.3.3 Day Three: Experimental Protocol

Day three of testing consisted of the experimental protocol. Participants began day three with instrumentation, including an esophageal and gastric balloon catheter placed into the participants. Next, a 15-minute rest period to obtain resting cardiac ultrasound images and resting heart rate was collected. Participants performed a 15-minute warm up on the same modified ergometer as day one and two. Participants then began the experimental protocol, the protocol consisted of each participant completing a series of exercise trials at three different exercise intensities: 30%, 60% and 80% W_{\max} . The order of exercise intensities was not randomized (so as to avoid any sympathetic carry over effects) and occurred in a successive order from low to high exercise intensity. For each exercise intensity, participants performed both control (spontaneous breathing) and respiratory muscle unloading trials (PAV/unloaded breathing) (120). Each exercise intensity trial was continuous and lasted approximately 12-15 minutes. The first three minutes ensured the participant reached a steady state. The remaining minutes consisted of ~3-5 minutes of control, 3-5 minutes of PAV, and 3-5 minutes of control. Between the continuous exercise trials, participants

had ~15 minutes of rest or until their heart rate fell to resting values (± 10 beats pre-exercise HR) (**Figure 4**). All trials were completed at a cadence between 60-70 rpm to standardize cadence and ensure quality of the cardiac images. Echocardiography measurements were taken during the duration of all exercise trials.

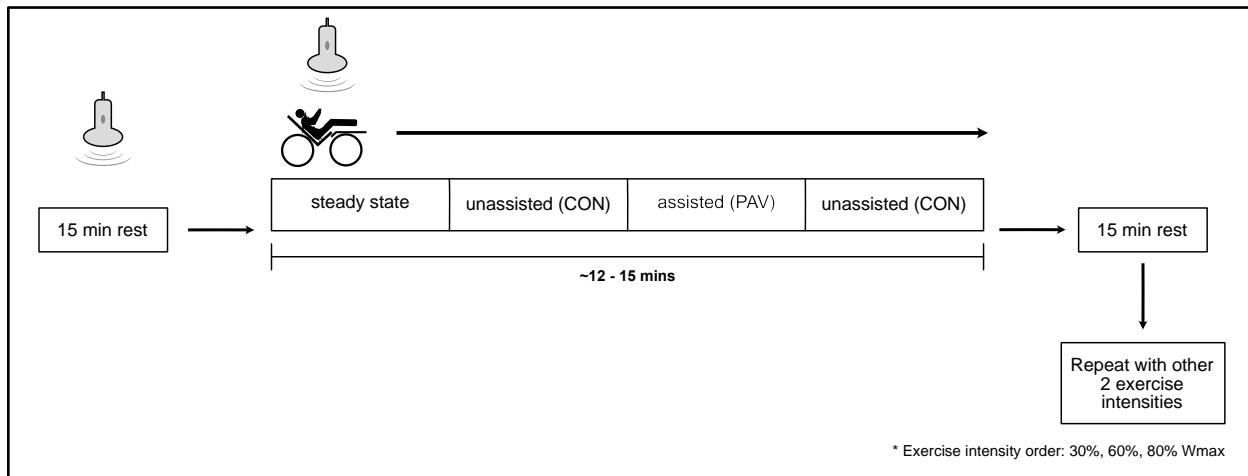


Figure 4. Schematic of day 3 experimental protocol.

4.4 Data Collection

4.4.1 Respiratory Flow and Volume

Raw data was recorded at 200 Hz with a 16-channel analog-to-digital data acquisition system (PowerLab/16SP model ML 795; ADInstruments, Colorado Springs, CO). Inspiratory and expiratory flow was continuously measured by having participants breathe through the mouthpiece, which was attached to two pneumotachographs located on either end of the breathing circuit connected to the proportional assist ventilator. The expired pneumotach was heated to 37°C while the inspired was kept at room temperature. Both pneumotachs were calibrated using room air and a 3-L syringe. Mixed-expired gases were sampled from the mixing chamber from a sample line connected to calibrated oxygen (O₂) and carbon dioxide (CO₂) analyzers (AEI Technologies S-3-A/I and CD-3Am, respectively; Applied Electrochemistry, Bastrop, TX) during the duration of the experimental protocol to allow for the calculation of $\dot{V}O_2$ and carbon dioxide output ($\dot{V}CO_2$). All

collected gas was dried using nafion tubing inside a sealed glass jar filled with Drierite to ensure the gases contain 0% humidity prior to entering the gas analyzers. End-tidal CO₂ was sampled at the mouth using a sample line connected to a CO₂ analyzer (VacuMed; Ventura, CA). End-tidal gas was dried using a separate glass jar containing Drierite to ensure end-tidal gases contain 0% humidity prior to entering the gas analyzer.

Heart rate was measured using two 3-lead electrocardiograms (one for ultrasound and one for LabChart) throughout the duration of the experiment.

Photoelectric plethysmography (Human NIBP Nano Interface, ADInstruments) was used to non-invasively measure blood pressure. A blood pressure cuff was placed on the participants' middle finger on their right hand to collect beat-by-beat blood pressure during the duration of the exercise protocol (Day 3). Prior to testing, the correct cuff size was determined using the finger cuff guide provided by ADInstruments. The height correction unit was used to account for height changes of the finger and calibrated prior to use.

4.4.2 Intrathoracic/intrabdominal Pressure Surrogate (Esophageal/Gastric Pressure)

A topical anesthetic (Xilocaine®, Lidocaine Hydrochloride) was applied to the subject's nares and nasal conchae before passing a balloon catheter (Ackrad Laboratories Inc., Cranford, NJ) through the nose. One balloon was positioned in the lower third of the esophagus, the other balloon was positioned at the entry of the stomach (gastric pressure). Participants were asked to perform a brief Valsalva manoeuvre while the catheters were open to the atmosphere to empty the balloons and then 1 mL (esophageal balloon) or 2 mL (gastric balloon) of air was administered into the balloon using a glass syringe. The validity of each balloon's position was assessed using a dynamic occlusion test before being secured in place. The balloon catheters were connected to two separate differential pressure transducers (DP45-34, Validyne Engineering, Northridge, CA USA).

Mouth pressure was measured at the mouth via a sample line connected to a differential pressure transducer (DP45-34, Validyne Engineering, Northridge, CA USA). The signal from all pressure transducers was converted to a digital signal using a data acquisition system (PowerLab/16SP) and sampled at 200Hz. All pressure transducers were calibrated at baseline and before and after each test using a digital manometer (2021P, Digitron, Torquay UK).

4.4.3 Echocardiography

Echocardiographic images of the heart were acquired by a trained individual in accordance with current guidelines (130), and recorded on a commercially available ultrasound system (Vivid iq; GE Healthcare) using a M5Sc-RS Phased Array Transducer 1.5-4.6 MHz probe for 2D imaging. Echocardiographic images were recorded at end-expiration to mitigate the lateral displacement of left ventricular structures due to respiration. All images were acquired at rest and during exercise on a semi-recumbent cycle ergometer where participants had their upper body shifted leftwards so as to simulate a left lateral decubitus position. The leftwards shift functioned to bring the heart closer to the chest wall and slightly left of the sternum to make for optimal cardiac windows. All participants were given the opportunity to wear an ultrasound gown that covers part of the chest but allows access to the center and left side of the chest. Echocardiographic windows included apical views obtained from the left lateral window along the 4-6th intercostal space for the assessment of left ventricular end-diastolic volume, left ventricular end-systolic volume, stroke volume and cardiac output (130). To image the apex of the heart, the probe was placed between the 4-6th intercostal space with the footprint of the transducer facing upwards (towards the participants head) to visualize the apical 4-chamber view with a focus on the left ventricle. Additionally, apical 2-chamber views were obtained by placing the probe in the same position as the apical 4-chamber view but rotating the probe 90° in a counter-clockwise direction. Apical 2-

and 4-chamber image acquisition was used to maximize left ventricular areas and avoid foreshortening of the left ventricle which would result in an underestimation of left ventricular volumes (130). The sonographer followed established protocols for optimizing left ventricular length and avoiding foreshortening by moving the probe between adjacent rib spaces to compensate for any chest wall movement during cardiac imaging (130). Moreover, during image acquisition, the ultrasound settings were optimized to include the entire left ventricular endocardial border and excluded additional structures that were not assessed.

Data was recorded and stored for offline analysis (EchoPAC, GE Medical, Horton, Norway), which included the quantification of left ventricular end-diastolic volume, left ventricular end-systolic volume, stroke volume and cardiac output. The acquisition of cardiac images in both males and females during exercise has been completed successfully and safely by the trained sonographer that performed the measurements in the present study (131,132).

4.4.4 Manipulation of Intrathoracic Pressure

During the experimental day (Day 3), intrathoracic pressure was attenuated through the use of the PAV. The PAV functions to add additional compressed room air to the inspired circuit during inspiration. The amount of air and the timing will be determined using the equation of motion incorporated into customized software that triggers a proportional solenoid valve. The pressure at the mouth will be maintained at <15 cmH₂O, as measured by a manometer port in the mouthpieces, via both software control and physical release valves. This level of P_m is less than what is commonly incurred by individuals using a non-invasive sleep apnea support devices, for extended periods (>1 hr) and does not cause ill effects. The addition of the air to the circuit results in the respiratory muscles not having to work as hard during normal exercise hyperpnea. Moreover, the use of the term “unloaded breathing” in the present study is referring to the PAV unloading the

respiratory muscles and therefore making it easier for the participant to breath while on the PAV. The term “unloaded breathing” is referring to the unloading of the respiratory system and not the cardiovascular system.

4.5 Data Analysis

4.5.1 Respiratory Flow and Volume

The measured flow from the inspiratory pneumotach was numerically integrated to determine volume which allowed for the determination of both tidal volume and breathing frequency. Inspiratory ventilation was calculated as the product of tidal volume and breathing frequency which was converted into expiratory ventilation using the Haldane transformation, both are expressed in body temperature pressure saturated. Inspiratory and expiratory volumes were determined by numerical integration of inspiratory and expiratory flow, respectively. Oxygen consumption was determined by taking the difference between the inspired and expired oxygen using inspiratory ventilation and expiratory ventilation. Both $\dot{V}O_2$ and $\dot{V}CO_2$ were expressed in standard pressure temperature dry. Metabolic variables such as $\dot{V}O_2$, $\dot{V}CO_2$ and respiratory exchange ratio (RER) were analyzed in 30-second sections during the PAV and POST trials and compared with each other. Additionally, ventilatory data was analyzed at the time when the apical four and two chamber views of the heart were taken.

4.5.2 Heart Rate and Blood Pressure

Heart rate was analyzed from the R-R interval measured from the electrocardiogram connected to LabChart. Systolic blood pressure (SBP) and diastolic blood pressure (DBP) were derived from pulse pressure measured beat-to-beat via photoelectric plethysmography. Mean arterial pressure (MAP) was calculated via measurements collected via photoelectric plethysmography based on the equation 3:

$$\text{Eq 3. MAP} = [\text{DBP} + 1/3(\text{SBP}-\text{DBP})]$$

Heart rate, MAP, SBP, and DBP were analyzed in 30-second sections during the PAV and POST stages of each exercise intensity and compared with each other. Additionally, heart rate was analyzed at the time when the apical four and two chamber views of the heart were taken. Lastly, total peripheral resistance (TPR) was determined by dividing cardiac output from MAP.

4.5.3 Pressure

The maximal, minimal, means and magnitudes of esophageal, gastric, mouth and Pdi were analyzed during the PAV (unloaded) and spontaneous (POST) trials of the experiment. Pressures were analyzed at the time when the apical four and two chamber views of the heart were taken (~30-second sections) during the PAV and POST trials and compared with each other. Diaphragmic pressure was determined by calculating the difference between esophageal and gastric pressure.

4.5.4 Echocardiography

Data processing and analysis for the echocardiography measurements was recorded and stored for offline analysis (EchoPAC, GE Medical, Horton, Norway). Echocardiography measurements were recorded (Vivid iq; GE Healthcare) using a M5Sc-RS Phased Array Transducer 1.5-4.6 MHz probe for 2D imaging. Echocardiographic images acquired from the apical views obtained from the left lateral window along the 4-6th intercostal space were used for the assessment of left ventricular end-diastolic volume, left ventricular end-systolic volume, stroke volume and cardiac output using the Simpson's biplane method. The apical view of the heart provided two different images: 1) an apical 4-chamber view and 2) an apical 2-chamber view. The apical 4-chamber image provides views of the left atrium, left ventricle, right atrium and right ventricle, while the apical 2-chamber image provides views of the left atrium and left ventricle. The Simpson's biplane

method was used to determine left ventricular end-diastolic volume and left ventricular end-systolic volume in the apical 2- and 4-chamber views. The Simpson's biplane method involves manually tracing the left ventricular endocardial border. Tracing began at the mitral valve level closest to the interventricular septum and ended at the other side of the mitral valve closest to the left ventricular posterior wall. The trace was closed by connecting the two opposite sides of the mitral valve with a straight line. Left ventricular stroke volume was determined by taking the difference between left ventricular end-diastolic volume and left ventricular end-systolic volume ($SV = LVEDV - LVESV$).

An electrocardiogram (ECG) was connected to the ultrasound and used to produce an ECG trace on all cardiac images. The ECG trace was used to time the beginning and end of systolic ejection. End-diastole was identified by the frame with the largest left ventricle size immediately following mitral valve closure. End-systole was identified by the frame with the smallest left ventricle size immediately prior to mitral valve opening. Endocardial border tracing of end-diastolic and end-systolic images was performed according to the American Society of Echocardiography recommendations to measure left ventricular stroke volume ($LVSV = LVEDV - LVESV$) and cardiac output ($\dot{Q} = HR * SV$)(130).

Five consecutive cardiac cycles were recorded across several respiratory cycles. A respiratory trace was applied to all cardiac images to identify the phase of the respiratory cycle that corresponds to the cardiac cycles that were analyzed. For standardization purposes, all cardiac images were analyzed during expiration. Analysis of cardiac images at end-inspiration can be difficult and image quality can be low due to high lung volumes. As such, all cardiac analysis occurred during expiration as identified by the respiratory trace.

The Simpson's biplane method was used to assess left ventricular stroke volume and cardiac output for each stage (PAV and POST) during each exercise intensity (30%, 60%, and 80% W_{max}). The Simpson's biplane method involved analyzing an apical 2- and 4-chamber view of the heart at end-diastole and end-systole which provided an assessment of left ventricular end-diastolic volume and left ventricular end-systolic volume ($LVSV=LVEDV-LVESV$). The Simpson's biplane method was performed over three different cardiac cycles, if the measurements of stroke volume differed by $>10\%$, an additional cardiac cycle was analyzed. For each cardiac cycle analyzed, one stroke volume (Simpson's biplane method) and heart rate (ECG connected to ultrasound) value were obtained. To determine cardiac output, the three stroke volume values were averaged to get one stroke volume value, and the three heart rate values were averaged to get one heart rate value. Next, the single stroke volume and heart rate value were multiplied to determine cardiac output for the given stage and exercise intensity. For standardization purposes, all stroke volume analysis was conducted during expiration as identified by the breathing trace on the cardiac images. Cardiac output was determined for each stage (PAV and POST) during each exercise intensity (30%, 60%, and 80% W_{max}). Moreover, sex differences were not investigated as it was not the purpose of this thesis.

4.5.5 Work of Breathing

The work of breathing was calculated using oesophageal pressure–volume loop integration and inspiratory force was inferred using oesophageal and diaphragmatic pressure–time products (PTP) (123). Esophageal pressure (P_{es}) was used instead of transpulmonary pressure because transpulmonary pressure would be overestimated due to the high P_m from the PAV. The area within the pressure-volume loop was integrated and the sum was multiplied by breathing frequency. Since end-inspiratory can exceed end-expiratory pressure with the PAV, partitioning

the W_b into its elastic and resistive components was not possible. Moreover, pressure-time products were used to determine inspiratory and expiratory work. Esophageal and Pdi was integrated with respect to time throughout inspiration to determine inspiratory work. Gastric pressure was integrated with respect to time during expiration to determine expiratory work. The method of assessing the work of breathing was selected because Campbell diagrams and integrating transpulmonary pressure–volume loops are not valid during assisted ventilation because lung volumes cannot be determined (*e.g.* PAV) (120).

4.6 Statistical Analysis

Statistical analyses were conducted using GraphPad Software (Version 8.2.1). To determine if \dot{Q} decreased with respiratory muscle unloading, a dependent samples t-test was conducted to compare the PAV and POST conditions at each exercise intensity separately (30%, 60%, 80% W_{max}). The dependent samples t-tests were performed separately because there was no \dot{Q} data for one participant at 80% W_{max} . Therefore, to avoid violating the assumption of an ANOVA, dependent samples t-tests were completed separately for each exercise intensity.

One-way repeated measures ANOVAs were conducted to determine if there was a difference between the relative (percent) and absolute change (POST to PAV) between exercise intensities for all variables. Participants with a missing value for a variable at a given exercise intensity were removed from the ANOVA.

To determine if HR, SV and $\dot{V}O_2$ changed with respiratory muscle unloading, a dependent samples t-test was conducted for each of the above variables to compare the PAV and POST conditions for each exercise intensity separately. Moreover, dependent samples t-tests were completed for all ventilatory, W_b , metabolic, and respiratory pressure data to determine the difference between the PAV and POST breathing condition for each exercise intensity. All

dependent samples t-tests were conducted only if the assumption of normality (Shapiro-Wilk test) and homogeneity of variances (Levene test) were met. If the aforementioned assumptions were violated, then the Wilcoxon Signed Rank test (non-parametric equivalent) was completed.

Repeated measures correlations were used to examine the relationship between \dot{Q} and $\dot{V}O_2$, and between cardiovascular variables and the magnitude of ITP swings within each participant to compare the PAV and POST conditions for each exercise intensity (to address the violated assumption of independence). The repeated measures correlations were conducted using R (Version 4.0.3) (R library: rmcrr).

Lastly, Pearson Product Moment correlations were conducted to determine the relationship between the absolute change in \dot{Q} and the change in $\dot{V}O_2$. The difference between the PAV and POST conditions for \dot{Q} and $\dot{V}O_2$ (deltas) were examined for each exercise intensity. If the assumption of normality was violated, then a Kendall-Tau correlation (non-parametric equivalent) was conducted. For all statistical tests, significance was set at $p < 0.05$.

5.0 RESULTS

5.1 Participant Demographics and Baseline Data

A total of 13 participants (n= 7 males, n= 6 females) completed this study. Demographic and baseline data are presented in **Table 2**.

Table 2. Participant demographics and baseline data.

Variable	All Participants	Males	Females
Age (years)	25 ± 4	24 ± 4	25 ± 3
Height (cm)	174.8 ± 8.6	179.7 ± 6.1	169.1 ± 7.7
Weight (kg)	71.2 ± 11.1	75.7 ± 10.2	66.0 ± 10.5
BMI (kg/m ²)	23.2 ± 2.2	23.3 ± 2.2	22.9 ± 2.4
HR (bpm)	67.7 ± 10.2	65.1 ± 10.7	70.6 ± 9.7
LVEDV (mL)	137.9 ± 29.2	147.3 ± 27.5	127.0 ± 29.6
LVESV (mL)	59.9 ± 18.8	66.9 ± 21.3	51.8 ± 12.5
SV (mL)	77.9 ± 13.6	80.4 ± 7.9	75.2 ± 18.7
EF (%)	57.3 ± 5.4	55.7 ± 6.6	59.2 ± 3.3
Q̇ (L/min)	5.2 ± 0.6	5.2 ± 0.6	5.2 ± 0.7

Abbreviations: BMI, body mass index; HR, heart rate; LVEDV, left ventricular end-diastolic volume; LVESV, left ventricular end-systolic volume; SV, stroke volume; EF, ejection fraction; Q̇, cardiac output. Values are reported as mean ± SD.

5.2 Respiratory Muscle Unloading and Work of Breathing

5.2.1 Evidence of Respiratory Muscle Unloading via Proportional Assist Ventilation

During respiratory muscle unloading, the PAV elevated Pm which allowed Pes to decrease despite achieving a similar ventilatory output. Esophageal and Pdi were attenuated during unloaded (PAV) relative to spontaneous (POST) breathing (**Figure 5**). **Figure 5** shows representative respiratory pressures and flow data for one male subject at 80% Wmax. Group data displaying mean Pes and gastric pressure (Pgas) as well as the magnitude of Pes and Pdi swings are shown in **Figure 6**.

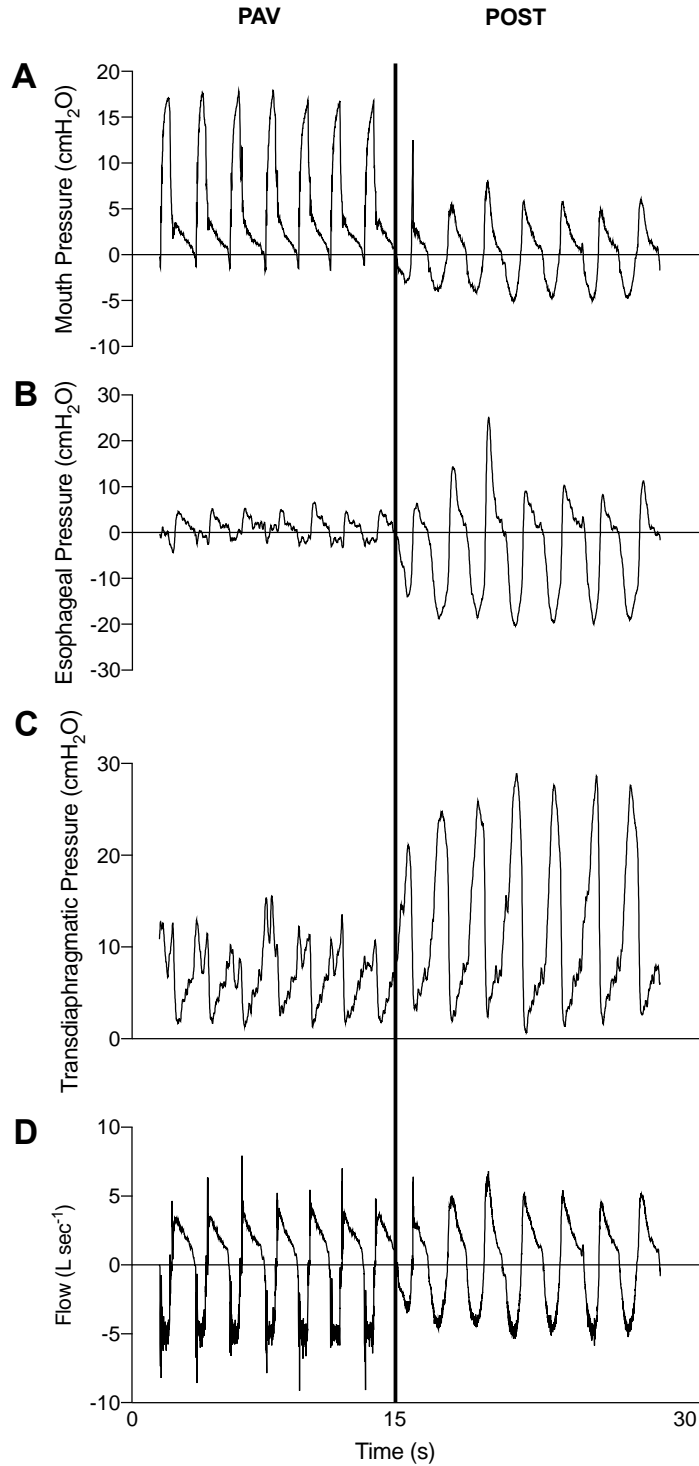


Figure 5. A raw tracing showing mouth pressure, esophageal pressure, transdiaphragmatic pressure, and flow for one male participant and the transition from unloaded to spontaneous breathing while exercising at 80% Wmax. The tracing highlights that when the participant is unloaded, mouth pressure is elevated and therefore esophageal pressure is attenuated. Continuous vertical line represents when the PAV was turned off.

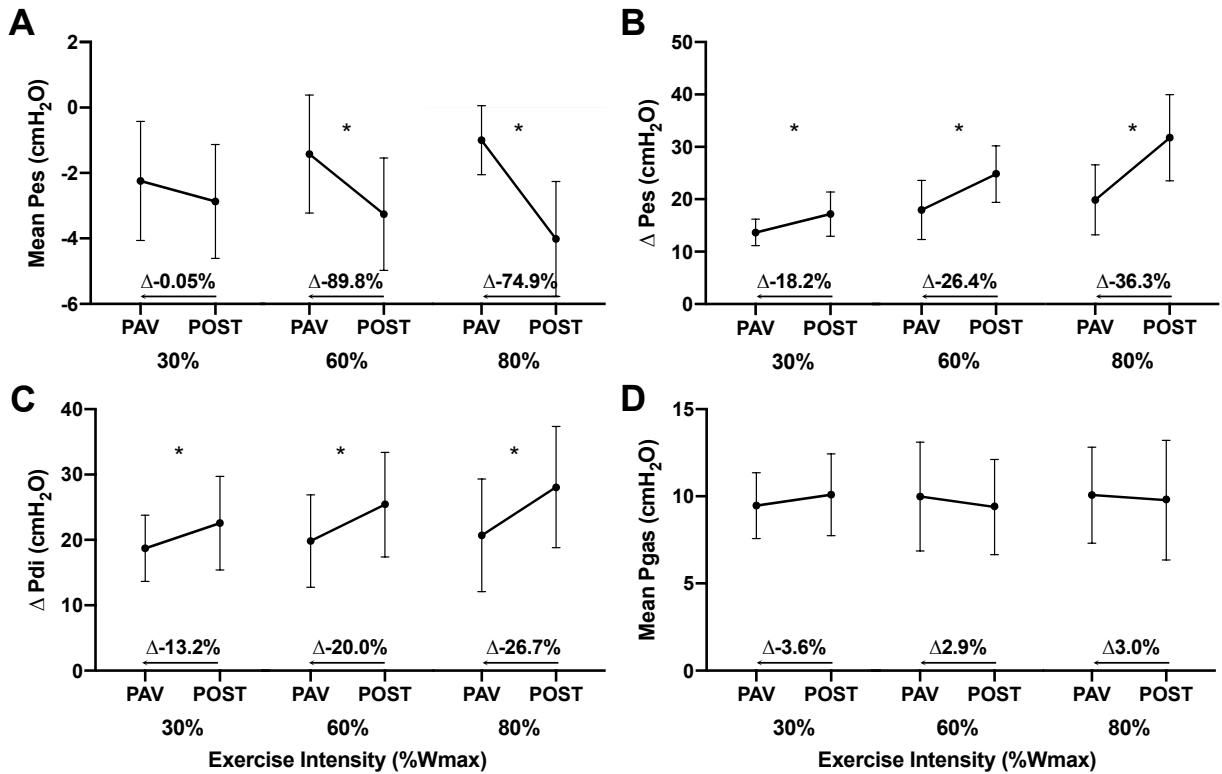


Figure 6. Respiratory pressures during unloaded (PAV) and spontaneous (POST) breathing at 30%, 60% and 80%Wmax. Panel A and B are showing average esophageal pressure (Pes) and magnitude of Pes swings (Δ Pes), respectively. Panel C is displaying magnitude of transdiaphragmatic pressure (Pdi) (Δ Pdi) swings. Lastly, Panel D is showing average gastric pressure (Pgas). Percent differences are showing changes from POST to PAV (as indicated by the arrows). *, significant difference between PAV and POST within the below-listed exercise intensity, $p < 0.05$.

The respiratory muscles were unloaded during the PAV condition at all exercise intensities (**Figure 6**). At the 30%Wmax exercise intensity, mean Pm during unloaded breathing was significantly greater than spontaneous breathing (2.6 ± 0.7 vs. 0.2 ± 0.3 cmH₂O, respectively ($p < 0.0001$)). Although a nonsignificant -0.7 ± 1.6 cmH₂O change in mean Pes was observed (**Figure 6A**) (from spontaneous to unloaded breathing), the magnitude of Pes swings was -3.5 ± 3.4 cmH₂O (smaller) during unloaded relative to spontaneous breathing ($p=0.0031$) (**Figure 6B**). The magnitude of Pdi decreased by -3.8 ± 5.6 cmH₂O during unloaded breathing ($p=0.02$) (**Figure 6C**),

while mean Pgas had a nonsignificant -0.6 ± 1.8 cmH₂O change between unloaded and spontaneous breathing ($p=0.23$) (**Figure 6D**).

During the 60% Wmax exercise intensity, mean Pm was greater during unloaded compared to spontaneous breathing (3.4 ± 0.9 vs. 0.2 ± 0.6 cmH₂O, respectively ($p < 0.0001$), with a significant -1.8 ± 2.6 cmH₂O change in mean Pes observed during unloaded breathing relative to spontaneous breathing ($p=0.02$) (**Figure 6A**). Along with a decrease in mean Pes, the magnitude of Pes swings decreased by -6.8 ± 6.4 cmH₂O during unloaded breathing ($p=0.0023$) (**Figure 6B**). The magnitude of Pdi swings also decreased during unloaded breathing by -5.6 ± 6.4 cmH₂O ($p=0.0084$) (**Figure 5C**), while no significant difference in mean Pgas was observed (0.6 ± 2.5 cmH₂O during unloaded relative to spontaneous breathing ($p=0.41$)) (**Figure 6D**).

Lastly, during the 80% Wmax exercise intensity, mean Pm was greater during unloaded relative to spontaneous breathing (4.8 ± 1.3 vs. 0.5 ± 0.5 cmH₂O, respectively ($p < 0.0001$). A significant -3.3 ± 1.5 cmH₂O change in mean Pes was observed during unloaded compared to spontaneous breathing ($p < 0.0001$) (**Figure 6A**). The magnitude swings in Pes as well as Pdi were also reduced during unloaded breathing by a -11.9 ± 7.9 cmH₂O ($p=0.0002$) and -7.4 ± 4.1 cmH₂O change from spontaneous breathing ($p < 0.0001$), respectively (**Figure 6B&C**). As with 30% and 60% Wmax, mean Pgas had a nonsignificant 0.3 ± 1.6 cmH₂O change during unloaded compared to spontaneous breathing ($p=0.51$) (**Figure 6D**).

The relative difference between unloaded and spontaneous breathing for mean Pes at 30% was different from 60% ($p=0.01$) and 80% ($p=0.009$). While Δ Pes at 30% was different from 80% Wmax ($p=0.02$) (**Table 3**). Moreover, the absolute difference between unloaded and spontaneous breathing for mean Pes and Δ Pes at 30% was different from 80% Wmax (mean Pes

$p=0.0001$; Δ Pes $p=0.01$) (**Table 4**). There was no difference in the relative or absolute change between exercise intensities for any other variable displayed in **Figure 6**.

5.2.2 Inspiratory and Total Work of Breathing Reduced by Proportional Assist Ventilation

During all unloaded breathing trials, the PAV reduced both inspiratory and total work of breathing. **Figure 7** is displaying Pes and Pdi PTPs, total W_b and ventilatory data such as breathing frequency, tidal volume and ventilation.

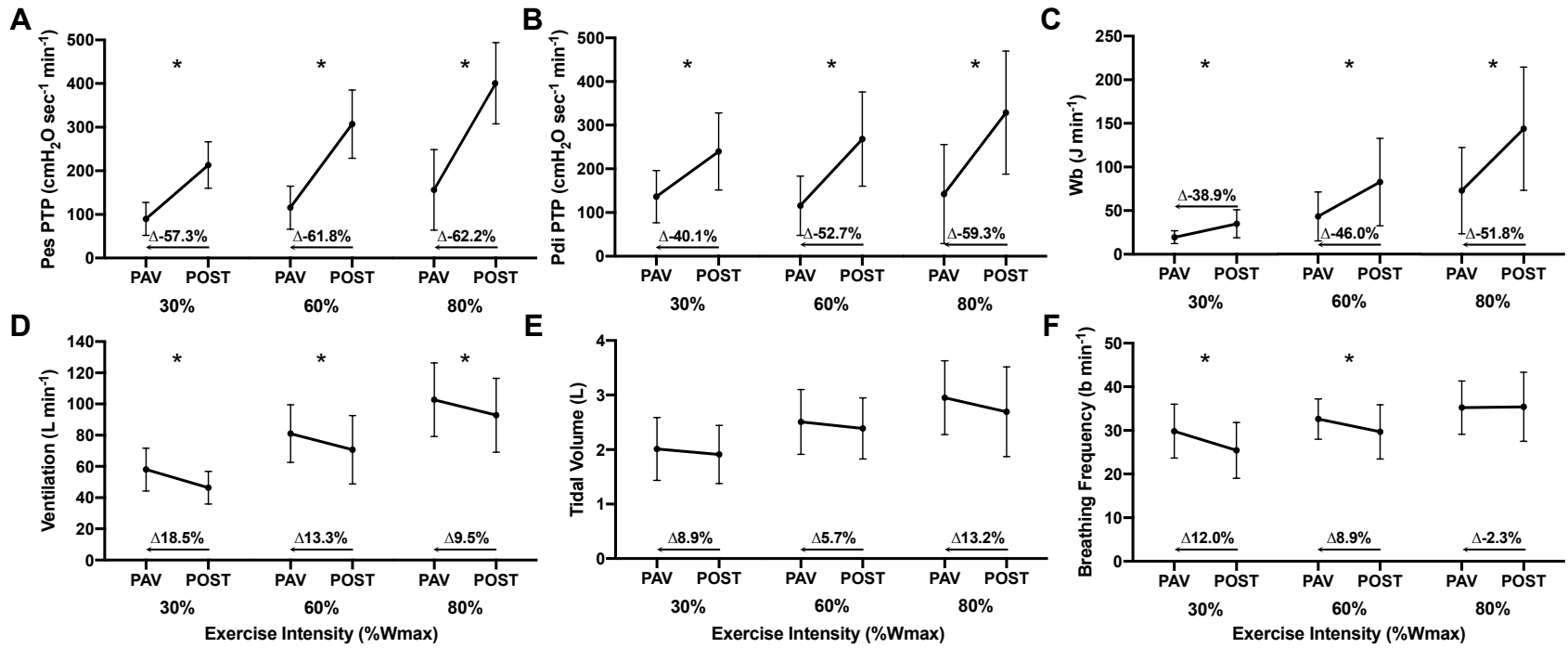


Figure 7. Work of breathing and ventilation data during unloaded and spontaneous breathing at 30%, 60%, and 80%W_{max}. Panel A and B display the esophageal (Pes) and transdiaphragmatic (Pdi) pressure-time products (PTP), respectively. Panel C shows total work of breathing (W_b) (inspiratory and expiratory work combined). Panel D, E and F are displaying ventilation, tidal volume and breathing frequency, respectively. Percent differences are showing changes from POST to PAV (as indicated by the arrows). *, significant difference between PAV and POST within the below-listed exercise intensity, $p < 0.05$.

During the 30% W_{max} exercise intensity, inspiratory W_b was significantly reduced during unloaded breathing as indicated by the Pes and Pdi pressure-time products. The Pes and Pdi PTPs decreased by -123.3 ± 55.6 ($p < 0.0001$) and -103.3 ± 87.5 $\text{cmH}_2\text{O sec}^{-1} \text{min}^{-1}$ during unloaded relative to spontaneous breathing, respectively ($p = 0.0011$) (**Figure 7A&B**). Total W_b decreased by -15.3 ± 12.7 J min^{-1} during unloaded relative to spontaneous breathing ($p = 0.0010$) (**Figure 7C**). Moreover, W_b per litre of ventilation was also lower during unloaded compared to spontaneous breathing (0.3 ± 0.1 vs. 0.7 ± 0.2 J L^{-1} , $p < 0.0001$). Ventilation increased by 11.6 ± 9.7 L min^{-1} ($p = 0.0010$) during unloaded relative to spontaneous breathing because of a rise in breathing frequency of 4.3 ± 6.7 breaths min^{-1} ($p = 0.03$) (**Figure 7D&F**). Tidal volume had a nonsignificant 0.1 ± 0.5 L change during unloaded compared to spontaneous breathing ($p = 0.54$) (**Figure 7E**).

During the 60% W_{max} exercise intensity, Pes and Pdi PTPs were reduced during unloaded compared to spontaneous breathing by -192.6 ± 68.8 and -153.4 ± 94.9 $\text{cmH}_2\text{O sec}^{-1} \text{min}^{-1}$, respectively (both $p < 0.0001$) (**Figure 7A&B**). Total W_b decreased by -39.5 ± 26.7 J min^{-1} ($p = 0.0002$) during unloaded relative to spontaneous breathing despite an increase in ventilation of 10.4 ± 9.5 L min^{-1} ($p = 0.002$) (**Figure 7C&D**). Additionally, W_b per litre of ventilation was lower during unloaded compared to spontaneous breathing (0.5 ± 0.2 vs. 1.1 ± 0.3 J L^{-1} , $p < 0.0001$). The rise in ventilation was attributed to an increase in breathing frequency of 2.9 ± 4.8 breaths min^{-1} ($p = 0.04$) as there was a nonsignificant change in tidal volume of 0.1 ± 0.4 L ($p = 0.3$) (**Figure 7E&F**).

Lastly, during the 80% W_{max} exercise intensity, the Pes and Pdi PTPs decreased by -246.1 ± 83.5 and -187.2 ± 89.0 $\text{cmH}_2\text{O sec}^{-1} \text{min}^{-1}$, respectively (both $p < 0.0001$) (**Figure 7A&B**). Total W_b decreased by -71.2 ± 32.5 J min^{-1} ($p < 0.0001$) despite a rise in ventilation of 10 ± 11.2 L min^{-1} during unloaded relative to spontaneous breathing ($p = 0.0073$) (**Figure 7C&D**). Furthermore, W_b

per litre of ventilation was lower during unloaded compared to spontaneous breathing (0.6 ± 0.3 vs. 1.5 ± 0.3 J L⁻¹, $p < 0.0001$). There was no change in breathing frequency and tidal volume as breathing frequency had a nonsignificant reduction of -0.2 ± 8.2 breaths min⁻¹ ($p = 0.9$) and tidal volume had a nonsignificant increase of 0.3 ± 0.7 L ($p = 0.2$) (**Figure 7E&F**).

The relative difference between spontaneous and unloaded breathing for Pdi PTP and breathing frequency (Fb) were different between 30% and 80% Wmax (Pdi PTP $p = 0.007$; Fb $p = 0.02$) (**Table 3**). While the absolute difference between spontaneous and unloaded breathing for Pdi PTP at 30% was different from 80% Wmax ($p = 0.001$) and Pes PTP at 30% was different from 60% ($p = 0.001$) and 80% Wmax ($p < 0.0001$) (**Table 4**). For W_b, the absolute difference between spontaneous and unloaded breathing at 30% was different from 60% ($p = 0.02$) and 80% ($p < 0.0001$) and 60% was different from 80% Wmax ($p < 0.0001$). Moreover, the absolute change in Fb was different between 30% and 80% Wmax ($p = 0.03$). There were no relative differences between spontaneous and unloaded breathing for W_b, ventilation, and Pes PTP between exercise intensities (all $p > 0.05$). As such, this displays that the relative reduction in the W_b, Pes PTP, and the change in ventilation was not different between exercise intensities.

Expiratory work as determined by the Pgas PTP was not different between the PAV and POST conditions at all exercise intensities. At 30% Wmax, the Pgas PTP was 136.7 ± 85.1 cmH₂O sec⁻¹ min⁻¹ and 133.3 ± 86.2 cmH₂O sec⁻¹ min⁻¹ during the PAV and POST condition, respectively ($p = 0.86$). At 60% Wmax, the Pgas PTP was 164.7 ± 147.4 cmH₂O sec⁻¹ min⁻¹ and 141.6 ± 158.2 cmH₂O sec⁻¹ min⁻¹ during the PAV and POST condition, respectively ($p = 0.36$). Lastly, at 80% Wmax, the Pgas PTP was 153.6 ± 149.8 cmH₂O sec⁻¹ min⁻¹ and 138.9 ± 214.2 cmH₂O sec⁻¹ min⁻¹ during the PAV and POST condition, respectively ($p = 0.66$).

5.3 Metabolic Implications of Respiratory Muscle Unloading

Metabolic variables including $\dot{V}O_2$, $\dot{V}CO_2$, and RER are represented in **Figure 8**.

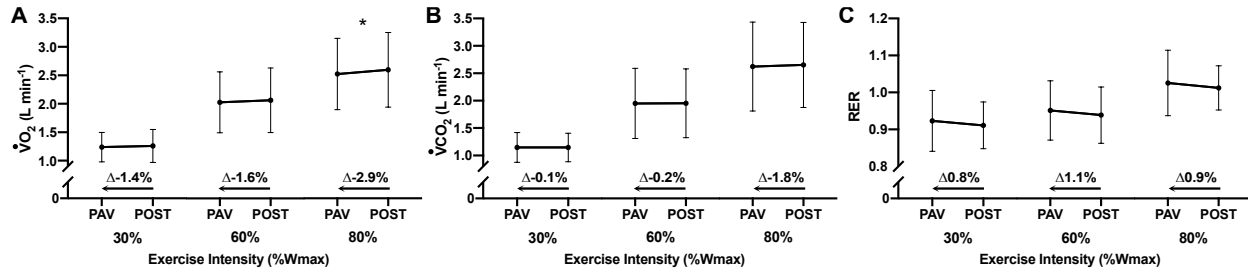


Figure 8. Metabolic variables during unloaded and spontaneous breathing at 30%, 60%, and 80% Wmax. Panel A displays oxygen consumption ($\dot{V}O_2$). Panel B displays carbon dioxide output ($\dot{V}CO_2$) and Panel C is showing the respiratory exchange ratio (RER). Percent differences are showing changes from POST to PAV (as indicated by the arrows). *, significant difference between PAV and POST within the below-listed exercise intensity, $p < 0.05$. Data in the above figure includes values from $n = 12$ subjects.

At 30% Wmax, $\dot{V}O_2$, $\dot{V}CO_2$ and RER were not different between unloaded and spontaneous breathing (**Figure 8A-C**). Oxygen consumption had a nonsignificant -0.02 ± 0.09 L min⁻¹ reduction ($p = 0.46$), while $\dot{V}CO_2$ and RER had a nonsignificant -0.002 ± 0.04 L min⁻¹ ($p = 0.8$) and 0.01 ± 0.06 rise during unloaded compared to spontaneous breathing, respectively ($p = 0.5$). At 60% Wmax, $\dot{V}O_2$ had a nonsignificant -0.03 ± 0.1 L min⁻¹ reduction ($p = 0.3$), while $\dot{V}CO_2$ and RER had a nonsignificant reduction of -0.0008 ± 0.2 L min⁻¹ ($p = 0.9$) and a rise of 0.01 ± 0.06 during unloaded compared to spontaneous breathing, respectively ($p = 0.4$) (**Figure 8A-C**). At 80% Wmax, a decrease in $\dot{V}O_2$ of -0.07 ± 0.06 L min⁻¹ was observed ($p = 0.002$). Carbon dioxide output had a nonsignificant decrease of -0.02 ± 0.1 L min⁻¹ ($p = 0.4$) while RER had a nonsignificant increase of 0.01 ± 0.06 during unloaded relative to spontaneous breathing ($p = 0.5$) (**Figure 8A-C**). The relative and absolute change in $\dot{V}O_2$, $\dot{V}CO_2$ and RER between spontaneous and unloaded breathing was not different between exercise intensities (all $p > 0.05$) (**Figure 8**).

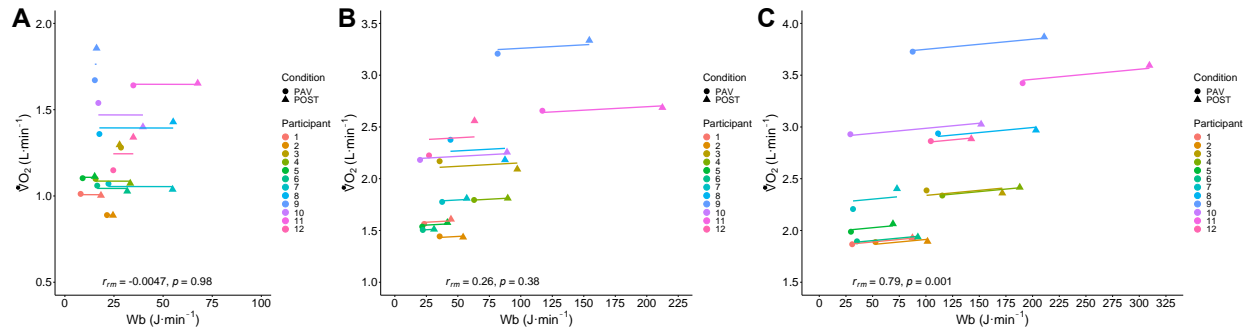


Figure 9. Relationship between work of breathing (W_b) and oxygen consumption ($\dot{V}O_2$) when combining all participants' repeated measures during unloaded (PAV; circles) and spontaneous (POST; triangles) breathing. Panel A to C is displaying 30%, 60%, and 80% W_{max} , respectively. Each colour represents a different participant. The length of each line represents each participant's response range. Data in this figure are representing values from $n=12$ subjects.

Figure 9 shows the relationship between $\dot{V}O_2$ and the W_b . There is a strong positive relationship between $\dot{V}O_2$ and W_b observed at 80% W_{max} ($p=0.001$) and not a 30% ($p=0.98$) and 60% W_{max} ($p=0.38$). No relationship is observed at low and moderate intensity exercise because the change in W_b is too small to observe a measurable change in $\dot{V}O_2$.

5.4 Cardiovascular Changes with Respiratory Muscle Unloading

Respiratory muscle unloading induced changes to multiple cardiac variables at all exercise intensities. **Figure 10** displays how attenuating ITP at different exercise intensities impacts \dot{Q} , HR, SV, LVEDV and LVESV. **Figure 11** demonstrates how attenuating ITP can impact MAP, SBP, DBP, and TPR.

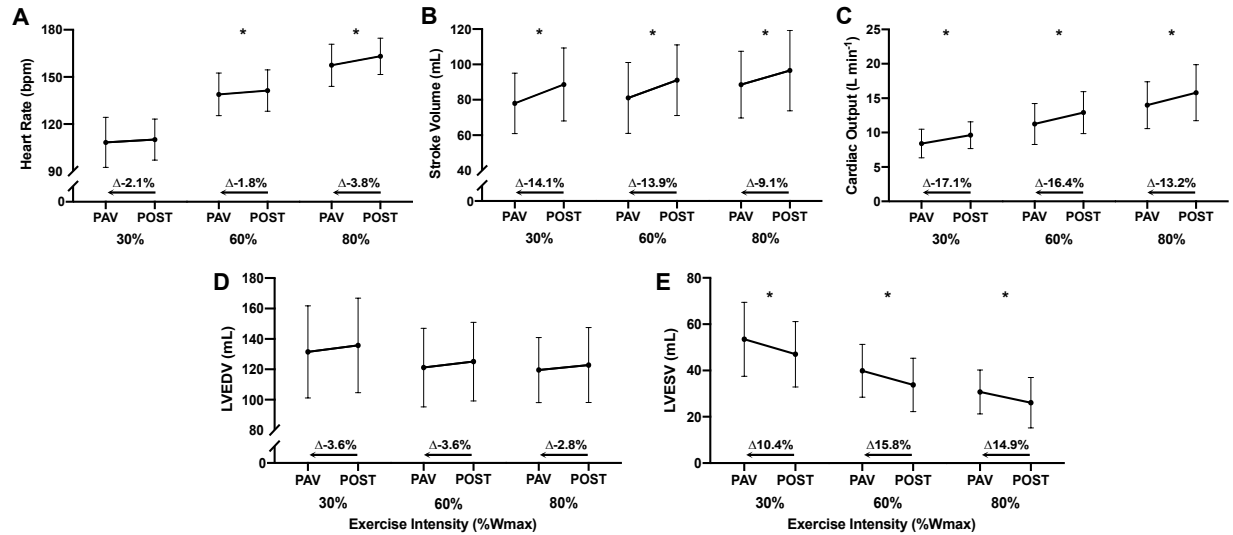


Figure 10. Cardiac variables during unloaded and spontaneous breathing at 30%, 60%, and 80% Wmax. Panel A, B and C display heart rate, stroke volume, and cardiac output, respectively. Panel D and E show left ventricular end-diastolic volume (LVEDV) and left ventricular end-systolic volume (LVESV), respectively. Percent differences are showing changes from POST to PAV (as indicated by the arrows). *, significant difference between PAV and POST within the below-listed exercise intensity, $p < 0.05$. Data in the above figure include values from $n = 12$ subjects.

At 30% Wmax, HR had a nonsignificant decrease of -1.7 ± 4.9 bpm from spontaneous to unloaded breathing ($p = 0.21$) (**Figure 10A**) while SV and \dot{Q} decreased by -10.7 ± 11.2 mL and -1.2 ± 1.3 L min^{-1} during unloaded breathing compared to spontaneous breathing, respectively (both $p = 0.005$) (**Figure 10B&C**). The decrease in SV is attributed to a rise in LVESV of 6.4 ± 10.1 mL ($p = 0.04$) as LVEDV had a nonsignificant decline of -4.2 ± 13.1 mL ($p = 0.26$) (**Figure 10D&E**).

At 60% Wmax, HR, SV and \dot{Q} decreased by -2.4 ± 2.7 bpm ($p = 0.008$), -10.1 ± 10.2 mL ($p = 0.003$), and -1.6 ± 1.4 L min^{-1} ($p = 0.001$) during unloaded compared to spontaneous breathing, respectively (**Figure 10A-C**). As with 30% Wmax, LVEDV had a nonsignificant decrease of -3.9 ± 9.9 mL ($p = 0.17$) while LVESV increased by 6.1 ± 4.7 mL ($p = 0.0005$) during unloaded relative to spontaneous breathing (**Figure 10D&E**).

At 80% Wmax, HR, SV, and \dot{Q} decreased by -5.7 ± 3.9 bpm ($p=0.0004$), -8.0 ± 12.3 mL ($p=0.04$), and -1.8 ± 2.0 L min⁻¹ ($p=0.009$) during unloaded relative to spontaneous breathing, respectively (**Figure 10A-C**). Moreover, LVESV increased by 4.7 ± 6.2 mL ($p=0.02$) while LVEDV had a nonsignificant decrease of -3.3 ± 12.9 mL ($p=0.39$) during unloaded compared to spontaneous breathing (**Figure 10D&E**).

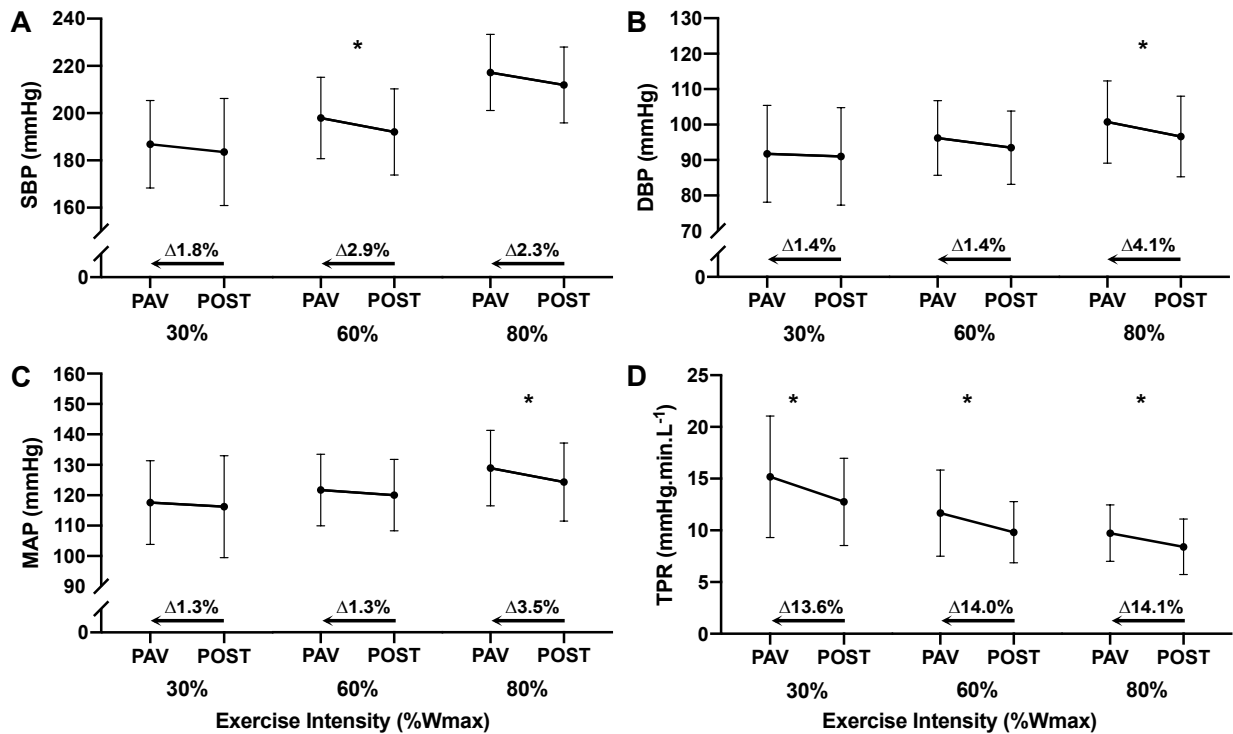


Figure 11. Cardiovascular variables during unloaded and spontaneous breathing at 30%, 60%, and 80% Wmax. Panel A and B display systolic blood pressure (SBP) and diastolic blood pressure (DBP), respectively. Panel C and D show mean arterial pressure (MAP) and total peripheral resistance (TPR), respectively. Percent differences are showing changes from POST to PAV (as indicated by the arrows). *, significant difference between PAV and POST within the below-listed exercise intensity, $p < 0.05$. At 80% Wmax, all variables in this figure were determined using $n=12$ subjects.

At 30% Wmax, a nonsignificant rise in SBP, DBP, and MAP was observed (3.3 ± 10.6 mmHg ($p=0.28$), 1.1 ± 3.4 mmHg ($p=0.28$), and 1.3 ± 4.9 mmHg ($p=0.33$), respectively) during unloaded compared to spontaneous breathing (**Figure 11A-C**). Total peripheral resistance

increased by 2.4 ± 2.8 mmHg.min. L⁻¹ during unloaded relative to spontaneous breathing ($p=0.008$) (**Figure 11D**).

At 60% Wmax, SBP increased by 5.9 ± 6.9 mmHg ($p=0.009$) despite a nonsignificant rise in DBP of 1.4 ± 3.9 mmHg ($p=0.24$) and MAP of 3.9 ± 3.4 mmHg ($p=0.08$) during unloaded compared to spontaneous breathing (**Figure 11A-C**). Total peripheral resistance increased by 1.9 ± 1.9 mmHg.min. L⁻¹ during unloaded relative to spontaneous breathing ($p=0.004$) (**Figure 11D**).

Lastly, at 80% Wmax, DBP increased by 4.1 ± 2.8 mmHg ($p=0.0002$) while a nonsignificant rise in SBP of 5.3 ± 9.3 ($p=0.06$) and a significant increase in MAP of 4.5 ± 4.6 mmHg ($p=0.004$) was observed during unloaded relative to spontaneous breathing (**Figure 11A-C**). Total peripheral resistance increased by 1.3 ± 0.9 mmHg.min. L⁻¹ during unloaded relative to spontaneous breathing ($p=0.0004$) (**Figure 11D**). Lastly, the absolute difference between spontaneous and unloaded breathing for DBP at 30% was different from 80% Wmax ($p=0.04$) (**Table 4**), with no other relative or absolute differences between exercise intensities for the other variables displayed in **Figure 11**.

5.5 Integrative Influence of Respiratory Muscle Unloading on Cardiovascular and Metabolic Variables

The relationship between \dot{Q} and $\dot{V}O_2$ is altered during respiratory muscle unloading compared to spontaneous breathing. **Figure 12** displays correlations between the absolute change in \dot{Q} and $\dot{V}O_2$ at each exercise intensity. **Figure 13** shows the relationship between \dot{Q} and $\dot{V}O_2$ when combining all participants' repeated measures during unloaded and spontaneous breathing at each exercise intensity.

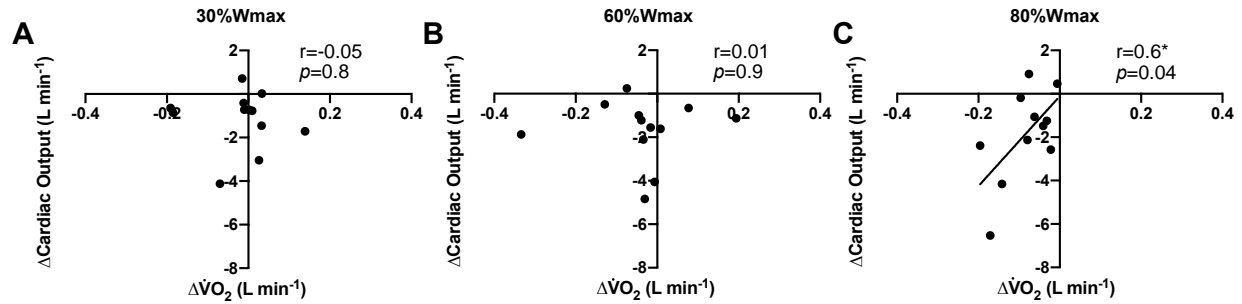


Figure 12. Pearson product moment correlations examining the relationship between absolute changes in cardiac output and oxygen consumption ($\dot{V}O_2$). Panel A to C are displaying correlations at 30%, 60% and 80% Wmax, respectively. Panel A&B is determined using 12 subjects while panel C is determined using 11 subjects.

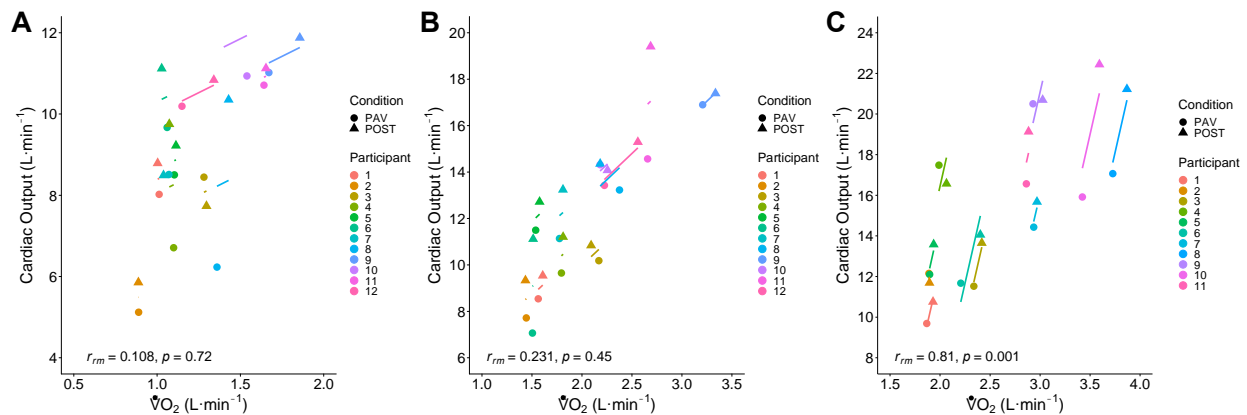


Figure 13. Relationship between cardiac output and oxygen consumption ($\dot{V}O_2$) when combining all participants' repeated measures during unloaded (PAV; circles) and spontaneous (POST; triangles) breathing. Panel A to C is displaying 30%, 60%, and 80% Wmax, respectively. Each colour represents a different participant. The length of each line represents each participant's response range. Panel A&B is determined using 12 subjects while panel C is determined using 11 subjects.

At 30% and 60% Wmax, no relationship was observed between the absolute (**Figure 12A&B**) or relative change in \dot{Q} and $\dot{V}O_2$ (30% Wmax: $r = -0.2$, $p = 0.9$; 60% Wmax: $r = -0.04$, $p = 0.8$). Moreover, in the repeated measures correlation analysis, there was no relationship between \dot{Q} and $\dot{V}O_2$ when combining data from both breathing conditions (**Figure 13A&B**).

At 80% Wmax, a moderate positive relationship was observed between the absolute change in \dot{Q} and $\dot{V}O_2$ ($r=0.6, p=0.04$) (**Figure 12C**), however, no relationship was observed when comparing the relative change in \dot{Q} and $\dot{V}O_2$ ($r=0.4, p=0.1$). Lastly, the repeated measures correlation analysis revealed a strong positive relationship between \dot{Q} and $\dot{V}O_2$ when combining data from both breathing conditions (**Figure 13C**). Thereby suggesting that the relationship between \dot{Q} and $\dot{V}O_2$ is stronger at 80% Wmax when the relative contribution of $\dot{V}O_2$ to determining \dot{Q} is greater.

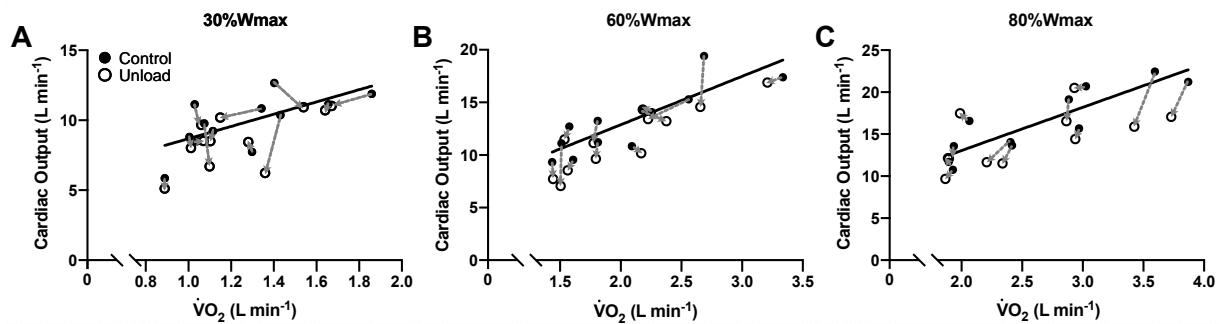


Figure 14. Relationship between cardiac output and oxygen consumption ($\dot{V}O_2$) at each exercise intensity. Black circles represent spontaneous (control) and white circles represent unloaded breathing. Solid black line in each graph represents the control regression line. This figure highlights how the relationship between cardiac output and $\dot{V}O_2$ change during unloaded and spontaneous breathing. Panel A&B is determined using 12 subjects while panel C is determined using 11 subjects.

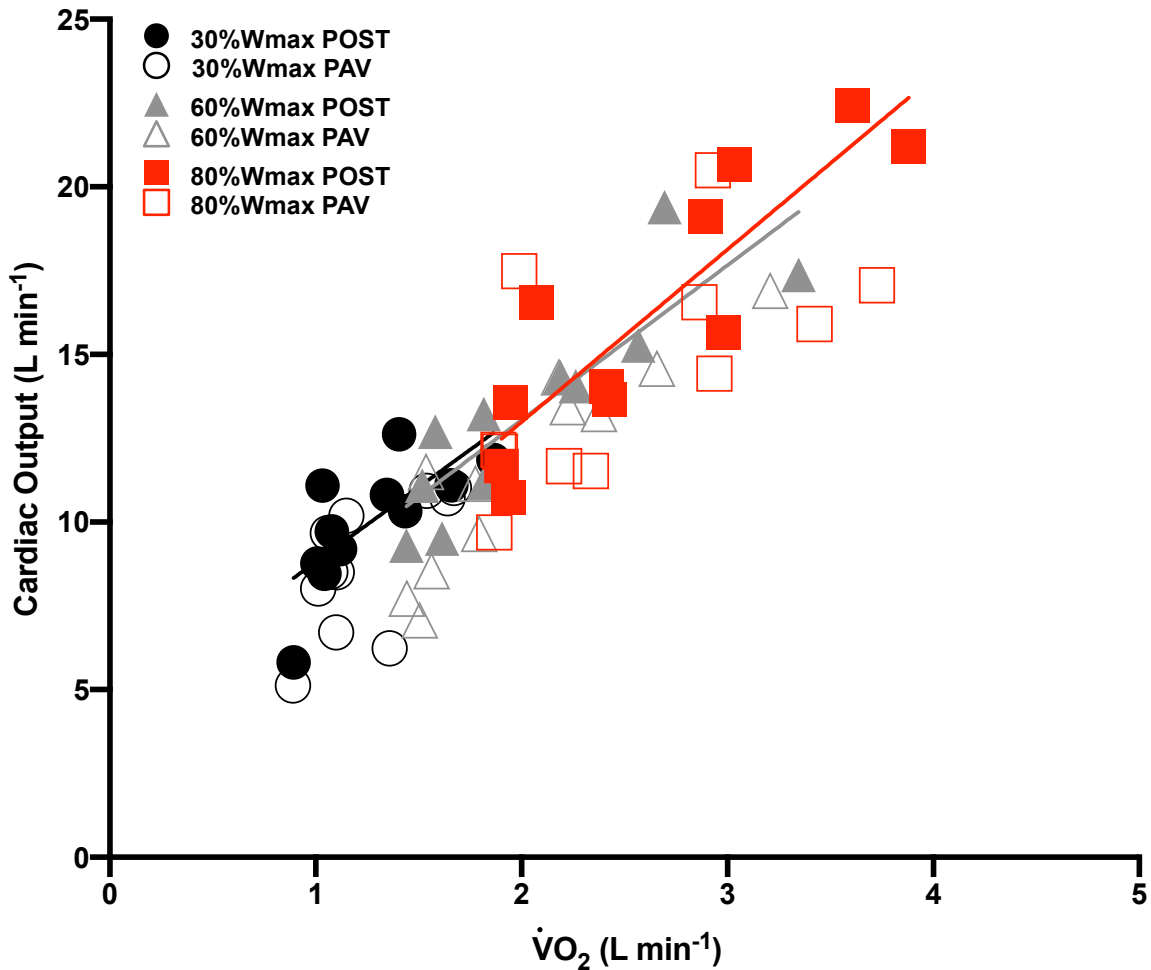


Figure 15. Relationship between cardiac output and oxygen consumption ($\dot{V}O_2$) for each exercise intensity on one graph. Circles represent 30%Wmax (black = spontaneous (POST), white = unloaded (PAV)). Triangles represent 60%Wmax (gray = spontaneous (POST), white = unloaded (PAV)). Squares represent 80%Wmax (red = spontaneous (POST), white = unloaded (PAV)). Solid lines represent the control (POST) regression lines for the respective exercise intensity. This figure highlights that at 30% and 60%Wmax during unloaded breathing cardiac output goes down for a similar $\dot{V}O_2$ (unloaded dots move down relative to regression line), suggesting mechanisms other than $\dot{V}O_2$ are causing a reduction in cardiac output. Moreover, at 80%Wmax during unloaded breathing, the unloaded dots move down and leftwards suggesting a stronger relationship between cardiac output and $\dot{V}O_2$, yet because the dots moved downwards, something other than $\dot{V}O_2$ is leading at the reduction in cardiac output at 80%Wmax. 30% and 60%Wmax in the above graph is determined using 12 subjects while 80%Wmax is determined using 11 subjects.

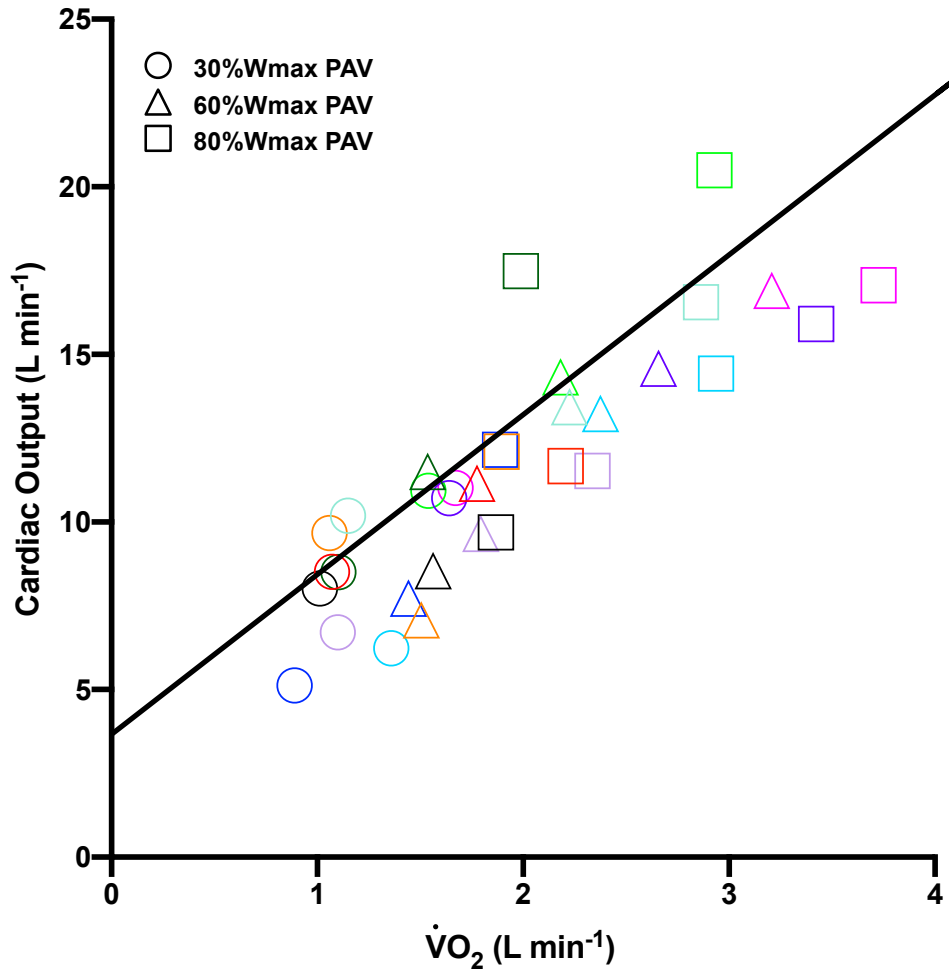


Figure 16. Relationship between cardiac output and oxygen consumption ($\dot{V}O_2$) for each individual at each exercise intensity. Black solid line represents the relationship between \dot{Q} and $\dot{V}O_2$ during spontaneous (control) breathing. Circles represent 30% W_{max} , triangles represent 60% W_{max} , and squares represent 80% W_{max} . Each colour represents a different participant. 11 subjects are being represented in this graph.

The relationship between \dot{Q} and $\dot{V}O_2$ during unloaded breathing differs between exercise intensity. **Figure 14** is showing how this relationship differs during unloaded breathing (from spontaneous breathing) at each exercise intensity separately. **Figure 15** demonstrates the same concept as **Figure 14**, but on the same graph. Both **Figures 14&15** highlight that at 30% and 60% W_{max} , \dot{Q} seems to decrease despite a similar $\dot{V}O_2$ during unloaded breathing. At 80% W_{max} , \dot{Q} decreases with a reduction in $\dot{V}O_2$, however, the unloaded dots/shapes drop down below the

control regression line. For all intensities, these graphs are suggesting that a mechanism(s) other than $\dot{V}O_2$ are causing a reduction in \dot{Q} ; however, these other mechanisms are more prevalent at 30% and 60% W_{max} when $\dot{V}O_2$ is not contributing to the change in \dot{Q} . **Figure 16** is showing the relationship between \dot{Q} and $\dot{V}O_2$ for each individual at each intensity. As such, some individuals saw no change in their $\dot{Q}/\dot{V}O_2$ relationship from spontaneous to unloaded breathing, however, the general trend is consistent with that seen in **Figures 14&15**.

As highlighted in **Figures 15&16**, \dot{Q} is decreasing at 30% and 60% W_{max} for a similar $\dot{V}O_2$. As such, other mechanisms that could account for the observed reduction in \dot{Q} may be related to changes in ITP (**Figure 17**).

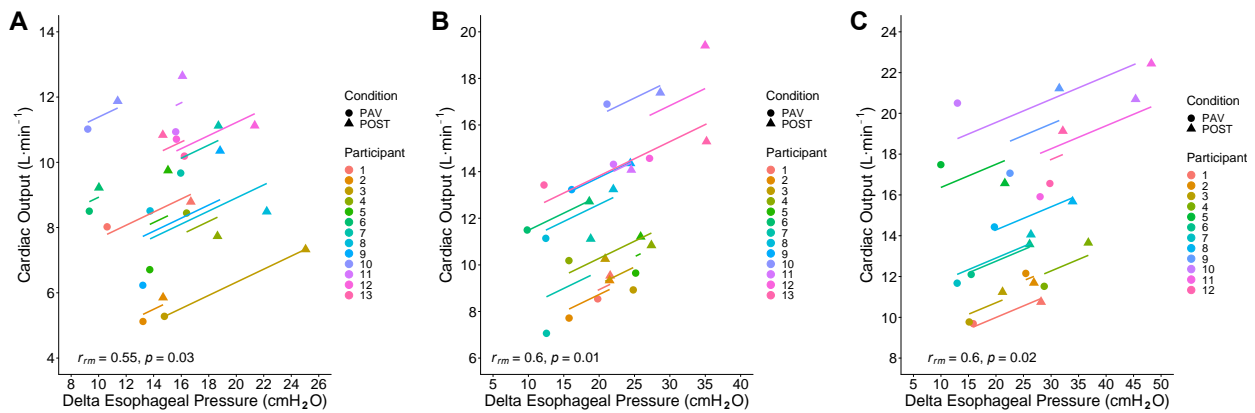


Figure 17. Relationship between cardiac output and the magnitude of esophageal pressure changes when combining all participants' repeated measures during unloaded (PAV; circles) and spontaneous (POST; triangles) breathing. Panel A to C is displaying 30%, 60%, and 80% W_{max} , respectively. Each colour represents a different participant. The length of each line represents each participant's response range. Panel C is determined using 12 subjects.

At all exercise intensities, there is a strong positive relationship between the magnitude of Pes swings and \dot{Q} (**Figure 17**). Whereby when the magnitude of Pes becomes smaller as with respiratory muscle unloading, \dot{Q} decreases. When considering the relationship between \dot{Q} and mean Pes, there was a strong negative relationship identified at all exercise intensities ($r=-0.61, p=0.02$;

$r=-0.73$, $p=0.002$; $r=-0.59$, $p=0.03$, for 30%, 60%, and 80% Wmax, respectively). Esophageal pressure changes are primarily impacting \dot{Q} via changes to SV (**Figure 18**).

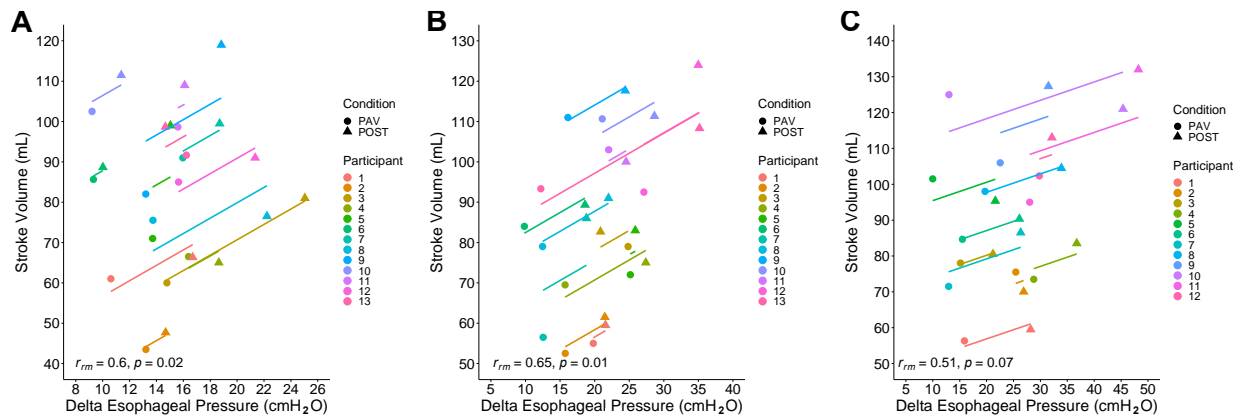


Figure 18. Relationship between stroke volume and the magnitude of esophageal pressure swings when combining all participants’ repeated measures during unloaded (PAV; circles) and spontaneous (POST; triangles) breathing. Panel A to C is displaying 30%, 60%, and 80% Wmax, respectively. Each colour represents a different participant. The length of each line represents each participant’s response range. Panel C is determined using $n=12$ subjects.

When considering the relationship between SV and the magnitude of Pes swings, there was a strong positive relationship determined at all exercise intensities (**Figure 18**), whereby when the magnitude of Pes swings gets smaller, SV decreases. Moreover, there was a strong negative relationship between SV and mean Pes at 30% ($r=-0.75$, $p=0.001$) and 60% Wmax ($r=-0.70$, $p=0.005$). There was also a moderate negative relationship between SV and mean Pes at 80% Wmax, however this relationship was not significant ($r=-0.52$, $p=0.06$). Moreover, the magnitude of Pes swings only influenced HR at 80% Wmax ($r=0.61$, $p=0.02$), with no relationship determined at 30% and 60% Wmax ($r=0.23$, $p=0.43$; $r=0.23$, $p=0.42$). There was a strong negative relationship between HR and mean Pes at 80% Wmax ($r=-0.65$, $p=0.01$), a moderate negative relationship at 30% Wmax ($r=-0.54$, $p=0.04$), with no relationship at 60% Wmax ($r=-0.51$, $p=0.06$). Furthermore, the magnitude of Pes swings had no influence on LVEDV (**Figure 19**).

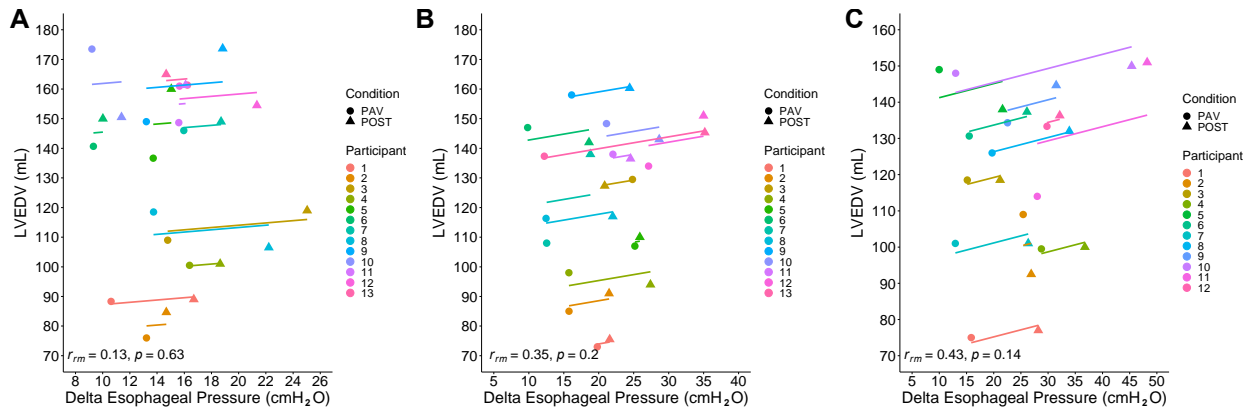


Figure 19. Relationship between left ventricular end-diastolic volume (LVEDV) and the magnitude of esophageal pressure swings when combining all participants' repeated measures during unloaded (PAV; circles) and spontaneous (POST; triangles) breathing. Panel A to C is displaying 30%, 60%, and 80% Wmax, respectively. Each colour represents a different participant. The length of each line represents each participant's response range. Panel C is determined using 12 subjects.

At all exercise intensities, there was no relationship observed between LVEDV and the magnitude of Pes swings (**Figure 19**). There was also no relationship observed between mean Pes and LVEDV at 30%, 60%, and 80% Wmax ($r=-0.43$, $p=0.12$; $r=0.23$, $p=0.43$; $r=-0.29$, $p=0.33$, respectively).

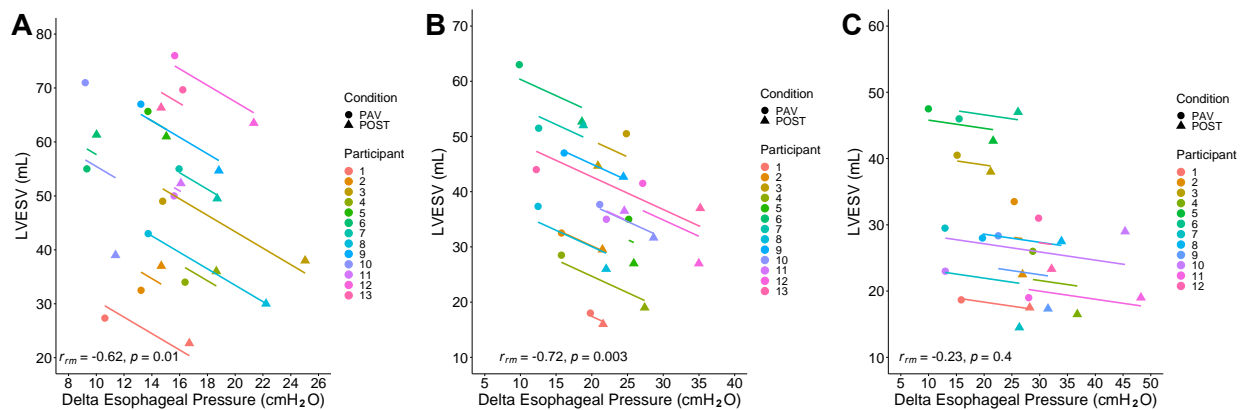


Figure 20. Relationship between left ventricular end-systolic volume (LVESV) and the magnitude of esophageal pressure swings when combining all participants' repeated measures during unloaded (PAV; circles) and spontaneous (POST; triangles) breathing. Panel A to C is displaying 30%, 60%, and 80% Wmax, respectively. Each colour represents a different participant. The length of each line represents each participant's response range. Panel C is determined using 12 subjects.

Figure 20 shows the relationship between LVESV and the magnitude of Pes swings. At 30% and 60% Wmax, there was a strong negative relationship between LVESV and the magnitude of esophageal pressure swings (**Figure 20**). However, at 80% Wmax, there was no relationship observed between LVESV and the magnitude of Pes swings (**Figure 20**). There was also no relationship observed between LVESV and mean Pes at 30%, 60%, and 80% Wmax ($r=0.23$, $p=0.42$; $r=0.51$, $p=0.06$; $r=0.44$, $p=0.13$, respectively). The rise in LVESV may be the result of the influence the magnitude of Pes swings has on MAP (**Figure 21**).

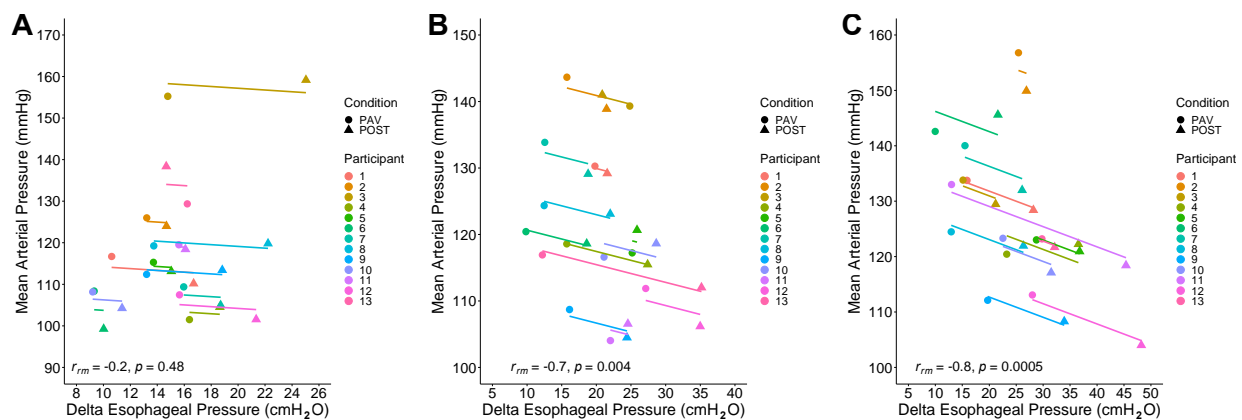


Figure 21. Relationship between mean arterial pressure (MAP) and the magnitude of esophageal pressure swings when combining all participants' repeated measures during unloaded (PAV; circles) and spontaneous (POST; triangles) breathing. Panel A to C is displaying 30%, 60%, and 80% Wmax, respectively. Each colour represents a different participant. The length of each line represents each participant's response range.

There was no relationship between MAP and the magnitude of Pes swings at 30% Wmax; however, there was a strong negative relationship observed at 60% ($r=-0.7$, $p=0.004$) and 80% Wmax ($r=-0.8$, $p=0.0005$) (**Figure 21**). Lastly, the reduction in \dot{Q} observed at 80% may be the result of a HR related decrease in $\dot{V}O_2$ (**Figure 22**).

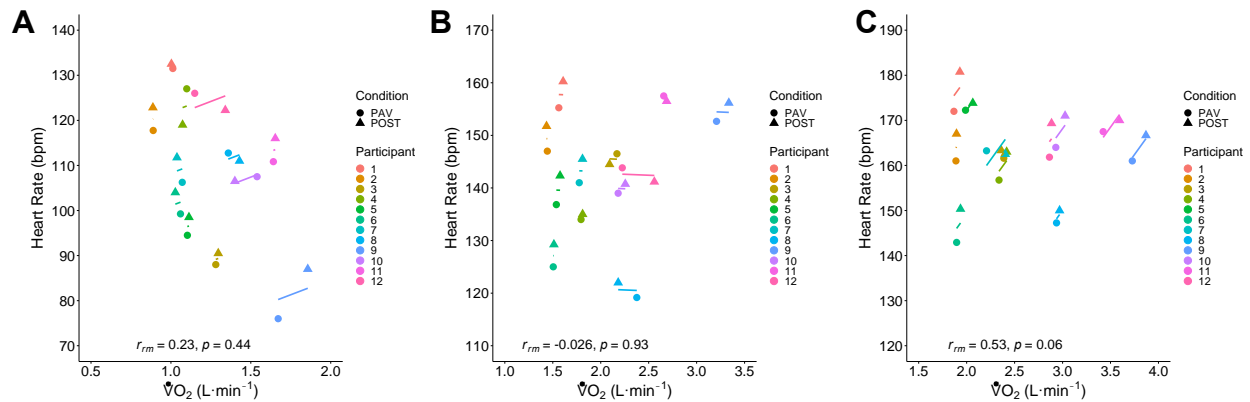


Figure 22. Relationship between heart rate and oxygen consumption ($\dot{V}O_2$) when combining all participants' repeated measures during unloaded (PAV; circles) and spontaneous (POST; triangles) breathing. Panel A to C is displaying 30%, 60%, and 80% W_{max} , respectively. Each colour represents a different participant. The length of each line represents each participant's response range. The data in this figure is derived from $n=12$ subjects.

There was no relationship observed between HR and $\dot{V}O_2$ at any exercise intensity (all $p>0.05$). However, at 80% W_{max} there was a moderate positive nonsignificant relationship between HR and $\dot{V}O_2$ ($r=0.53$, $p=0.06$).

Relative (**Table 3**) and absolute (**Table 4**) differences between each exercise intensity from spontaneous (POST) to unloaded breathing (PAV) are presented below. There were no relative or absolute differences between spontaneous and unloaded breathing for any cardiovascular or metabolic variables between the exercise intensities. However, there were several relative and absolute differences observed between exercise intensities for variables relating to respiratory pressures and the W_b (**Tables 3&4**).

Table 3. Relative (percent) differences for each exercise intensity from spontaneous (POST) to unloaded (PAV) breathing.

Variable	30% Wmax	60% Wmax	80% Wmax
Mean Pes (cmH ₂ O)	-0.05 ± 94.2*†	-81.8 ± 67.5	-74.9 ± 29.2
Δ Pes (cmH ₂ O)	-18.2 ± 15.4†	-26.4 ± 22.0	-36.3 ± 18.3
Δ Pdi (cmH ₂ O)	-13.2 ± 24.4	-20.0 ± 20.4	-26.7 ± 14.9
Mean Pgas (cmH ₂ O)	-3.6 ± 18.4	2.8 ± 19.4	3.0 ± 20.3
Pes PTP (cmH ₂ O sec ⁻¹ min ⁻¹)	-57.3 ± 18.1	-61.8 ± 14.4	-62.2 ± 19.7
Pdi PTP (cmH ₂ O sec ⁻¹ min ⁻¹)	-40.1 ± 23.9†	-52.7 ± 22.8	-59.3 ± 21.5
W _b (J min ⁻¹)	-38.9 ± 22.4	-46.1 ± 14.1	-51.8 ± 14.1
Ṁ _E (L min ⁻¹)	18.5 ± 14.9	13.3 ± 11.1	9.5 ± 11.5
V _t (L)	8.8 ± 30.5	5.7 ± 15.8	13.2 ± 22.6
F _b (b min ⁻¹)	12.1 ± 26.3†	8.9 ± 15.5	-2.3 ± 24.2
ṀO ₂ (L min ⁻¹)	-1.4 ± 6.8	-1.7 ± 5.4	-2.9 ± 2.6
ṀCO ₂ (L min ⁻¹)	-0.1 ± 4.5	-0.2 ± 3.6	-1.8 ± 7.0
RER	0.9 ± 7.4	1.1 ± 6.2	0.9 ± 6.8
Q̇ (L min ⁻¹)	-17.1 ± 20.7	-16.4 ± 15.1	-13.2 ± 12.7
HR (bpm)	-2.2 ± 5.1	-1.8 ± 1.9	-3.8 ± 3.0
SV (mL)	-14.1 ± 15.2	-13.9 ± 14.8	-9.1 ± 13.1
LVEDV (mL)	-3.6 ± 9.2	-3.7 ± 8.7	-2.8 ± 11.1
LVESV (mL)	10.4 ± 17.0	15.8 ± 12.1	14.9 ± 21.9
MAP (mmHg)	1.4 ± 4.2	1.4 ± 2.7	3.5 ± 3.6
SBP (mmHg)	1.8 ± 5.9	2.9 ± 3.5	2.4 ± 4.4
DBP (mmHg)	1.4 ± 3.7	1.4 ± 4.6	4.1 ± 2.7
TPR (mmHg min L ⁻¹)	13.7 ± 13.8	14.0 ± 10.9	14.1 ± 10.6

Abbreviations: Pes, esophageal pressure; Pdi, diaphragmatic pressure; Pgas, gastric pressure; PTP, pressure-time product; W_b, work of breathing; Ṁ_E, ventilation; V_t, tidal volume; F_b, breathing frequency; ṀO₂, oxygen consumption; ṀCO₂, carbon dioxide output; RER, respiratory exchange ratio; Q̇, cardiac output; HR, heart rate; SV, stroke volume; LVEDV, left ventricular end-diastolic volume; LVESV, left ventricular end-systolic volume; MAP, mean arterial pressure; SBP, systolic blood pressure; DBP, diastolic blood pressure; TPR, total peripheral resistance. *, significant difference from 60%Wmax. †, significant difference from 80%Wmax. All data are presented as means ± SD.

Table 4. Absolute differences for each exercise intensity from spontaneous (POST) to unloaded (PAV) breathing.

Variable	30% Wmax	60% Wmax	80% Wmax
Mean Pes (cmH ₂ O)	-0.6 ± 1.6 [†]	-1.8 ± 2.6	-3.3 ± 1.5
Δ Pes (cmH ₂ O)	-3.5 ± 3.4 [†]	-6.9 ± 6.4	-11.9 ± 7.9
Δ Pdi (cmH ₂ O)	-3.8 ± 5.6	-5.6 ± 6.4	-7.4 ± 4.2
Mean Pgas (cmH ₂ O)	-0.6 ± 1.8	0.6 ± 2.6	0.3 ± 1.6
Pes PTP (cmH ₂ O sec ⁻¹ min ⁻¹)	-123.4 ± 55.7 ^{*†}	-192.6 ± 68.8	-246.1 ± 83.6
Pdi PTP (cmH ₂ O sec ⁻¹ min ⁻¹)	-103.4 ± 87.5 [†]	-153.4 ± 94.9	-187.3 ± 89.0
W _b (J min ⁻¹)	-15.3 ± 12.7 ^{*†}	-39.6 ± 26.7 [†]	-71.2 ± 32.5
Ṡ _E (L min ⁻¹)	11.6 ± 9.7	10.4 ± 9.6	10.0 ± 11.2
V _t (L)	0.1 ± 0.6	0.1 ± 0.4	0.3 ± 0.7
F _b (b min ⁻¹)	4.4 ± 6.7 [†]	2.9 ± 4.8	-0.2 ± 8.2
Ṡ _{O₂} (L min ⁻¹)	-0.02 ± 0.09	-0.035 ± 0.123	-0.074 ± 0.067
Ṡ _{CO₂} (L min ⁻¹)	-0.002 ± 0.04	-0.0008 ± 0.06	-0.02 ± 0.1
RER	0.01 ± 0.06	0.01 ± 0.06	0.01 ± 0.06
Ḡ (L min ⁻¹)	-1.2 ± 1.3	-1.7 ± 1.4	-1.8 ± 2.0
HR (bpm)	-1.8 ± 4.9	-2.4 ± 2.7	-5.7 ± 3.9
SV (mL)	-10.7 ± 11.2	-10.1 ± 10.2	-8.0 ± 12.3
LVEDV (mL)	-4.2 ± 13.2	-3.9 ± 9.9	-3.3 ± 12.9
LVESV (mL)	6.4 ± 10.1	6.1 ± 4.7	4.7 ± 6.2
MAP (mmHg)	1.3 ± 4.9	1.7 ± 3.2	4.6 ± 4.6
SBP (mmHg)	3.3 ± 10.6	5.9 ± 6.9	5.3 ± 9.3
DBP (mmHg)	1.1 ± 3.4 [†]	1.4 ± 3.9	4.1 ± 2.8
TPR (mmHg min L ⁻¹)	2.4 ± 2.8	1.9 ± 1.9	1.3 ± 0.9

Abbreviations: Pes, esophageal pressure; Pdi, diaphragmatic pressure; Pgas, gastric pressure; PTP, pressure-time product; W_b, work of breathing; Ṡ_E, ventilation; V_t, tidal volume; F_b, breathing frequency; Ṡ_{O₂}, oxygen consumption; Ṡ_{CO₂}, carbon dioxide output; RER, respiratory exchange ratio; Ḡ, cardiac output; HR, heart rate; SV, stroke volume; LVEDV, left ventricular end-diastolic volume; LVESV, left ventricular end-systolic volume; MAP, mean arterial pressure; SBP, systolic blood pressure; DBP, diastolic blood pressure; TPR, total peripheral resistance. *, significant difference from 60%Wmax. †, significant difference from 80%Wmax. All data are presented as means ± SD.

6.0 DISCUSSION

6.1 Main Findings

The purpose of this study was to determine 1) if respiratory muscle unloading causes a change in \dot{Q} at different exercise intensities, and 2) if \dot{Q} does change, is this change due to HR, SV or $\dot{V}O_2$. As such, the present study has two main findings. First, \dot{Q} decreases during respiratory muscle unloading at all exercise intensities. Second, at 30% W_{max} \dot{Q} may have decreased due to a reduction in SV, at 60% W_{max} , \dot{Q} likely decreased due to reductions in SV and HR and at 80% W_{max} , \dot{Q} may have decreased due to reductions in SV, HR and $\dot{V}O_2$. Moreover, the present study observed a disrupted relationship between \dot{Q} and $\dot{V}O_2$ during respiratory muscle unloading and that other mechanisms are causing a change in \dot{Q} independent of $\dot{V}O_2$. Overall, attenuating ITP has implications on cardiac function. By attenuating ITP, the influence of respiration on the heart is diminished. Therefore, the normally occurring swings in ITP are critical to maintaining normal cardiac function during exercise.

6.2 Cardiac Output Decreases During Respiratory Muscle Unloading

During respiratory muscle unloading, the positive pressure provided by the PAV reduces the work of the respiratory muscles as the pressure gradient to breathe is altered compared to spontaneous breathing. During spontaneous breathing, the pressure gradient to breathe is driven primarily by a more negative ITP. However, during unloaded breathing, ITP may still be negative, but the more positive P_m is now driving the pressure gradient to breathe (120). As such, ITP does not get as negative and the attenuated ITP has implications on \dot{Q} . Cardiac output decreased at all exercise intensities during respiratory muscle unloading with no change in the relative or absolute differences between exercise intensities (**Figure 10C, Tables 3&4**). A reduction in SV contributed to the decrease in \dot{Q} at every exercise intensity, while HR contributed at 60% and 80% W_{max}

(**Figure 10A&B**). Moreover, a reduction in $\dot{V}O_2$ contributed to the decline in \dot{Q} at 80% W_{max} (**Figure 8A**).

The reduction in \dot{Q} with the use of proportional assist ventilation is consistent with others investigating the implications of mechanical ventilation on cardiac function (1,29,126). Since both conventional mechanical ventilation (*e.g.*, PSV) and proportional assist ventilation provide a positive mouth/airway pressure and reduce ITP (less negative), the primary mechanisms determined to cause a decrease in \dot{Q} are those that impact preload and afterload (*e.g.*, venous return and LV ejection). For example, attenuating ITP will reduce the respiratory pump and VR will decrease as less blood will be pulled back to the heart. As such, RSV and LV preload will decrease and subsequently cause a reduction in \dot{Q} as there will be less blood leaving the heart compared to spontaneous breathing. Moreover, changes in afterload will make it harder for the LV to pump blood out of the heart as it must generate greater pressures. Therefore, LV ejection and \dot{Q} may also decrease. Furthermore, our findings are consistent with researchers using proportional assist ventilation to unload the respiratory muscles during exercise (126). At maximal exercise, \dot{Q} was significantly reduced while on the PAV, and this reduction was hypothesized to be due to alterations in SV (126).

6.2.1 Reductions in Stroke Volume with Respiratory Muscle Unloading

Stroke volume decreased at all exercise intensities during respiratory muscle unloading and was the primary reason for a reduction in \dot{Q} at 30% W_{max} (**Figure 10B**). The reduction in SV with respiratory muscle unloading is consistent with previous research that showed a nonsignificant decrease in SV at maximal exercise (126). However, the study had a small sample size ($n=8$) which may account for the nonsignificant finding. The researchers hypothesized this reduction in SV to be due to decreases in metabolic demand, increases in PVR, and attenuations in ITP (126). For

example, by reducing respiratory muscle work, the respiratory muscles require less oxygen and blood flow and therefore SV and \dot{Q} may decrease. Moreover, increasing PVR will increase RV afterload thereby increasing RVESV. Therefore, as RVESV decreases, LVSV will also decrease via both series and direct ventricular interactions. Lastly, attenuating ITP will reduce venous return and therefore RV and LV preload (via series ventricular interactions) and subsequently LVSV. In other studies investigating the implications of positive pressure ventilation on cardiac function, the primary causes for a reduction in \dot{Q} are attributed to changes on both sides of the heart, namely preload (*e.g.*, VR) and LV afterload (1,3,4,27,29).

Typically during positive pressure ventilation, the resulting attenuation in ITP will reduce the pressure gradient for VR resulting in less blood coming back to the heart and a reduction in LV preload (or LVEDV). As such, it was anticipated that SV would decrease due to reductions in LVEDV, yet there were no significant differences in LVEDV between unloaded and spontaneous breathing at any exercise intensity (**Figure 10D**). In the present study, we observed a nonsignificant reduction in LVEDV during unloaded breathing which we believe will change with a greater sample size as the effect of attenuating ITP on LVEDV may be smaller than its effect on LVESV. Therefore, the reductions in SV observed in the present study were driven primarily by increases in LVESV (**Figure 10E**).

Although no difference was observed in LVEDV in the present study, a pressure gradient that can influence VR is the abdomino-thoracic pressure gradient (49). The abdomino-thoracic pressure gradient determines the amount of VR from the abdominal cavity to the thoracic cavity ($P_{ab} \rightarrow$ ITP). For example, during inspiration as the diaphragm contracts, P_{ab} will increase and compress the IVC thereby decreasing VR from the lower limbs (12,51). Moreover, the more negative ITP associated with spontaneous breathing and increased P_{ab} will enhance VR from the abdominal

cavity towards the thoracic cavity. However, whether IVC blood flow and VR will increase depends on the volume status of the IVC (49). When IVC blood volume is elevated, compression will increase relative VR (promoting more blood flow from the abdominal cavity towards the thoracic cavity). However, if IVC blood volume is low, compression will likely leave VR unchanged or decreased relative to the previous amount of blood flow back to the heart (52). Therefore, with respiratory muscle unloading, the abdomino-thoracic pressure gradient is attenuated as ITP will not become as negative. As such, changes in Pab will likely have a relatively greater influence on the abdomino-thoracic pressure gradient during unloaded breathing.

Left ventricular end-systolic volume significantly increased during unloaded breathing at every exercise intensity with no difference in the relative or absolute change from spontaneous and unloaded breathing between exercise intensities (**Figure 10E, Tables 3&4**). It is generally understood that attenuating ITP decreases the pressure gradient for LV ejection and therefore enhances LV function (and SV) when LV afterload remains unchanged (1). When considering the ITP side of the LV ejection pressure gradient (between ITP and arterial pressure), we found that LVESV and ΔP_{es} had a strong negative relationship at 30% and 60% W_{max} , suggesting that when the magnitude of P_{es} swings is reduced, LVESV increases (**Figure 20**). There was no relationship between LVESV and ΔP_{es} at 80% W_{max} which may be the result of a smaller sample as we had to remove one participant from the analysis due to poor image quality. Moreover, at high intensity exercise, the cardiovascular system is in a very different state compared to lower exercise intensities as mechanisms to enhance cardiac function (to meet the body's oxygen demands) are more prevalent (133). For example, at high exercise intensities, cardiovascular variables such as sympathetic nerve activity, cardiac contractility, heart rate, and venous return are elevated relative to low exercise intensities. Therefore, the impact of altering respiratory pressures may simply not

have as much of an impact at high intensity exercise and may be the reason for no relationship observed between LVESV and ΔP_{es} at 80% W_{max} .

Another potential reason for the rise in LVESV could be due to changes to the other side of the LV ejection pressure gradient, namely arterial pressure. Mean arterial pressure remained unchanged (nonsignificant increase) at 30% and 60% W_{max} with a significant rise at 80% W_{max} during unloaded compared to spontaneous breathing (**Figure 11C**). The rise in MAP at 80% W_{max} could explain why LVESV was elevated at that exercise intensity because when MAP (LV afterload) is elevated, the LV has to work harder to overcome the greater pressure and usually leads to a rise in LVESV and a decrease in SV (26). The findings regarding the increase in MAP observed is consistent with previous work that measured MAP during respiratory muscle unloading at submaximal exercise intensities (50% and 75% $\dot{V}O_{2max}$), such that a nonsignificant rise in MAP was observed (134). Although not significant, the magnitude increases in MAP observed at 30% and 60% W_{max} in the present study are similar to those others have observed at 50% and 75% $\dot{V}O_{2max}$ (134). However, the study investigating MAP at submaximal exercise intensities had a smaller sample size ($n=10$) and therefore likely had a smaller statistical power compared to the present study which could account for the nonsignificant result. Conversely, others have observed a nonsignificant decrease in MAP at maximal exercise (126), and submaximal exercise intensities (40% and 60% W_{max}) (117).

A possible explanation for the elevation in MAP during respiratory muscle unloading observed in the present study may be attributed to the arterial baroreceptors. The arterial baroreceptors located in the aortic arch will sense the reduction in arterial wall deformation and will send signals to the central nervous system to enhance sympathetic nerve activity (SNA) to the heart and vasculature in response (133). As such, this increase in SNA will increase HR, cardiac

contractility, and vascular resistance, which may explain why we observed increases in TPR and MAP (**Figure 11C&D**). However, HR decreased during unloaded breathing at 60% and 80% W_{max} (**Figure 10A**), therefore, if MAP increased due to action from the arterial baroreceptors, then it may be possible this stimulus was not sufficient to increase HR. Furthermore, another possible explanation for the observed rise in MAP may be due to action from the cardiopulmonary baroreceptors. The attenuated ITP will reduce the pressure gradient for VR resulting in less blood coming back to the heart. As such, less blood in the heart and pulmonary circulation will reduce the stretch of the cardiopulmonary baroreceptors and subsequently increase baroreceptor activity. As a result, SNA will increase which will cause a rise in vascular resistance to enhance blood flow back to the heart (133). Therefore, both the arterial and cardiopulmonary baroreceptors may be contributing to the observed rise in MAP and TPR with respiratory muscle unloading. Lastly, in the present study we investigated the PAV and the POST breathing conditions but did not examine the PRE breathing condition. It was decided to only examine the PAV and POST breathing conditions for the present study as the ventilatory and W_b data was more comparable than the PRE and PAV breathing conditions. Moreover, some participants did not completely reach a steady state during the PRE condition, especially at the higher exercise intensities, therefore, it was more feasible to use the POST breathing condition. Therefore, we are unable to provide information on how MAP changes from the PRE condition to the PAV condition or from the PRE condition to the POST condition. Both of which may display differing results from the present observations of how MAP is altered from the PAV to POST breathing condition.

Furthermore, another potential reason for the rise in LVESV observed during unloaded breathing at all exercise intensities could be due to changes in cardiac contractility. Currently, the mechanisms by which mechanical ventilation and attenuating ITPs on cardiac contractility remains

incompletely understood (1,3,4). However, mechanical ventilation may reduce cardiac contractility by altering 1) preload and afterload (1,3,4), 2) heart rate (135), 3) coronary perfusion (136,137), 4) modulation of ventricular geometry (136,138), and 5) muscle sympathetic nerve activity (MSNA) (117).

Cardiac contractility can be influenced by both preload and afterload. A rise in preload can increase the force of ventricular contraction via the Frank-Starling law of the heart as there is an increase in cross-bridge formation. As such, this could have enhanced cardiac contractility, however, a rise in afterload can also increase contractility via the Anrep effect (136). The Frank-Starling law of the heart relates that when preload is increased, more sarcomeres are recruited to increase the force of contraction to pump the greater blood volume out of the heart (139,140). However, there may be more complex mechanisms at work than just enhanced cross-bridge formation (141,142). Moreover, when afterload is elevated, LVESV increases and this will increase sarcomere length and subsequently increase the force of ventricular contraction (143). Moreover, since attenuating ITPs can decrease LV afterload, this theory would reduce contractility given the Anrep effect. Moreover, others have speculated that the associated rise in PVR with mechanical ventilation may attenuate LV contractility via a reduction in LV compliance. Since mechanical ventilation can increase PVR, this would increase RV afterload and RVESV thereby inhibiting the filling and contractile ability of the LV and therefore decreasing contractility (1). However, in the present study we observed a nonsignificant reduction in preload and a significant rise in LVESV. As such, from the Frank-Starling perspective, contractility would decrease, however, the observed rise in LVESV would increase contractility. Therefore, from a preload and afterload perspective, there is conflicting information regarding what could be happening with cardiac contractility.

Cardiac contractility can also be influenced by HR according to the Bowditch effect. The Bowditch effect explains that as HR increases, the myocardium has less time to remove intracellular calcium, allowing for more calcium to accumulate and subsequently lead to an increase in the force of myocardial contraction (3,135,144). As such, in the present study HR decreased significantly at 60% and 80% Wmax. Therefore, from a Bowditch perspective, reducing HR may reduce cardiac contractility and could have led to the observed rise in LVESV at 60% and 80% Wmax.

The implications of elevated ITPs on coronary blood flow has been hypothesized as a reason for a reduction in contractility during mechanical ventilation. A study investigating increases in pressure around an isolated heart found that myocardial blood flow decreased (145), with the idea that the greater pressures would disrupt myocardial blood flow and therefore contractile ability would be diminished. However, studies in intact dogs (146,147) and ICU patients found that coronary blood flow was not influenced by positive pressure mechanical ventilation or positive end-expiratory pressure (148). Moreover, others have suggested that mechanical ventilation has no influence on LV contractility, but the attenuated ITPs may decrease RV myocardial blood flow instead (137). Overall, the impact of mechanical ventilation on coronary blood flow requires further investigation.

Mechanical ventilation may influence cardiac contractility through changes in ventricular geometry. In dogs, LV geometry has been altered by positive pressure ventilation (149,150) and could lead to a reduction in cardiac contractility (136). Moreover, in dogs that underwent a vagotomy, systolic function was diminished suggesting that because neural involvement was attenuated, the changes in ventricular contractility were suggested to be due to the positive pressure impacting cardiac geometry (151). Furthermore, modulation of cardiac geometry can greatly

influence LV rotation and twist (152). LV twist mechanics can be altered by the degree of contraction and relaxation of the myocardium (153). As such, any aspect that increases cardiac contractility will increase rotation/twist and vice versa. Moreover, a rise in preload and/or afterload will either increase or decrease left ventricular rotation, respectively. It has been observed that when LVEDV is increased with a constant LVESV, LV twist will increase. Conversely, increasing LVESV with a constant LVEDV will decrease LV twist (154). Moreover, LV rotation can be enhanced by increases in SNA and when considering the present study, at high exercise intensities, SNA was likely elevated and could have impacted cardiac contractility. Conversely, since afterload can negatively impact contractility (from a LV twist mechanic perspective), at 80% Wmax when we observed an elevation in MAP, this may have reduced cardiac contractility. With respect to longitudinal strain, a study conducted in critically ill ICU patients found that there was a substantial reduction in RA, RV, and LA longitudinal strain during positive end-expiratory pressure ventilation with no change in LV longitudinal strain (155). Overall, to determine if respiratory muscle unloading impacts left ventricular twist mechanics and subsequently cardiac contractility requires further investigation in the future.

Lastly, cardiac contractility may be influenced by attenuations in MSNA (117). In a study investigating MSNA during respiratory muscle unloading found that MSNA was significantly reduced at all exercise intensities (40%, 60% and 80% Wmax) (117). Increases in SNA can cause increases in cardiac contractility and HR (156). Although not of similar magnitude, both SNA and MSNA may increase/decrease in the same direction. For example, if SNA is elevated, then it is probable that MSNA is also elevated. Therefore, if MSNA is reduced during respiratory muscle unloading, it is likely that SNA is also reduced. As such, a potential reduction in SNA may have

decreased cardiac contractility and led to the observed rise in LVESV. However, we did not measure MSNA in the present study.

6.2.2 Reductions in Heart Rate with Respiratory Muscle Unloading

The reduction in \dot{Q} observed during respiratory muscle unloading at 60% and 80% W_{max} was facilitated by a reduction in HR (**Figure 10A**). A reduction in HR is consistent with previous work looking at respiratory muscle unloading at different submaximal (40%, 60%, and 80% W_{max} (117) and maximal exercise intensities (126). It was hypothesized that the reduction in HR with unloaded breathing was due to action from the cardiopulmonary baroreceptors (117). The cardiopulmonary baroreceptors monitor blood volume in the heart and lungs. As such, since the PAV provides a positive P_m , this higher pressure may be sensed as a greater volume of blood in the thorax and will therefore cause the cardiopulmonary baroreceptors to signal the central nervous system to inhibit sympathetic nervous system activity, thereby resulting in a reduction in HR and systemic vascular resistance (133). However, others have suggested that the cardiopulmonary baroreceptors facilitate the resetting of the arterial baroreflex and impact blood pressure, with no impact on heart rate (157).

The arterial baroreceptors may also be responsible for a reduction in HR during respiratory muscle unloading. It may be possible that with the positive pressure provided by the PAV, this could be compressing the aortic arch and thereby having the arterial baroreceptors sense an increased blood pressure, thereby signalling the central nervous system to decrease SNA to the heart, such as HR and contractility and to modulate the vasculature resistance as well (133,158,159). The response by the arterial baroreceptors would cause a reduction in HR, but MAP should decrease via this mechanism as well. However, no change in MAP was observed in the present study at 30% and 60% W_{max} , with a significant rise at 80% W_{max} (**Figure 11C**). Overall,

the ITPs observed in the present study are unlikely to compress the aortic arch and there are many conflicting mechanisms at work during mechanical ventilation and the resulting attenuated ITPs that it is difficult to determine how the body may be responding. Moreover, it has been previously hypothesized that during mechanical ventilation, the fall in \dot{Q} and subsequently blood pressure would cause an increase in HR via the arterial baroreflex response (136). However, it has since been understood that with positive pressure ventilation, the expected rise in HR is attenuated (136). Several studies investigating the hemodynamics of mechanical ventilation have also observed a reduction in HR (146,147,160).

6.3 Relationship Between Cardiac Output and Oxygen Consumption

During respiratory muscle unloading, the relationship between \dot{Q} and $\dot{V}O_2$ was disrupted in the present study (**Figures 12, 13&15**). Oxygen consumption was only observed to decrease at 80% W_{max} with no change at 30% and 60% W_{max} (**Figure 8**). During spontaneous breathing while exercising at high intensities, there is a considerable increase in ventilation compared to that of rest and low exercise intensities (12). This rise in ventilation has an exponential relationship with the W_b whereby small increases in ventilation can cause large increases in the W_b (111). As such, during high intensity exercise, there are higher levels of ventilation and a greater W_b . At maximal exercise, respiratory muscle $\dot{V}O_2$ is approximately 9-15% (125,161) of total $\dot{V}O_2$ and requires a similar amount of \dot{Q} (126). Therefore, during maximal exercise, blood flow is preferentially sent to the respiratory muscles and away from the working locomotor muscles (127). With respiratory muscle unloading, it has been shown that this competition for blood flow between the respiratory muscles and the limb locomotor muscles is reduced as respiratory muscle work decreases, decreasing $\dot{V}O_2$ and subsequently \dot{Q} whereby since the competition is gone, leg blood flow increases and performance is enhanced (127). In the present study, we observed a strong

positive relationship between the W_b and $\dot{V}O_2$ at 80%, but not at 30% and 60% W_{max} (**Figure 9**). Respiratory muscle $\dot{V}O_2$ is not substantial at low and moderate exercise intensities. As such, when the respiratory muscles were unloaded, the work of the respiratory muscles was reduced, thereby decreasing oxygen demand. There was likely no relationship observed between the W_b and $\dot{V}O_2$ at 30% and 60% W_{max} when considering respiratory muscle unloading because the change in W_b was likely too small to induce a notable change in $\dot{V}O_2$. For every 1 J min^{-1} reduction in the W_b , it is understood that there should approximately be a 1 mL min^{-1} reduction in $\dot{V}O_2$ (125,161). In the present study, we observed this relationship between W_b and $\dot{V}O_2$ to remain true as we observed similar reductions in $\dot{V}O_2$ for a decrease in the W_b . Specifically, at 30% W_{max} , there was an absolute reduction in W_b of 15.3 J min^{-1} , therefore the predicted drop in $\dot{V}O_2$ was ~15 mL min^{-1} and the observed drop was 20 mL min^{-1} . At 60% W_{max} , W_b decreased by 39.6 J min^{-1} therefore $\dot{V}O_2$ was predicted to decrease by ~39 mL min^{-1} and it decreased by 35 mL min^{-1} . Lastly, the W_b decreased by 71.2 J min^{-1} at 80% W_{max} and the predicted reduction in $\dot{V}O_2$ was ~71 mL min^{-1} and we observed at 74 mL min^{-1} reduction in $\dot{V}O_2$ (**Table 4**). We attribute the changes in $\dot{V}O_2$ with respiratory muscle unloading to be due to changes in respiratory muscle $\dot{V}O_2$ as locomotor muscle $\dot{V}O_2$ should not be different between unloaded and spontaneous breathing. Moreover, at low relative to high exercise intensities, respiratory muscle $\dot{V}O_2$ is not very high as ventilation and respiratory muscle work is lower. Taken together, the primary reason for the observed reduction in $\dot{V}O_2$ at 80% W_{max} in the present study is likely because of the reduction in W_b causing a reduction in $\dot{V}O_2$ and therefore \dot{Q} . Lastly, the reason why there is a relationship between \dot{Q} and $\dot{V}O_2$ at 80% W_{max} when considering respiratory muscle unloading (**Figure 13**) is because of the increased work of breathing at higher exercise intensities from the elevated ventilations that require a greater $\dot{V}O_2$ and \dot{Q} . Therefore when respiratory muscle work is decreased, $\dot{V}O_2$ and \dot{Q} also

decrease. There is not a relationship between \dot{Q} and $\dot{V}O_2$ at 30% and 60% W_{max} during respiratory muscle unloading because \dot{Q} has not yet been maximized and respiratory muscle $\dot{V}O_2$ is not changing significantly at lower exercise intensities.

Lastly, another potential reason for the reduction in $\dot{V}O_2$ observed at 80% W_{max} could be the result of a reduction in HR. There was a nonsignificant moderate positive relationship observed between HR and $\dot{V}O_2$ at 80% W_{max} ($p=0.06$) (**Figure 22C**). The idea behind this relationship is that when HR decreases (as with respiratory muscle unloading), this will decrease the myocardial work and contribute to a reduction in $\dot{V}O_2$ (117,162).

Overall, during respiratory muscle unloading the relationship between \dot{Q} and $\dot{V}O_2$ was only significant at 80% W_{max} (**Figure 13**), thereby suggesting that \dot{Q} decreased by mechanisms independent of $\dot{V}O_2$ at 30% and 60% W_{max} . Moreover, the reduction in \dot{Q} observed at 30% and 60% W_{max} appears to be linked to attenuating the magnitude swings in P_{es} rather than mean P_{es} (**Figure 17**). The reductions in \dot{Q} are primarily the result of decreases in SV (**Figure 18**) rather than HR, with a rise in LVESV observed (**Figure 20**) rather than reductions in LVEDV (**Figure 19**). Lastly, this reduction in \dot{Q} at 80% W_{max} could also be due to the relationship observed between HR and $\dot{V}O_2$.

6.4 Case Studies

The following two sections describe the physiological responses to respiratory muscle unloading in two participants. Both participants had very different responses to proportional assist ventilation and the attenuation in ITPs. One participant had the greatest reduction in \dot{Q} out of all the participants, while the other observed an increase in \dot{Q} . The participants in the present study did not all have the same response to respiratory muscle unloading as there was some variability. For example, some participants observed a reduction in LVEDV, while others had no change or

an increase in LVEDV. Therefore, the purpose of this section is to describe the potential physiological reasons for why these two participants had very different responses to respiratory muscle unloading.

6.4.1 Participant with the Greatest Reduction in Cardiac Output also had the Greatest rise in Intrathoracic Pressure

Participant 026 was exercising at 80% W_{max} when the PAV was turned on and mean P_m increased by 6.9 cmH₂O to reach a mean P_m of 7.8 cmH₂O. Mean P_{es} decreased by -11.3 cmH₂O to reach a mean P_{es} of -0.9 cmH₂O. With the magnitude of P_{es} swings decreasing by 10.1 cmH₂O for an average ΔP_{es} of 28.0 cmH₂O while on the PAV. Therefore, the pressure gradient for breathing changed during unloaded breathing whereby breathing was not being driven by the more negative ITP, rather it was the more positive P_m driving the pressure gradient to breath, as such, mean P_{es} and the magnitude of P_{es} swings decreased as a result. The less negative ITPs decreased the pressure gradient for VR. Although not ideal, we determined VR by assessing LVEDV in the present study. Therefore, LVEDV decreased by 37 mL, whereby LVEDV during unloaded breathing was 114 mL and increased to 151 mL during spontaneous breathing. As a result, SV also decreased by 37 mL, leading to a SV of 95 mL during unloaded breathing and 132 mL during spontaneous breathing. The reduction in SV was the result of a reduction in LVEDV as there was no change in LVESV between unloaded and spontaneous breathing (both 19 mL). In this participant, MAP in the PRE condition (before the PAV was turned on), was 124.9 mmHg and decreased by 3.8 mmHg when the PAV was turned on. When examining the PAV and POST condition, MAP was elevated by 9.1 mmHg during the PAV condition compared to the POST condition whereby on the PAV, MAP was 113.1 mmHg and during the POST condition it was 103.9 mmHg. As such, the transmural LV ejection pressure gradient (ITP \rightarrow MAP) was increased

on the PAV (154.7 cmH₂O vs. 147.7 cmH₂O, during unloaded (PAV) and spontaneous breathing (POST), respectively), thereby placing more work onto the LV to pump blood out of the heart. However, no change was observed in LVESV in this participant.

A potential mechanism for a reduction in LVEDV could be the result of changes in the abdomino-thoracic pressure gradient between unloaded and spontaneous breathing. Mean P_{ab} was 7.2 cmH₂O during unloaded breathing and 2.9 cmH₂O during spontaneous breathing. As such, it was determined that the transmural pressure was less during unloaded breathing compared to spontaneous breathing (8.2 cmH₂O vs. 9.3 cmH₂O for unloaded and spontaneous breathing, respectively). Therefore, suggesting that during unloaded breathing the pressure gradient for blood flow from the abdomen to thorax was reduced compared to spontaneous breathing therefore this may have contributed to the reduction in LVEDV observed. Moreover, an elevated P_{ab} can compress the IVC and decrease VR from the lower limbs.

Moreover, HR decreased during unloaded breathing by 2.5 bpm whereby HR during unloaded breathing was 167.5 bpm and 170 bpm during spontaneous breathing. This reduction in HR could have decreased this participants' myocardial work and therefore $\dot{V}O_2$ as well. Moreover, there was a substantial reduction in the W_b . The W_b decreased by 118.8 J min⁻¹ from spontaneous to unloaded breathing whereby during unloaded breathing the W_b was 190.6 J min⁻¹ and during spontaneous breathing it was 309.5 J min⁻¹. This reduction in respiratory muscle work caused $\dot{V}O_2$ to decrease by 0.13 L min⁻¹ from spontaneous to unloaded breathing. Overall, the reduction in $\dot{V}O_2$ as well as HR and SV contributed to a reduction in \dot{Q} .

In this participant, the large increase (less negative) in ITP impacted the heart considerably. The less negative ITP combined with the more positive P_{ab} reduced the pressure gradient for VR from the abdomen compared with spontaneous breathing. This reduction in VR decreased LV

preload which subsequently decreased SV and \dot{Q} . Moreover, as respiratory muscle work was reduced, $\dot{V}O_2$ and \dot{Q} decreased as well. Lastly, because of the known influence of greater/more positive Pm on the cardiopulmonary baroreceptors, the higher pressure likely caused action from the cardiopulmonary baroreceptors to ultimately decrease SNA and HR. As such, this reduction in HR likely contributed to a reduction in myocardial work and therefore $\dot{V}O_2$ as well. Overall, this participant had the greatest reduction in mean Pes and a large reduction in the magnitude of Pes swings which resulted in the greatest change in \dot{Q} from spontaneous to unloaded breathing.

6.4.2 Participant with the Smallest Change in Cardiac Output had the Smallest Reduction in the Magnitude of Intrathoracic Pressure Swings

Participant 015 was exercising at 80% Wmax when the PAV was turned on and Pm increased by 3.1 cmH₂O, whereby mean Pm was 3.7 cmH₂O during unloaded breathing and 0.6 cmH₂O during spontaneous breathing. As such, this rise in Pm altered the pressure gradient for breathing as mean Pes increased by 2.9 cmH₂O whereby during unloaded breathing, mean Pes was -0.7 cmH₂O and -3.6 cmH₂O during spontaneous breathing. Therefore, during unloaded breathing, the pressure gradient for breathing was driven primarily by the more positive Pm rather than the more negative Pes as is with spontaneous breathing. The magnitude of esophageal pressure swings decreased by 1.5 cmH₂O, whereby the magnitude of Pes pressure swings was 25.4 cmH₂O during unloaded breathing and 26.9 cmH₂O during spontaneous breathing. The small difference in Δ Pes between unloaded and spontaneous breathing suggests that the heart was exposed to a similar magnitude of ITP changes and that VR was likely similar between breathing conditions as well. The pressure gradient for VR from the abdomen (Pab \rightarrow ITP), was very similar and a bit greater during spontaneous breathing (13.1 vs. 13.7 cmH₂O for unloaded and spontaneous breathing, respectively). Abdominal pressure increased during unloaded breathing by 2.3 cmH₂O with a mean

Pab of 12.5 cmH₂O during unloaded and 10.1 cmH₂O during spontaneous breathing. However, since ITP was made less negative while breathing on the PAV, the overall pressure gradient for VR from the abdomen decreased by 0.6 cmH₂O suggesting that there was slightly less VR from the abdomen during unloaded breathing. Moreover, since Pab was elevated during unloaded breathing, this may have compressed the IVC and hindered VR from this mechanism as well. However, Δ Pab was greater in this individual during unloaded breathing (13.6 vs. 10.5 cmH₂O for unloaded and spontaneous breathing, respectively). As such, the larger swings in Pab could have contributed to a greater VR which may have led to the observed rise in LVEDV in this participant. Overall, preload may have increased from several mechanisms that we were unable to measure in the present study (*e.g.*, IVC blood volume, circulating catecholamines, skeletal muscle pump, etc).

During unloaded breathing, LVEDV increased by 16.5 mL, whereby LVEDV was 109 mL during unloaded and 92.5 mL during spontaneous breathing. Due to the elevation in preload, SV increased by 5.5 mL (75.5 mL during unloaded breathing and 70 mL during spontaneous breathing). This rise in SV led \dot{Q} to increase by 0.46 L min⁻¹ as \dot{Q} was 12.1 L min⁻¹ during unloaded and 11.7 L min⁻¹ during spontaneous breathing. Left ventricular afterload was elevated during unloaded breathing as MAP increased by 6.9 mmHg, with an average MAP of 156.8 mmHg during unloaded and 149.4 mmHg during spontaneous breathing. This elevation in LV afterload may have led to a rise in LVESV of 11 mL as LVESV was 33.5 mL during unloaded and 22.5 mL during spontaneous breathing. Moreover, LV transmural pressure was greater during unloaded breathing compared to spontaneous breathing (212.5 vs. 199.5 cmH₂O for unloaded and spontaneous breathing respectively). The elevated LV transmural pressure suggests that it was more difficult for the LV to pump blood out of the heart during unloaded breathing.

Despite a rise in \dot{Q} of 0.46 L min^{-1} during unloaded breathing, there was a reduction in HR by 6 bpm whereby HR was 161 bpm during unloaded and 167 bpm during spontaneous breathing. Given that a reduction in HR should decrease \dot{Q} , the elevation in SV likely maintained \dot{Q} in this participant. Overall, the observed decrease in HR likely prevented \dot{Q} from increasing greater than 0.46 L min^{-1} during unloaded breathing.

Lastly, the W_b decreased by 48.8 J min^{-1} with a W_b of 52.7 J min^{-1} during unloaded breathing and 101.5 J min^{-1} during spontaneous breathing. Subsequently leading to a 0.044 L min^{-1} reduction in $\dot{V}O_2$, whereby $\dot{V}O_2$ was 1.85 L min^{-1} during unloaded and 1.894 L min^{-1} during spontaneous breathing. The reduction in HR may have also contributed to the decrease in $\dot{V}O_2$ and likely prevented \dot{Q} from increasing more than 0.46 L min^{-1} . Overall, this participant had the smallest change in the magnitude of Pes swings and a minor change in mean Pes changes which led to a similar \dot{Q} between unloaded and spontaneous breathing. Despite relatively no difference in the abdomino-thoracic pressure gradient between unloaded and spontaneous breathing, VR was likely enhanced by mechanisms we were unable to measure which led to a rise in LVEDV. Lastly, afterload was elevated in this participant which may have contributed to the observed rise in LVESV during unloaded breathing. Overall, this participant had the smallest reduction in ΔPes which led to a minor increase in \dot{Q} from spontaneous to unloaded breathing.

6.5 Technical Considerations and Limitations

There are several limitations to the present study which warrant further discussion. First, the participants performed all aspects of this study in a semi-recumbent position so as to allow for high quality echocardiographic image acquisition. The semi-recumbent position does not reflect upright exercise as there are many cardiovascular differences associated with changes in body position. For example, in the semi-recumbent position, hydrostatic pressure is more evenly

distributed which can enhance venous return, preload and \dot{Q} compared to the upright position. A higher thoracic blood volume and cardiac filling will trigger action from the cardiopulmonary baroreceptors which will lead to the inhibition of sympathetic nervous system activity causing reductions to chronotropic, inotropic and vascular resistance activity (163). Moreover, due to the semi-recumbent position, participants likely did not reach a true $\dot{V}O_2\text{max}$ during experimental testing day 1 (117). Second, we used photoelectric plethysmography to measure beat-by-beat blood pressure which requires the hand and finger that the blood pressure cuff is attached to remain still for the duration of the blood pressure measurement. Due to the intensity of exercise performed, it was challenging for participants to keep their hand still despite verbal encouragement. Precautions were taken to improve the quality of the blood pressure measurement such as correcting for height, calibrating before use and warming the participants hand and fingers when needed. Despite the precautions taken, our blood pressure measurements were susceptible to motion artefacts. Third, the exercise intensities performed in this study were sequential and not randomized so as to avoid potential sympathetic carryover effects. For example, if the 80% W_{max} exercise intensity was performed before the 30% W_{max} intensity, the effects of greater sympathetic stimulation developed during the high exercise intensity would remain elevated for a longer time following completion of the exercise, such as elevated heart rate and contractility. Since this study focused on SV, HR and \dot{Q} , an elevation in baseline chronotropic and inotropic activity before beginning an exercise trial would skew our results as greater HR and contractility can reduce the time for cardiac filling and SV and \dot{Q} measures would not be accurate. As such, we were unable to control for the multiple treatment interference threat to external validity. Fourth, we were unable to blind the participants to the intervention (unloaded breathing) due to the sensation of positive pressure applied by the ventilator as well as the familiarization trial that occurred on experimental

testing day 2. We needed to perform the familiarization trial in order to coach the participants on how to accept the ventilatory support and relax the respiratory muscles so as to maximize the potential for respiratory muscle unloading on experimental testing day 3. Moreover, because we coached the participants during the familiarization trial, this may have altered breathing pattern and the control of breathing (120). Fifth, cardiac output determination using the Simpson's Biplane analysis can underestimate SV and \dot{Q} measurements compared to that of the velocity time integral method (164) as well as magnetic resonance imaging (165). When comparing the use of echocardiography in general to determine \dot{Q} (including Doppler and two-dimensional echocardiography), echocardiography has been shown to obtain similar results when compared to thermodilution techniques at rest (166) and to the Fick equation during exercise (167). However, others have suggested that echocardiography can determine directional changes in \dot{Q} , but the magnitude of change may vary considerably when compared with thermodilution (168). Moreover, the accuracy of echocardiography on LV volumetric analysis is dependent on the ability of the sonographer to obtain quality cardiac images (e.g. remaining on axis) as well as the participant having optimal cardiac windows. As such, we chose a sonographer with previous experience collecting cardiac images during exercise and we only included participants that had good quality cardiac windows as determined by participant screening prior to data collection. Acquisition of quality left ventricular cardiac images depends on multiple factors, such as the risk of foreshortening which can lead to volume underestimation (130). The typical protocol for obtaining cardiac images is to have participants exhale and hold their breath at a static lung volume at or near functional residual capacity during image acquisition so as to limit lung interference and improve cardiac image quality. However, we did not have participants perform a static breath hold and rather collected the cardiac images during spontaneous breathing which may have decreased

our image quality. However, to promote the accuracy of our cardiac analysis, we analyzed multiple cardiac cycles per trial/stage during expiration and we were conservative with the Simpson's Biplane analysis. Moreover, we were unable to perform the cardiac analysis strictly at end-expiration and rather performed the analysis during expiration because there were not enough cardiac cycles at end-expiration to analyze per person/per trial. Therefore, we chose to analyze the cardiac cycles during expiration as determined by the respiratory trace. Lastly, we did not calculate a-vO₂ difference in the present study as our absolute values may be inaccurate compared to others. There are two potential discrepancies with our absolute a-vO₂ difference values. First, since our measure of \dot{Q} via echocardiography is underestimated compared to other methods of determining \dot{Q} , the absolute values for a-vO₂ difference in our study may overestimate those of others. Second, our measurements of $\dot{V}O_2$ and \dot{Q} were not completed at the same time which may account for discrepancies in the magnitude change in our values of a-vO₂ difference.

6.6 Future Directions

There are several avenues for future directions from the present study. First, obtaining a more accurate measure of blood pressure through the use of arterial catheters would be beneficial for the investigation of blood pressure regulation during respiratory muscle unloading. Using arterial catheters rather than photoelectric plethysmography would eliminate measurement error and allow for a better determination of blood pressure and the potential changes to LV ejection and TPR. Second, investigations into LV geometry and twist mechanics with respiratory muscle unloading should be completed to determine their potential influence on cardiac contractility. Determining cardiac contractility would better elucidate the mechanisms behind the observed elevation in LVESV at all exercise intensities with respiratory muscle unloading. Third, investigating the implications of sex differences on cardiac function with respiratory muscle

unloading may warrant future investigations. Although not the purpose of the present study, females generally have smaller conducting airways compared to males (119,169), thereby potentially resulting in greater magnitude changes in ITP. Due to enhanced ITP swings, it is possible females may rely on respiration more for cardiac preload and SV compared to males. Lastly, examining cardiorespiratory interactions during exercise in older individuals would be beneficial. Aging is associated with several detriments to the lungs, airways, chest wall, and respiratory muscles (170,171), such as destruction of the lung parenchyma (172), stiffening of the thoracic cage (173), and reduction in respiratory muscle strength (174). Therefore, compared to younger individuals, older individuals have a greater W_b for a given ventilation. As such, older individuals may rely on greater respiratory pressures for VR, preload, SV, and \dot{Q} . Moreover, older individuals may have a greater percentage of \dot{Q} distributed to the respiratory muscles during exercise. Therefore, determining how respiratory muscle unloading influences cardiac function in healthy aging would be beneficial in determining how aging influences the cardiorespiratory system.

7.0 CONCLUSION

Attenuating ITPs with the use of proportional assist ventilation has considerable influence on cardiac function. Cardiac output decreased at all exercise intensities with respiratory muscle unloading. The reductions in \dot{Q} were mediated primarily by the impact of attenuating ITP on SV and reducing metabolic demand secondary to a decline in the W_b . At low exercise intensities, \dot{Q} decreased primarily by attenuations in SV. During moderate intensity exercise, \dot{Q} decreased by both reductions in SV and HR, while at high intensity exercise, \dot{Q} decreased due to reductions in SV, HR and $\dot{V}O_2$. Therefore, by attenuating ITP, the importance of normally occurring swings in ITP is demonstrated with respect to aiding cardiac function. In conclusion, respiration and its associated pressures are helpful in maintaining \dot{Q} during exercise.

REFERENCES

1. Mahmood SS, Pinsky MR. Heart-lung interactions during mechanical ventilation: the basics. *Ann Transl Med.* 2018 Sep;6(18):349.
2. Cheyne WS, Harper MI, Gelinac JC, Sasso JP, Eves ND. Mechanical cardiopulmonary interactions during exercise in health and disease. *J Appl Physiol Bethesda Md* 1985. 2020 May 1;128(5):1271–9.
3. Grübler MR, Wigger O, Berger D, Blöchlinger S. Basic concepts of heart-lung interactions during mechanical ventilation. *Swiss Med Wkly.* 2017;147:w14491.
4. Pinsky MR. The hemodynamic consequences of mechanical ventilation: an evolving story. *Intensive Care Med.* 1997 May;23(5):493–503.
5. Stray-Gundersen J, Musch TI, Haidet GC, Swain DP, Ordway GA, Mitchell JH. The effect of pericardiectomy on maximal oxygen consumption and maximal cardiac output in untrained dogs. *Circ Res.* 1986 Apr;58(4):523–30.
6. Lloyd TC. Mechanical cardiopulmonary interdependence. *J Appl Physiol.* 1982 Feb;52(2):333–9.
7. Taylor RR, Covell JW, Sonnenblick EH, Ross J. Dependence of ventricular distensibility on filling of the opposite ventricle. *Am J Physiol.* 1967 Sep;213(3):711–8.
8. Belenkie I, Dani R, Smith E R, Tyberg J V. Ventricular interaction during experimental acute pulmonary embolism. *Circulation.* 1988 Sep 1;78(3):761–8.
9. Moreno AH, Katz AI, Gold LD. An integrated approach to the study of the venous system with steps toward a detailed model of the dynamics of venous return to the right heart. *IEEE Trans Biomed Eng.* 1969 Oct;16(4):308–24.
10. Johnson BD, Babcock MA, Suman OE, Dempsey JA. Exercise-induced diaphragmatic fatigue in healthy humans. *J Physiol.* 1993;460(1):385–405.
11. Guenette JA, Querido JS, Eves ND, Chua R, Sheel AW. Sex differences in the resistive and elastic work of breathing during exercise in endurance-trained athletes. *Am J Physiol Regul Integr Comp Physiol.* 2009 Jul;297(1):R166-175.
12. Sheel AW, Romer LM. Ventilation and respiratory mechanics. *Compr Physiol.* 2012 Apr;2(2):1093–142.
13. Henke KG, Sharratt M, Pegelow D, Dempsey JA. Regulation of end-expiratory lung volume during exercise. *J Appl Physiol.* 1988 Jan 1;64(1):135–46.
14. Sheel AW. Respiratory Muscle Training in Healthy Individuals. *Sports Med.* 2002 Aug 1;32(9):567–81.

15. Dominelli P, Wiggins C, Roy T, Secomb T, Curry T, Joyner M. The oxygen cascade during exercise in health and disease. *Mayo Clinic Proceedings*;
16. Kubiak GM, Ciarka A, Biniecka M, Ceranowicz P. Right Heart Catheterization—Background, Physiological Basics, and Clinical Implications. *J Clin Med*. 2019 Aug 28;8(9):1331.
17. Miller JD, Pegelow DF, Jacques AJ, Dempsey JA. Skeletal muscle pump versus respiratory muscle pump: modulation of venous return from the locomotor limb in humans. *J Physiol*. 2005 Mar 15;563(Pt 3):925–43.
18. Guyton AC, Lindsey AW, Abernathy B, Richardson T. Venous return at various right atrial pressures and the normal venous return curve. *Am J Physiol*. 1957 Jun;189(3):609–15.
19. Wise RA, Robotham JL, Summer WR. Effects of spontaneous ventilation on the circulation. *Lung*. 1981 Dec 1;159(1):175–86.
20. Stickland MK, Welsh RC, Petersen SR, Tyberg JV, Anderson WD, Jones RL, et al. Does fitness level modulate the cardiovascular hemodynamic response to exercise? *J Appl Physiol Bethesda Md* 1985. 2006 Jun;100(6):1895–901.
21. Pinsky MR. Cardiopulmonary Interactions: Physiologic Basis and Clinical Applications. *Ann Am Thorac Soc*. 2018 Feb;15(Suppl 1):S45–8.
22. Brecher GA, Hubay CA. Pulmonary Blood Flow and Venous Return During Spontaneous Respiration. *Circ Res*. 1955 Mar 1;3(2):210–4.
23. Scharf SM, Graver LM, Khilnani S, Balaban K. Respiratory phasic effects of inspiratory loading on left ventricular hemodynamics in vagotomized dogs. *J Appl Physiol*. 1992 Sep 1;73(3):995–1003.
24. Aliverti A, Bovio D, Fullin I, Dellacà RL, Lo Mauro A, Pedotti A, et al. The abdominal circulatory pump. *PloS One*. 2009;4(5):e5550.
25. Wexler L, Bergel DH, Gabe IT, Makin GS, Mills CJ. Velocity of blood flow in normal human venae cavae. *Circ Res*. 1968 Sep;23(3):349–59.
26. Pinsky MR. Heart-lung interactions. *Curr Opin Crit Care*. 2007 Oct;13(5):528–31.
27. Pinsky MR. The Hemodynamic Effects of Artificial Ventilation. In: Vincent JL, editor. *Update 1988* [Internet]. Berlin, Heidelberg: Springer; 1988 [cited 2021 May 13]. p. 187–201. (Update in Intensive Care and Emergency Medicine). Available from: https://doi.org/10.1007/978-3-642-83392-2_26
28. Buda AJ, Pinsky MR, Ingels NB, Daughters GT, Stinson EB, Alderman EL. Effect of intrathoracic pressure on left ventricular performance. *N Engl J Med*. 1979 Aug 30;301(9):453–9.

29. Pinsky MR, Summer WR, Wise RA, Permutt S, Bromberger-Barnea B. Augmentation of cardiac function by elevation of intrathoracic pressure. *J Appl Physiol*. 1983 Apr;54(4):950–5.
30. Shuey CB, Pierce AK, Johnson RL. An evaluation of exercise tests in chronic obstructive lung disease. *J Appl Physiol*. 1969 Aug;27(2):256–61.
31. Beyar R, Goldstein Y. Model studies of the effects of the thoracic pressure on the circulation. *Ann Biomed Eng*. 1987;15(3–4):373–83.
32. Saltin B, Rådegran G, Koskolou MD, Roach RC. Skeletal muscle blood flow in humans and its regulation during exercise. *Acta Physiol Scand*. 1998;162(3):421–36.
33. Summer WR, Permutt S, Sagawa K, Shoukas AA, Bromberger-Barnea B. Effects of spontaneous respiration on canine left ventricular function. *Circ Res*. 1979 Dec 1;45(6):719–28.
34. De Troyer A, Wilson TA. Effect of acute inflation on the mechanics of the inspiratory muscles. *J Appl Physiol Bethesda Md* 1985. 2009 Jul;107(1):315–23.
35. Grimby G, Goldman M, Mead J. Respiratory muscle action inferred from rib cage and abdominal V-P partitioning. *J Appl Physiol*. 1976 Nov;41(5 Pt. 1):739–51.
36. Guenette JA, Witt JD, McKenzie DC, Road JD, Sheel AW. Respiratory mechanics during exercise in endurance-trained men and women. *J Physiol*. 2007;581(3):1309–22.
37. Dempsey JA, La Gerche A, Hull JH. Is the Healthy Respiratory System Built Just Right, Overbuilt or Underbuilt to Meet the Demands Imposed by Exercise? *J Appl Physiol* [Internet]. 2020 Aug 13 [cited 2020 Oct 7]; Available from: <https://journals.physiology.org/doi/abs/10.1152/jappphysiol.00444.2020>
38. Whittenberger JL, McGregor M, Berglund E, Borst HG. Influence of state of inflation of the lung on pulmonary vascular resistance. *J Appl Physiol*. 1960 Sep 1;15(5):878–82.
39. Permutt S, Wise RA. Mechanical Interaction of Respiration and Circulation. In: *Comprehensive Physiology* [Internet]. American Cancer Society; 2011 [cited 2021 May 11]. p. 647–56. Available from: <https://onlinelibrary.wiley.com/doi/abs/10.1002/cphy.cp030336>
40. Katayama K, Dominelli PB, Foster GE, Kipp S, Leahy MG, Ishida K, et al. Respiratory modulation of sympathetic vasomotor outflow during graded leg cycling. *J Appl Physiol Bethesda Md* 1985. 2021 Aug 1;131(2):858–67.
41. West JB. *Respiratory Physiology: The Essentials*. Lippincott Williams & Wilkins; 2012. 211 p.
42. Steingrub JS, Tidswell M, Higgins TL. Hemodynamic Consequences of Heart-Lung Interactions. *J Intensive Care Med*. 2003 Mar 1;18(2):92–9.

43. Cassidy SS, Ramanathan M. Dimensional analysis of the left ventricle during PEEP: relative septal and lateral wall displacements. *Am J Physiol.* 1984 Jun;246(6 Pt 2):H792-805.
44. Morgan BC, Dillard DH, Guntheroth WG. Effect of cardiac and respiratory cycle on pulmonary vein flow, pressure, and diameter. *J Appl Physiol.* 1966 Jul;21(4):1276-80.
45. Howell JBL, Permutt S, Proctor DF, Riley RL. Effect of inflation of the lung on different parts of pulmonary vascular bed. *J Appl Physiol.* 1961 Jan 1;16(1):71-6.
46. Scharf SM, Brown R, Tow DE, Parisi AF. Cardiac effects of increased lung volume and decreased pleural pressure in man. *J Appl Physiol.* 1979 Aug 1;47(2):257-62.
47. Janicki JS. Influence of the pericardium and ventricular interdependence on left ventricular diastolic and systolic function in patients with heart failure. *Circulation.* 1990 Feb;81(2 Suppl):III15-20.
48. Kovacs G, Olschewski A, Berghold A, Olschewski H. Pulmonary vascular resistances during exercise in normal subjects: a systematic review. *Eur Respir J.* 2012 Feb 1;39(2):319-28.
49. Takata M, Wise RA, Robotham JL. Effects of abdominal pressure on venous return: abdominal vascular zone conditions. *J Appl Physiol.* 1990 Dec 1;69(6):1961-72.
50. Glenny RW, Bernard S, Robertson HT, Hlastala MP. Gravity is an important but secondary determinant of regional pulmonary blood flow in upright primates. *J Appl Physiol Bethesda Md* 1985. 1999 Feb;86(2):623-32.
51. Willeput R, Rondeux C, De Troyer A. Breathing affects venous return from legs in humans. *J Appl Physiol.* 1984 Oct;57(4):971-6.
52. Takata M, Robotham JL. Effects of inspiratory diaphragmatic descent on inferior vena caval venous return. *J Appl Physiol Bethesda Md* 1985. 1992 Feb;72(2):597-607.
53. Guyton AC, Adkins LH. Quantitative aspects of the collapse factor in relation to venous return. *Am J Physiol.* 1954 Jun;177(3):523-7.
54. Ainsworth DM, Smith CA, Eicker SW, Henderson KS, Dempsey JA. The effects of locomotion on respiratory muscle activity in the awake dog. *Respir Physiol.* 1989 Nov;78(2):145-62.
55. Grassino AE, Derenne JP, Almirall J, Milic-Emili J, Whitelaw W. Configuration of the chest wall and occlusion pressures in awake humans. *J Appl Physiol.* 1981 Jan;50(1):134-42.
56. Rowell LB, Rowell P of P and BLB. *Human Cardiovascular Control.* Oxford University Press; 1993. 522 p.
57. Hogan MC, Grassi B, Samaja M, Stary CM, Gladden LB. Effect of contraction frequency on the contractile and noncontractile phases of muscle venous blood flow. *J Appl Physiol Bethesda Md* 1985. 2003 Sep;95(3):1139-44.

58. Stewart JM, Medow MS, Montgomery LD, McLeod K. Decreased skeletal muscle pump activity in patients with postural tachycardia syndrome and low peripheral blood flow. *Am J Physiol Heart Circ Physiol*. 2004 Mar;286(3):H1216-1222.
59. Miller JD, Pegelow DF, Jacques AJ, Dempsey JA. Effects of augmented respiratory muscle pressure production on locomotor limb venous return during calf contraction exercise. *J Appl Physiol*. 2005 Nov 1;99(5):1802–15.
60. Perko MJ, Nielsen HB, Skak C, Clemmesen JO, Schroeder TV, Secher NH. Mesenteric, coeliac and splanchnic blood flow in humans during exercise. *J Physiol*. 1998;513(3):907–13.
61. Thomas DP, Fregin GF. Cardiorespiratory and metabolic responses to treadmill exercise in the horse. *J Appl Physiol*. 1981 Apr;50(4):864–8.
62. Stewart IB, Warburton DER, Hodges ANH, Lyster DM, McKenzie DC. Cardiovascular and splenic responses to exercise in humans. *J Appl Physiol*. 2003;94:8.
63. Aliverti A, Uva B, Laviola M, Bovio D, Mauro AL, Tarperi C, et al. Concomitant ventilatory and circulatory functions of the diaphragm and abdominal muscles. *J Appl Physiol*. 2010 Sep 2;109(5):1432–40.
64. Uva B, Aliverti A, Bovio D, Kayser B. The “Abdominal Circulatory Pump”: An Auxiliary Heart during Exercise? *Front Physiol* [Internet]. 2016 [cited 2021 May 11];6. Available from: <https://www.frontiersin.org/articles/10.3389/fphys.2015.00411/full>
65. Laviolette L, O’Donnell DE, Webb KA, Hamilton AL, Kesten S, Maltais F. Performance during constant workrate cycling exercise in women with COPD and hyperinflation. *COPD*. 2009 Oct;6(5):340–51.
66. Rocha A, Arbex FF, Sperandio PA, Mancuso F, Marillier M, Bernard AC, et al. Exercise intolerance in comorbid COPD and heart failure: the role of impaired aerobic function. *Eur Respir J*. 2019 Apr;53(4):1802386.
67. Behnia M, Wheatley CM, Avolio A, Johnson BD. Alveolar–capillary reserve during exercise in patients with chronic obstructive pulmonary disease. *Int J Chron Obstruct Pulmon Dis*. 2017 Oct 24;12:3115–22.
68. Smith JR, Johnson BD, Olson TP. Impaired central hemodynamics in chronic obstructive pulmonary disease during submaximal exercise. *J Appl Physiol Bethesda Md 1985*. 2019 Sep 1;127(3):691–7.
69. O’donnell DE, D’arsigny C, Raj S, Abdollah H, Webb KA. Ventilatory Assistance Improves Exercise Endurance in Stable Congestive Heart Failure. *Am J Respir Crit Care Med*. 1999 Dec 1;160(6):1804–11.
70. Wheatley CM, Kannan T, Bornschlegl S, Kim C ho, Gastineau DA, Dietz AB, et al. Conducting Maximal and Submaximal Endurance Exercise Testing to Measure Physiological

- and Biological Responses to Acute Exercise in Humans. *J Vis Exp JoVE*. 2018 Oct 17;(140):58417.
71. Laughlin MH. Cardiovascular response to exercise. *Adv Physiol Educ*. 1999;22(1):16.
 72. Gledhill N, Cox D, Jamnik R. Endurance athletes' stroke volume does not plateau: major advantage is diastolic function. *Med Sci Sports Exerc*. 1994 Sep;26(9):1116–21.
 73. Proctor DN, Beck KC, Shen PH, Eickhoff TJ, Halliwill JR, Joyner MJ. Influence of age and gender on cardiac output-VO₂ relationships during submaximal cycle ergometry. *J Appl Physiol Bethesda Md* 1985. 1998 Feb;84(2):599–605.
 74. Wiebe CG, Gledhill N, Jamnik VK, Ferguson S. Exercise cardiac function in young through elderly endurance trained women. *Med Sci Sports Exerc*. 1999 May;31(5):684–91.
 75. Barker RC, Hopkins SR, Kellogg N, Olfert IM, Brutsaert TD, Gavin TP, et al. Measurement of cardiac output during exercise by open-circuit acetylene uptake. *J Appl Physiol Bethesda Md* 1985. 1999 Oct;87(4):1506–12.
 76. Warburton DE, Gledhill N, Jamnik VK, Krip B, Card N. Induced hypervolemia, cardiac function, VO₂max, and performance of elite cyclists. *Med Sci Sports Exerc*. 1999 Jun;31(6):800–8.
 77. Warburton DE, Gledhill N, Quinney HA. Blood volume, aerobic power, and endurance performance: potential ergogenic effect of volume loading. *Clin J Sport Med Off J Can Acad Sport Med*. 2000 Jan;10(1):59–66.
 78. Warburton DER, Haykowsky MJ, Quinney HA, Blackmore D, Teo KK, Taylor DA, et al. Blood volume expansion and cardiorespiratory function: effects of training modality. *Med Sci Sports Exerc*. 2004 Jun;36(6):991–1000.
 79. Ferguson S, Gledhill N, Jamnik VK, Wiebe C, Payne N. Cardiac performance in endurance-trained and moderately active young women. *Med Sci Sports Exerc*. 2001 Jul;33(7):1114–9.
 80. Zhou B, Conlee RK, Jensen R, Fellingham GW, George JD, Fisher AG. Stroke volume does not plateau during graded exercise in elite male distance runners. *Med Sci Sports Exerc*. 2001 Nov;33(11):1849–54.
 81. Trinity JD, Lee JF, Pahnke MD, Beck KC, Coyle EF. Attenuated relationship between cardiac output and oxygen uptake during high-intensity exercise. *Acta Physiol*. 2012;204(3):362–70.
 82. Stringer WW, Hansen JE, Wasserman K. Cardiac output estimated noninvasively from oxygen uptake during exercise. *J Appl Physiol Bethesda Md* 1985. 1997 Mar;82(3):908–12.
 83. Stringer WW, Whipp BJ, Wasserman K, Pórszász J, Christenson P, French WJ. Non-linear cardiac output dynamics during ramp-incremental cycle ergometry. *Eur J Appl Physiol*. 2005 Mar;93(5–6):634–9.

84. Calbet JAL, Gonzalez-Alonso J, Helge JW, Søndergaard H, Munch-Andersen T, Boushel R, et al. Cardiac output and leg and arm blood flow during incremental exercise to exhaustion on the cycle ergometer. *J Appl Physiol Bethesda Md* 1985. 2007 Sep;103(3):969–78.
85. Bevegard S, Holmgren A, Jonsson B. Circulatory studies in well trained athletes at rest and during heavy exercise. With special reference to stroke volume and the influence of body position. *Acta Physiol Scand*. 1963 Feb;57:26–50.
86. Astrand PO, Cuddy TE, Saltin B, Stenberg J. CARDIAC OUTPUT DURING SUBMAXIMAL AND MAXIMAL WORK. *J Appl Physiol*. 1964 Mar;19:268–74.
87. Higginbotham MB, Morris KG, Williams RS, McHale PA, Coleman RE, Cobb FR. Regulation of stroke volume during submaximal and maximal upright exercise in normal man. *Circ Res*. 1986 Feb;58(2):281–91.
88. Flamm SD, Taki J, Moore R, Lewis SF, Keech F, Maltais F, et al. Redistribution of regional and organ blood volume and effect on cardiac function in relation to upright exercise intensity in healthy human subjects. *Circulation*. 1990 May;81(5):1550–9.
89. Seals DR, Hagberg JM, Spina RJ, Rogers MA, Schechtman KB, Ehsani AA. Enhanced left ventricular performance in endurance trained older men. *Circulation*. 1994 Jan;89(1):198–205.
90. McCole SD, Brown MD, Moore GE, Zmuda JM, Cwynar JD, Hagberg JM. Cardiovascular hemodynamics with increasing exercise intensities in postmenopausal women. *J Appl Physiol Bethesda Md* 1985. 1999 Dec;87(6):2334–40.
91. González-Alonso J, Calbet JAL. Reductions in systemic and skeletal muscle blood flow and oxygen delivery limit maximal aerobic capacity in humans. *Circulation*. 2003 Feb 18;107(6):824–30.
92. González-Alonso J, Dalsgaard MK, Osada T, Volianitis S, Dawson EA, Yoshiga CC, et al. Brain and central haemodynamics and oxygenation during maximal exercise in humans. *J Physiol*. 2004 May 15;557(Pt 1):331–42.
93. Poliner LR, Dehmer GJ, Lewis SE, Parkey RW, Blomqvist CG, Willerson JT. Left ventricular performance in normal subjects: a comparison of the responses to exercise in the upright and supine positions. *Circulation*. 1980 Sep;62(3):528–34.
94. Stöhr EJ, González-Alonso J, Shave R. Left ventricular mechanical limitations to stroke volume in healthy humans during incremental exercise. *Am J Physiol Heart Circ Physiol*. 2011 Aug;301(2):H478-487.
95. Parker JO, Khaja F, Case RB. Analysis of left ventricular function by atrial pacing. *Circulation*. 1971 Feb;43(2):241–52.

96. Munch GDW, Svendsen JH, Damsgaard R, Secher NH, González-Alonso J, Mortensen SP. Maximal heart rate does not limit cardiovascular capacity in healthy humans: insight from right atrial pacing during maximal exercise. *J Physiol*. 2014 Jan 15;592(Pt 2):377–90.
97. Vieillard-Baron A, Schmitt JM, Augarde R, Fellahi JL, Prin S, Page B, et al. Acute cor pulmonale in acute respiratory distress syndrome submitted to protective ventilation: incidence, clinical implications, and prognosis. *Crit Care Med*. 2001 Aug;29(8):1551–5.
98. Brinker JA, Weiss JL, Lappé DL, Rabson JL, Summer WR, Permutt S, et al. Leftward septal displacement during right ventricular loading in man. *Circulation*. 1980 Mar;61(3):626–33.
99. Braunwald E, Binion JT, Morgan WL, Sarnoff SJ. Alterations in central blood volume and cardiac output induced by positive pressure breathing and counteracted by metaraminol (aramine). *Circ Res*. 1957 Nov;5(6):670–5.
100. Räsänen J, Heikkilä J, Downs J, Nikki P, Väisänen I, Viitanen A. Continuous positive airway pressure by face mask in acute cardiogenic pulmonary edema. *Am J Cardiol*. 1985 Feb 1;55(4):296–300.
101. Vieillard-Baron A, Matthay M, Teboul JL, Bein T, Schultz M, Magder S, et al. Experts' opinion on management of hemodynamics in ARDS patients: focus on the effects of mechanical ventilation. *Intensive Care Med*. 2016 May;42(5):739–49.
102. Vieillard-Baron A, Loubieres Y, Schmitt JM, Page B, Dubourg O, Jardin F. Cyclic changes in right ventricular output impedance during mechanical ventilation. *J Appl Physiol Bethesda Md* 1985. 1999 Nov;87(5):1644–50.
103. Morimont P, Lambermont B, Ghuysen A, Gerard P, Kolh P, Lancellotti P, et al. Effective arterial elastance as an index of pulmonary vascular load. *Am J Physiol Heart Circ Physiol*. 2008 Jun;294(6):H2736-2742.
104. Denault AY, Gorcsan J, Pinsky MR. Dynamic effects of positive-pressure ventilation on canine left ventricular pressure-volume relations. *J Appl Physiol Bethesda Md* 1985. 2001 Jul;91(1):298–308.
105. Fessler HE, Brower RG, Wise RA, Permutt S. Effects of positive end-expiratory pressure on the canine venous return curve. *Am Rev Respir Dis*. 1992 Jul;146(1):4–10.
106. Cheyne WS, Williams AM, Harper MI, Eves ND. Heart-lung interaction in a model of COPD: importance of lung volume and direct ventricular interaction. *Am J Physiol - Heart Circ Physiol*. 2016 Dec 1;311(6):H1367–74.
107. Cheyne WS, Williams AM, Harper MI, Eves ND. Acute volume loading exacerbates direct ventricular interaction in a model of COPD. *J Appl Physiol*. 2017 Nov 1;123(5):1110–7.
108. Cheyne WS, Gelinas JC, Eves ND. Hemodynamic effects of incremental lung hyperinflation. *Am J Physiol-Heart Circ Physiol*. 2018 May 4;315(3):H474–81.

109. Cheyne WS, Gelinas JC, Eves ND. The haemodynamic response to incremental increases in negative intrathoracic pressure in healthy humans. *Exp Physiol*. 2018 Apr 1;103(4):581–9.
110. Naughton MT, Rahman MA, Hara K, Floras JS, Bradley TD. Effect of continuous positive airway pressure on intrathoracic and left ventricular transmural pressures in patients with congestive heart failure. *Circulation*. 1995 Mar 15;91(6):1725–31.
111. Mann LM, Granger EA, Chan JS, Yu A, Molgat-Seon Y, Dominelli PB. Minimizing airflow turbulence in women lowers the work of breathing to levels similar to men. *J Appl Physiol*. 2020 Jul 23;129(2):410–8.
112. Babb TG. Ventilatory response to exercise in subjects breathing CO₂ or HeO₂. *J Appl Physiol Bethesda Md* 1985. 1997 Mar;82(3):746–54.
113. Eves ND, Petersen SR, Haykowsky MJ, Wong EY, Jones RL. Helium-hyperoxia, exercise, and respiratory mechanics in chronic obstructive pulmonary disease. *Am J Respir Crit Care Med*. 2006 Oct 1;174(7):763–71.
114. Molgat-Seon Y, Ramsook AH, Peters CM, Schaeffer MR, Dominelli PB, Romer LM, et al. Manipulation of mechanical ventilatory constraint during moderate intensity exercise does not influence dyspnoea in healthy older men and women. *J Physiol*. 2019 Mar;597(5):1383–99.
115. Dominelli PB, Foster GE, Dominelli GS, Henderson WR, Koehle MS, McKenzie DC, et al. Exercise-induced arterial hypoxaemia and the mechanics of breathing in healthy young women. *J Physiol*. 2013 Jun 15;591(12):3017–34.
116. Dominelli PB, Archiza B, Ramsook AH, Mitchell RA, Peters CM, Molgat-Seon Y, et al. Effects of respiratory muscle work on respiratory and locomotor blood flow during exercise. *Exp Physiol*. 2017;102(11):1535–47.
117. Dominelli PB, Katayama K, Vermeulen TD, Stuckless TJR, Brown CV, Foster GE, et al. Work of breathing influences muscle sympathetic nerve activity during semi-recumbent cycle exercise. *Acta Physiol Oxf Engl*. 2019 Apr;225(4):e13212.
118. Dominelli PB, Molgat-Seon Y, Griesdale DEG, Peters CM, Blouin JS, Sekhon M, et al. Exercise-induced quadriceps muscle fatigue in men and women: effects of arterial oxygen content and respiratory muscle work. *J Physiol*. 2017 Aug 1;595(15):5227–44.
119. Mann LM, Angus SA, Doherty CJ, Dominelli PB. Evaluation of sex-based differences in airway size and the physiological implications. *Eur J Appl Physiol*. 2021 Jul 31;
120. Dominelli PB, Henderson WR, Sheel AW. A proportional assist ventilator to unload respiratory muscles experimentally during exercise in humans. *Exp Physiol*. 2016 Jun 1;101(6):754–67.
121. Younes M. Proportional assist ventilation, a new approach to ventilatory support. *Theory. Am Rev Respir Dis*. 1992 Jan;145(1):114–20.

122. Jonkman AH, Rauseo M, Carreaux G, Telias I, Sklar MC, Heunks L, et al. Proportional modes of ventilation: technology to assist physiology. *Intensive Care Med.* 2020 Dec;46(12):2301–13.
123. Dominelli PB, Sheel AW. Experimental approaches to the study of the mechanics of breathing during exercise. *Respir Physiol Neurobiol.* 2012 Mar 15;180(2):147–61.
124. Janicki JS, Sheriff DD, Robotham JL, Wise RA. Cardiac Output During Exercise: Contributions of the Cardiac, Circulatory, and Respiratory Systems. In: *Comprehensive Physiology* [Internet]. American Cancer Society; 2011 [cited 2021 Sep 14]. p. 649–704. Available from: <https://onlinelibrary.wiley.com/doi/abs/10.1002/cphy.cp120115>
125. Aaron EA, Seow KC, Johnson BD, Dempsey JA. Oxygen cost of exercise hyperpnea: implications for performance. *J Appl Physiol.* 1992 May 1;72(5):1818–25.
126. Harms CA, Wetter TJ, McClaran SR, Pegelow DF, Nickele GA, Nelson WB, et al. Effects of respiratory muscle work on cardiac output and its distribution during maximal exercise. *J Appl Physiol.* 1998 Aug 1;85(2):609–18.
127. Harms CA, Babcock MA, McClaran SR, Pegelow DF, Nickele GA, Nelson WB, et al. Respiratory muscle work compromises leg blood flow during maximal exercise. *J Appl Physiol Bethesda Md* 1985. 1997 May;82(5):1573–83.
128. Cross TJ, Sabapathy S, Beck KC, Morris NR, Johnson BD. The resistive and elastic work of breathing during exercise in patients with chronic heart failure. *Eur Respir J.* 2012 Jun;39(6):1449–57.
129. Calbet J a. L, Jensen-Urstad M, van Hall G, Holmberg HC, Rosdahl H, Saltin B. Maximal muscular vascular conductances during whole body upright exercise in humans. *J Physiol.* 2004 Jul 1;558(Pt 1):319–31.
130. Lang RM, Badano LP, Victor MA, Afilalo J, Armstrong A, Ernande L, et al. Recommendations for cardiac chamber quantification by echocardiography in adults: An update from the American Society of Echocardiography and the European Association of Cardiovascular Imaging. *J Am Soc Echocardiogr.* 2015;28(1):1-39.e14.
131. Meah VL, Backx K, Cockcroft JR, Shave RE, Stöhr EJ. Left ventricular mechanics in late second trimester of healthy pregnancy. *Ultrasound Obstet Gynecol.* 2019;54(3):350–8.
132. Nio AQX, Rogers S, Mynors-Wallis R, Meah VL, Black JM, Stembridge M, et al. The Menopause Alters Aerobic Adaptations to High-Intensity Interval Training. *Med Sci Sports Exerc.* 2020 Oct;52(10):2096–106.
133. Farrell PA, Joyner MJ, Caiozzo VJ. *ACSM's Advanced Exercise Physiology.* 2nd ed. Wolters Kluwer Health, Lippincott Williams & Wilkins; 2012.

134. Wetter TJ, Harms CA, Nelson WB, Pegelow DF, Dempsey JA. Influence of respiratory muscle work on $\dot{V}O_2$ and leg blood flow during submaximal exercise. *J Appl Physiol*. 1999 Aug;87(2):643–51.
135. Koch-Weser J, Blinks JR. THE INFLUENCE OF THE INTERVAL BETWEEN BEATS ON MYOCARDIAL CONTRACTILITY. *Pharmacol Rev*. 1963 Sep;15:601–52.
136. Welsh DA, Summer WR, deBoisblanc B, Thomas D. Hemodynamic Consequences of Mechanical Ventilation. *Clin Pulm Med*. 1999 Jan;6(1):52–65.
137. Cheifetz IM. Cardiorespiratory Interactions: The Relationship Between Mechanical Ventilation and Hemodynamics. *Respir Care*. 2014 Dec 1;59(12):1937–45.
138. Huang SJ, McLean AS. Appreciating the Strengths and Weaknesses of Transthoracic Echocardiography in Hemodynamic Assessments. *Cardiol Res Pract*. 2012;2012:894308.
139. Patterson SW, Starling EH. On the mechanical factors which determine the output of the ventricles. *J Physiol*. 1914 Sep 8;48(5):357–79.
140. Ross J, Braunwald E. STUDIES ON STARLING'S LAW OF THE HEART. IX. THE EFFECTS OF IMPEDING VENOUS RETURN ON PERFORMANCE OF THE NORMAL AND FAILING HUMAN LEFT VENTRICLE. *Circulation*. 1964 Nov;30:719–27.
141. Ait-Mou Y, Hsu K, Farman GP, Kumar M, Greaser ML, Irving TC, et al. Titin strain contributes to the Frank–Starling law of the heart by structural rearrangements of both thin- and thick-filament proteins. *Proc Natl Acad Sci*. 2016 Feb 23;113(8):2306–11.
142. Kobirumaki-Shimozawa F, Inoue T, Shintani SA, Oyama K, Terui T, Minamisawa S, et al. Cardiac thin filament regulation and the Frank–Starling mechanism. *J Physiol Sci*. 2014 Jul;64(4):221–32.
143. Cingolani HE, Pérez NG, Cingolani OH, Ennis IL. The Anrep effect: 100 years later. *Am J Physiol Heart Circ Physiol*. 2013 Jan 15;304(2):H175-182.
144. Lakatta EG. Beyond Bowditch: the convergence of cardiac chronotropy and inotropy. *Cell Calcium*. 2004 Jun;35(6):629–42.
145. Fessler HE, Brower RG, Wise R, Permutt S. Positive pleural pressure decreases coronary perfusion. *Am J Physiol*. 1990 Mar;258(3 Pt 2):H814-820.
146. Fewell JE, Abendschein DR, Carlson CJ, Rapaport E, Murray JF. Mechanism of decreased right and left ventricular end-diastolic volumes during continuous positive-pressure ventilation in dogs. *Circ Res*. 1980 Sep;47(3):467–72.
147. Schulman DS, Biondi JW, Zohgbi S, Zaret BL, Soufer R. Coronary Flow Limits Right Ventricular Performance during Positive End-expiratory Pressure. *Am Rev Respir Dis*. 1990 Jun;141(6):1531–7.

148. Tittley JG, Fremes SE, Weisel RD, Christakis GT, Evans PJ, Madonik MM, et al. Hemodynamic and Myocardial Metabolic Consequences of PEEP. *Chest*. 1985 Oct 1;88(4):496–502.
149. Bell RC, Robotham JL, Badke FR, Little WC, Kindred MK. Left ventricular geometry during intermittent positive pressure ventilation in dogs. *J Crit Care*. 1987 Dec 1;2(4):230–44.
150. Cassidy SS, Mitchell JH, Johnson RL. Dimensional analysis of right and left ventricles during positive-pressure ventilation in dogs. *Am J Physiol-Heart Circ Physiol*. 1982 Apr;242(4):H549–56.
151. Robotham JL, Lixfeld W, Holland L, MacGregor D, Bromberger-Barnea B, Permutt S, et al. The Effects of Positive End-Expiratory Pressure on Right and Left Ventricular Performance. *Am Rev Respir Dis*. 1980 Apr;121(4):677–83.
152. Omar AMS, Vallabhajosyula S, Sengupta PP. Left Ventricular Twist and Torsion. *Circ Cardiovasc Imaging*. 2015 Jun;8(6):e003029.
153. Stöhr EJ, Shave RE, Baggish AL, Weiner RB. Left ventricular twist mechanics in the context of normal physiology and cardiovascular disease: a review of studies using speckle tracking echocardiography. *Am J Physiol-Heart Circ Physiol*. 2016 Sep;311(3):H633–44.
154. Badano LP, Muraru D. Twist Mechanics of the Left Ventricle. *Circ Cardiovasc Imaging*. 2019 Apr;12(4):e009085.
155. Franchi F, Faltoni A, Cameli M, Muzzi L, Lisi M, Cubattoli L, et al. Influence of Positive End-Expiratory Pressure on Myocardial Strain Assessed by Speckle Tracking Echocardiography in Mechanically Ventilated Patients. *BioMed Res Int*. 2013;2013:918548.
156. Charkoudian N, Rabbitts JA. Sympathetic Neural Mechanisms in Human Cardiovascular Health and Disease. *Mayo Clin Proc*. 2009 Sep;84(9):822–30.
157. Raven PB, Fadel PJ, Ogoh S. Arterial baroreflex resetting during exercise: a current perspective. *Exp Physiol*. 2006;91(1):37–49.
158. Bubshait K, Alabbasi Y. Influence of Spontaneous and Mechanical Ventilation on Frequency-Based Measures of Heart Rate Variability. *Crit Care Res Pract*. 2021 Dec 26;2021:e8709262.
159. Van de Louw A, Médigue C, Papelier Y, Cottin F. Breathing cardiovascular variability and baroreflex in mechanically ventilated patients. *Am J Physiol-Regul Integr Comp Physiol*. 2008 Dec;295(6):R1934–40.
160. Scharf SM, Brown R. Influence of the right ventricle on canine left ventricular function with PEEP. *J Appl Physiol*. 1982 Jan;52(1):254–9.

161. Dominelli PB, Render JN, Molgat-Seon Y, Foster GE, Romer LM, Sheel AW. Oxygen cost of exercise hyperpnoea is greater in women compared with men. *J Physiol*. 2015;593(8):1965–79.
162. Boerth RC, Covell JW, Pool PE, Ross J. Increased myocardial oxygen consumption and contractile state associated with increased heart rate in dogs. *Circ Res*. 1969 May;24(5):725–34.
163. Hinghofer-Szalkay H. Gravity, the hydrostatic indifference concept and the cardiovascular system. *Eur J Appl Physiol*. 2011 Feb 1;111(2):163–74.
164. Shahgaldi K, Manouras A, Brodin LÅ, Winter R. Direct Measurement of Left Ventricular Outflow Tract Area Using Three-Dimensional Echocardiography in Biplane Mode Improves Accuracy of Stroke Volume Assessment. *Echocardiography*. 2010;27(9):1078–85.
165. Hoffmann R, Barletta G, von Bardeleben S, Vanoverschelde JL, Kasprzak J, Greis C, et al. Analysis of Left Ventricular Volumes and Function: A Multicenter Comparison of Cardiac Magnetic Resonance Imaging, Cine Ventriculography, and Unenhanced and Contrast-Enhanced Two-Dimensional and Three-Dimensional Echocardiography. *J Am Soc Echocardiogr*. 2014 Mar 1;27(3):292–301.
166. Zhang Y, Wang Y, Shi J, Hua Z, Xu J. Cardiac output measurements via echocardiography versus thermodilution: A systematic review and meta-analysis. *PLoS ONE*. 2019 Oct 3;14(10):e0222105.
167. Christie J, Sheldahl LM, Tristani FE, Sagar KB, Ptacin MJ, Wann S. Determination of stroke volume and cardiac output during exercise: comparison of two-dimensional and Doppler echocardiography, Fick oximetry, and thermodilution. *Circulation*. 1987 Sep;76(3):539–47.
168. Wetterslev M, Møller-Sørensen H, Johansen RR, Perner A. Systematic review of cardiac output measurements by echocardiography vs. thermodilution: the techniques are not interchangeable. *Intensive Care Med*. 2016 Aug 1;42(8):1223–33.
169. Sheel AW, Dominelli PB, Molgat-Seon Y. Revisiting dysanapsis: sex-based differences in airways and the mechanics of breathing during exercise. *Exp Physiol*. 2016;101(2):213–8.
170. Johnson BD, Dempsey JA. Demand vs. capacity in the aging pulmonary system. *Exerc Sport Sci Rev*. 1991;19:171–210.
171. Molgat-Seon Y, Dominelli PB, Ramsook AH, Schaeffer MR, Molgat Sereacki S, Foster GE, et al. The effects of age and sex on mechanical ventilatory constraint and dyspnea during exercise in healthy humans. *J Appl Physiol Bethesda Md* 1985. 2018 Apr 1;124(4):1092–106.
172. Sharma G, Goodwin J. Effect of aging on respiratory system physiology and immunology. *Clin Interv Aging*. 2006 Sep;1(3):253–60.

173. Gillooly M, Lamb D. Airspace size in lungs of lifelong non-smokers: effect of age and sex. *Thorax*. 1993 Jan;48(1):39–43.
174. Enright PL, Kronmal RA, Manolio TA, Schenker MB, Hyatt RE. Respiratory muscle strength in the elderly. Correlates and reference values. Cardiovascular Health Study Research Group. *Am J Respir Crit Care Med*. 1994 Feb;149(2 Pt 1):430–8.